

## Accepted Manuscript

The role of ridge subduction in determining the geochemistry and Nd-Sr-Pb isotopic evolution of the Kodiak batholith in Southern Alaska

Robert A. Ayuso, Peter J. Haeussler, Dwight C. Bradley, David W. Farris, Nora K. Foley, Gregory A. Wandless

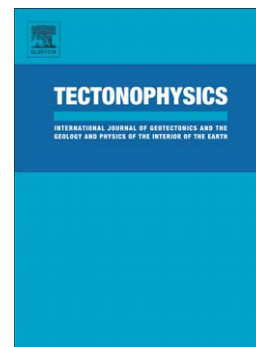
PII: S0040-1951(08)00444-7  
DOI: doi: [10.1016/j.tecto.2008.09.029](https://doi.org/10.1016/j.tecto.2008.09.029)  
Reference: TECTO 124337

To appear in: *Tectonophysics*

Received date: 9 May 2007  
Revised date: 25 August 2008  
Accepted date: 10 September 2008

Please cite this article as: Ayuso, Robert A., Haeussler, Peter J., Bradley, Dwight C., Farris, David W., Foley, Nora K., Wandless, Gregory A., The role of ridge subduction in determining the geochemistry and Nd-Sr-Pb isotopic evolution of the Kodiak batholith in Southern Alaska, *Tectonophysics* (2008), doi: [10.1016/j.tecto.2008.09.029](https://doi.org/10.1016/j.tecto.2008.09.029)

This is a PDF file of an unedited manuscript that has been accepted for publication. As a service to our customers we are providing this early version of the manuscript. The manuscript will undergo copyediting, typesetting, and review of the resulting proof before it is published in its final form. Please note that during the production process errors may be discovered which could affect the content, and all legal disclaimers that apply to the journal pertain.



**The role of ridge subduction in determining the geochemistry and Nd-Sr-Pb isotopic evolution of the Kodiak batholith in Southern Alaska**

Robert A. Ayuso<sup>a</sup>, Peter J. Haeussler<sup>b</sup>, Dwight C. Bradley<sup>b</sup>,  
David W. Farris<sup>c</sup>, Nora K. Foley<sup>a</sup>, and Gregory A. Wandless<sup>a</sup>

<sup>a</sup>, \* *Mail Stop 954 National Center, U.S. Geological Survey, Reston, VA 20192*

<sup>b</sup> *4200 University Drive, U.S. Geological Survey, Anchorage, AK 99508*

<sup>c</sup> *Department of Geological Sciences, University of Southern California, Los Angeles, CA 90089*

\* Corresponding author

E-mail address: [rayuso@usgs.gov](mailto:rayuso@usgs.gov) (R.A. Ayuso)

**Abstract**

The Paleocene Kodiak batholith, part of the Sanak-Baranof belt of Tertiary near-trench intrusive rocks, forms an elongate body (~150 km long) that transects Kodiak Island from SW to NE. The batholith consists of three zones (Southern, Central, and Northern) of kyanite-, muscovite-, and garnet-bearing biotite tonalite and granodiorite and less abundant granite that intruded an accretionary prism (Kodiak Formation, and Ghost Rocks Formation). Small and likely coeval bodies (Northern, Western, and Eastern satellite groups) of quartz gabbro, diorite, tonalite, granodiorite, and leucogranite flank the batholith. The batholith is calc-alkalic, has an aluminum saturation index of  $>1.1$ ,  $\text{FeO}_t/(\text{FeO}_t+\text{MgO}) \sim 0.65$  (at  $\text{SiO}_2 = 65$  wt. %), and increases in  $\text{SiO}_2$  (~61 wt. %–73 wt. %) and decreases in  $\text{TiO}_2$  (~0.9 wt. %–0.3 wt. %) from SW to NE. As a group, the granitic rocks have light REE-enriched chondrite-normalized patterns with small or no negative Eu anomalies, primitive mantle-normalized negative anomalies for Nb and Ti, and positive anomalies for Pb. Small to large negative anomalies for Th are also distinctive. The quartz gabbros and diorites are generally characterized by generally flat to light REE chondrite-normalized patterns (no Eu anomalies), and mantle-normalized negative anomalies for Nb, Ti, and P. Pb isotopic compositions ( $^{206}\text{Pb}/^{204}\text{Pb} = 18.850\text{--}18.960$ ;  $^{207}\text{Pb}/^{204}\text{Pb} = 15.575\text{--}15.694$ ;  $^{208}\text{Pb}/^{204}\text{Pb} = 38.350\text{--}39.039$ ) are intermediate between depleted mantle and average continental crust. The Southern zone and a portion of the Central zone are characterized by negative  $\epsilon_{\text{Nd}}$  values of -3.7 to -0.3 and  $T_{\text{DM}}$  ages ranging from ~ 838 Ma to 1011 Ma. Other granitic rocks from the Central and Northern zones have higher  $\epsilon_{\text{Nd}}$  values of -0.4 to +4.7 and younger  $T_{\text{DM}}$  ages of ~ 450 to 797 Ma. Granitic and mafic plutons from the Eastern satellites show a wide range of  $\epsilon_{\text{Nd}}$  values of -2.7 to +6.4, and  $T_{\text{DM}}$  ages from 204 Ma to 2124 Ma.  $^{87}\text{Sr}/^{86}\text{Sr}$  values of the Southern and Central zones overlap and tend to be slightly more radiogenic ( $^{87}\text{Sr}/^{86}\text{Sr} > 0.70426$ ) than the Northern zone ( $^{87}\text{Sr}/^{86}\text{Sr} < 0.70472$ ).  $^{206}\text{Pb}/^{204}\text{Pb}$  values increase slightly from the Southern and Central zones toward the Northern zone. There is no clear correlation of the major or trace elements with  $\epsilon_{\text{Nd}}$ , Pb or Sr isotopic values. Kodiak Formation and the Ghost Rocks Formation overlap the isotopic compositions (e.g.,  $^{206}\text{Pb}/^{204}\text{Pb} = 18.978$  to 19.165,  $^{87}\text{Sr}/^{86}\text{Sr}$  of 0.705715 to 0.707118, and  $\epsilon_{\text{Nd}}$  of -6.7 to -

1.5 at 59 Ma) and  $T_{DM}$  values (959 to 1489 Ma) of the batholith. Production of large volumes of granitic rocks in the Sanak-Baranof belt, and particularly on Kodiak Island, reflects a sequence of processes that includes underplating of mantle-derived mafic (possibly from the mantle wedge) and intermediate rocks under the accretionary flysch, interlayering of mantle-derived and flyschoid rocks, and partial melting of the mixed lithologic assemblages. Limited degrees of fractional crystallization or assimilation and fractional crystallization influenced compositions of the granitic rocks. The contribution of mantle-derived rocks that resided in the accretionary prism for only a short period of time prior to partial melting likely exceeds 40% (up to 80%). The balance (60 to 20%) is from a recently recycled crustal component represented by the Kodiak Formation. This type of progressive intracrustal melting from mixed sources controlled the geochemical character of the batholith and is most consistent with the hypothesis that the granitic rocks are associated with a slab-window produced by collision of a spreading oceanic center and a subduction zone and migration beneath the accretionary prism.

*Keywords:* Kodiak Batholith; Alaska; Geochemistry; Radiogenic Isotopes; Origin; Ridge Subduction, Slab Window

## **1. Introduction**

The Paleocene Kodiak batholith (located on Kodiak Island) is part of a plutonic belt of near-trench intrusions of gabbro, tonalite, granodiorite, and granite, which occur within rocks of the latest Cretaceous to Eocene composite accretionary prism of the Gulf of Alaska (Fig. 1). The belt is termed the Sanak-Baranof plutonic belt (Hudson et al., 1979), lies landward of the modern Aleutian Trench (Aleutian Megathrust) and in the forearc of the modern Aleutian oceanic island arc. It extends for about 2100 km from Sanak Island in the eastern Aleutian Islands to Baranof Island in southeast Alaska (Bradley et al., 2003). On Kodiak Island in the western part of the Gulf of Alaska, the accretionary prism consists dominantly of Late Cretaceous flysch and argillite such as the Kodiak Formation and Ghost Rocks Formation. The accretionary sequence has been referred to as the Chugach-Prince William composite

terrane in Alaska (Jones et al., 1987), one of several terranes that accreted to North America in latest Cretaceous to, perhaps, Paleocene (Hill et al., 1981; Moore et al., 1983; Plafker et al., 1977; 1989).

Silicic plutonism intruding the accretionary prism had been thought to reflect distinct pulses of magmatism occurring during the last stages of accretion (Hill et al., 1981; J.C. Moore referenced in Barker et al. 1992). Recent studies of the geological signature of early Tertiary ridge subduction in Alaska, however, emphasize continuous, rather episodic age progression from 61 to 50 Ma of the near-trench intrusive rocks of the Sanak-Baranof belt from western Alaska to Baranof Island (e.g., Bradley et al., 1993, 2003; Haeussler et al., 2003a, b). More importantly, there is a growing consensus that ridge-subduction best explains the age distribution, origin, and location of near-trench plutons along the Sanak-Baranof belt (e.g., Kusky et al., 2003, Sisson et al., 2003a, b, and references therein) even though occurrence of such plutons in the accretionary prism in a forearc setting is atypical when compared to classic plutonic distributions from orogenic, continental margin arcs. Moreover, in Alaska, an origin for the plutonic rocks as a result of ridge subduction is also thought to be consistent with other distinctive features found in the accretionary prism, such as its evolution in a high-T and low-P metamorphic environment (Sisson et al., 1989), its unique set of structural features (Pavlis and Sisson, 1995), and association with gold mineralization (Haeussler et al., 1995; 2003a).

The origin of the granitic magmas within the Kodiak batholith (Fig. 1) is considered in this paper on the basis of petrography, major and trace element variations, and Nd-Sr-Pb isotopic evolution. The geochemical results in this study provide insights into possible sources and processes that contributed to formation of the granitic magmas, and present key geochemical fingerprints for regional comparison of the granite sources along the Sanak-Baranof plutonic belt. We highlight geochemical features and the crustal evolution of the accretionary wedge hosting granitic magmas thought to have been produced by migration of the triple junction and during ridge subduction (see Bradley et al., 1993, 2003; Sisson et al., 2003a, b). However, because the identity of the tectonic plates along the Pacific rim of Alaska during the Late Cretaceous to the Eocene is not well established (see Bradley et al., 2003; Haeussler, et al., 2003b for summaries), it is difficult to conclusively attribute the origin of near-trench magmatism in southern

Alaska to a specific plate. Page and Engerbretson (1984) suggested two possible end-member locations for the trench-ridge-trench triple junction involving the Kula-Farallon plate in the Late Cretaceous to early Tertiary: a northern location in the state of Washington, and a southern location in Mexico. Neither of these locations would explain near-trench magmatism in southern Alaska thought to have been associated with ridge subduction. Others have proposed that intersection of the Kula-Farallon Ridge with the southern Alaska margin (e.g., Sisson et al., 1989; 2003a; Pavlis and Sisson, 1995, and references therein) explains the near-trench intrusions and the high temperature and low pressure metamorphism in the accretionary wedge. Intersection of the Kula-Farallon Ridge with the continental margin of the states of Washington, Oregon, and southern Vancouver Island in British Columbia has also been invoked to explain the origin of oceanic basalt basement in the Coast Ranges (e.g., Engerbretson et al., 1985; Thorkelson and Taylor, 1989, and references therein).

Recent work by Haeussler et al. (2003b) noted that a single trench-ridge-trench triple junction cannot explain simultaneous near-trench magmatism from areas separated by  $> 4000$  km. To explain the coeval near-trench magmatism from such widely separated areas, two contemporaneous slab windows associated with trench-ridge-trench triple junctions were proposed. As a consequence of this argument, another oceanic plate in the Pacific Basin in Paleocene-Eocene time was identified—the Resurrection plate, which is bound by two trench-ridge-trench triple junctions (Haeussler et al., 2003b). In this view, the western boundary of the Resurrection plate was located east of the Kula plate, and the southern boundary was located north of the Farallon plate. The northern trench-ridge-trench triple junction of the Resurrection plate intersected the southern Alaskan margin and migrated from west-to-east along a 2100 km-long coastal trend. Migration of this slab window was responsible for the Sanak-Baranof near-trench intrusives that were generated from 61 to 50 Ma, which include the Kodiak batholith at about 58 Ma. The southern ridge bounding the Resurrection plate intersected the continental margin of the states of Washington and Oregon, and also southern Vancouver Island in British Columbia. Magmatism in Washington, Oregon, and southern Vancouver Island is about 50 Ma old, and exhibits no clear record of age progression that can be linked to migration of the triple junction. Haeussler et al. (2003b) suggest that

the southern ridge was subducted sub-parallel to the continental margin and that the 50 Ma magmatic event marks the disappearance of the Resurrection plate.

## 2. Geologic Setting

The granitic rocks of the Kodiak batholith have been the focus of several geochemical studies (Hill et al., 1981; Moore et al., 1983). Only recently has a large portion of the batholith been examined in detail, however, to establish relevant ages, structural relations, and emplacement processes (Farris et al., 2006). The main mass of the batholith forms a narrow, irregular, interior belt on Kodiak Island, subparallel to the modern trench as well as the regional structural grain (Fig. 1). The granitic plutons intrude the Late Cretaceous Kodiak Formation (predominant host), which is flanked by pre-Late Cretaceous units to the north and northwest, and by the Paleocene Ghost Rocks Formation to the south and southeast.

### 2.1 *The Chugach-Prince William Accretionary Prism*

The Chugach-Prince William accretionary prism consists of belts of accreted ocean floor rocks that extend for more than 2000 km along the southern margin of Alaska and are younger in a seaward direction. A review of the geological history of these belts by Bradley et al. (2003, and references therein) is summarized below. The belts differ in age and grade of metamorphism. The most landward belt consists of Early Jurassic high pressure metamorphic rocks (Dusel-Bacon et al., 1993). Seaward from this belt is an argillite-matrix mélangé consisting of Triassic to Middle Cretaceous chert and basalt, greywacke, and limestone intruded by small near-trench plutons, dikes, and a few Triassic-Jurassic ultramafic-mafic complexes (Bradley and Kusky, 1992, and references therein). The next seaward belt is characterized by Upper Cretaceous flysch (assigned to the Shumagin Formation, Kodiak Formation, and Valdez Group, among others), which was particularly affected by relatively high temperature and low pressure metamorphism. This belt also contains the largest near-trench plutons, which include the Kodiak batholith. The plutons intruded the prism soon after it had been affected by penetrative deformation and

regional metamorphism during and shortly after subduction-accretion in the Jurassic to Paleocene time (Dusel-Bacon et al., 1993). Outboard of the Upper Cretaceous flysch belt, which contain the Ghost Rocks Formation and Orca Group, there are other belts of flysch (e.g., Moore et al., 1983, and references therein), and mafic and ultramafic rocks thought to have formed near the trench-ridge-trench triple junction (Bradley et al., 2003). Younger turbidites (Eocene Sitkalidak Formation and the outboard part of the Orca Group) were deposited and accreted after near-trench magmatism.

Sample and Reid (2003) provided a review of the evolution of the Chugach flysch terrane focused on the possible sources of the Kodiak Formation, which is the portion of the Chugach flysch closely associated with the genesis of the Kodiak batholith. The results constrain the tectonic origin of the terrane to latest Cretaceous time. Structural features of the Chugach flysch are thought to reflect underplating at a subduction zone (Plaker et al., 1977; Sample and Fisher, 1986; Sample and Moore, 1987; Fisher and Byrne, 1987), but there is controversy over where this subduction-accretion actually occurred. Detailed analysis of sandstone petrography, paleocurrent current and lithofacies information, and Nd isotopic analyses of the Kodiak Formation on Kodiak Island and vicinity by Sample and Reid (2003) indicated rapid deposition of the flysch in an area flanking an uplifting orogen. Moreover, the petrographic and isotopic data indicate that the Chugach flysch was deposited and accreted near its source along a convergent margin in latest Cretaceous time (adjacent to the Coast Mountains belt of British Columbia) and, subsequently, transported by dextral shear to its current location.

#### *Country rocks: Kodiak Formation and Ghost Rocks Formation*

The Kodiak Formation is dominantly a turbidite sequence (at least 3-5 km thick) consisting of deep-water sandstone-shale and nearly massive shale units cross-cut by shear zones (Nilsen and Moore, 1978) and by quartz veins (Vrolijk et al., 1988). Detailed descriptions of the Kodiak Formation are also given by Sample and Fisher (1986), Fisher and Byrne (1987), and Sample and Reid (2003). Regional grades of metamorphism are generally low, with maximum temperatures at about 200-250° C and pressures at 2-3 kbar (Sample and Moore, 1987). After deposition, the Kodiak Formation was subducted

(underplated) and became part of the accretionary prism (e.g., Nilsen and Moore, 1979; Fisher and Byrne, 1987; Sample and Moore, 1987). The metamorphic conditions were sufficient to transform shale-rich beds of the Kodiak Formation to argillites, but the greywacke-rich sections remained generally unaffected (Farris et al., 2006). Descriptions of the Ghost Rocks Formation are reported by Moore et al. (1983). The unit consists of deformed sandstone- and argillite-rich sedimentary units interbedded with a mafic plutonic-volcanic cycle of island-arc tholeiites and calc-alkaline andesites. These mafic igneous rocks flank the main mass of the granitic Kodiak batholith to the east (present-day trenchward), and may be coeval. Small igneous bodies, unconnected to the main mass of the Kodiak batholith at the surface, also intrude the Kodiak Formation to the west (present-day landward).

### **3. Petrography, Field, and Age Relations of the Kodiak Batholith**

#### *3.1 General Statement*

The Kodiak batholith covers greater than 700 km<sup>2</sup> in surface exposure. It is roughly 150 km in length and has a generally northeasterly trend on the interior of Kodiak Island. The batholith is dominantly composed of intermediate felsic rocks. Zircon from six samples (tonalite and granodiorite) selected from near the axis of the batholith (Fig. 1) and dated by the U-Pb method (thermal ionization mass spectrometry) indicate a northeastward decreasing age trend, from 59.2±0.2 Ma at the southwest end to 58.4±0.2 Ma at the northeast tip (Farris et al., 2006). Discrete granodiorite-granite bodies outcropping to the north, generally along strike of the main mass of the batholith, are termed the Northern satellite group. Flanking the main body of the batholith are discontinuous belts of smaller granitic and mafic plutons, dikes, and volcanic rocks forming discontinuous belts (called Western and Eastern satellite groups). K-Ar dating of biotite from plutons in the Eastern satellite group indicate ages of ~ 63-62 Ma (Moore et al., 1983), and although this group could be related to the Kodiak batholith, the relatively imprecise ages preclude conclusively linking all of the granitic rocks.

The Kodiak batholith ranges from biotite-, muscovite-, and garnet-bearing tonalite to granodiorite (Ayuso et al., 2005). It is easily recognizable in the field because of a relatively wide range in the

abundance of biotite, lack of amphibole, and distinctively zoned kyanite megacrysts. Mafic minerals (biotite, titanomagnetite, and accessory minerals) in the main body of the batholith account for up to 25% of the mode. Muscovite is locally very abundant. Typical field features include numerous country rock xenoliths ranging from meters to millimeters, varying in extent of mechanical disaggregation and reaction from discrete mineralogic (biotite-rich) bands to widely dispersed, remnant coarse clusters of biotite closely associated with fine-grained garnet. Other features in the batholith include scarcity of mafic enclaves, no petrographic evidence for reaction with a mafic magma and no field evidence (e.g. no large volumes of gabbro or diorite, abundant mafic enclaves, mafic dikes, etc.) for reaction with a mafic magma. Also notable are the scarcity of aplites, pegmatites, and miarolitic cavities.

The Kodiak batholith has not been mapped in detail, but existing field and petrographic information indicate several internal zones according to general petrographic variations along a trend from SW to NE (Fig. 1). Internal igneous contacts that would distinguish individual plutons within the zones have not been found. Characterization of the batholith using such regional variations is provided below, in a trend from the Southern zone, to the Central and Northern zones (Fig. 1). Here we give a brief description of the Northern, Western and Eastern satellite groups.

### *3.2 Southern Zone of the Kodiak Batholith*

Reconnaissance examination of the batholith from southwest to northeast indicates that variations are predominantly from tonalite to granodiorite (Fig. 2). In the Southern zone, the biotite-rich rocks are medium grained, muscovite- and garnet-bearing, and phenocryst-poor (plagioclase mega-phenocrysts <3%, up to ~1.5 cm in length). Textures are mostly hypidiomorphic-granular (equigranular and granitic). Plagioclase is generally free of inclusions, but may enclose an internal K-feldspar-rich zone or be rimmed by K-feldspar. The core of plagioclase can include a highly altered (fine-grained muscovite and epidote) euhedral zone that also contains euhedral biotite. This is consistent with plagioclase and biotite co-precipitation. Electron microprobe analyses indicate that most cores of plagioclase in the batholith range from An<sub>60</sub> to An<sub>20</sub> (R. Ayuso, unpublished data). The majority of K-feldspars are unzoned (no albitic

rims). Euhedral biotite occurs in all zones of the batholith, but may be more abundant in the Southern zone. In some rocks, biotite adjacent to quartz, feldspar, and garnet displays feathery, lobate reaction rims. However, biotite also encloses subhedral to euhedral garnet. Sparse, blue-green subhedral to euhedral aluminosilicate xenocrysts (<1 cm) display fine-grained muscovite and chlorite reaction rims and are intergrown with biotite. Fine-grained kyanite is also disseminated in the matrix, and, sheaves of very fine-grained fibrolite (?) are found as inclusions in clusters of biotite and quartz. Euhedral to subhedral fine-grained garnet (< 3 mm) is distributed in biotite clusters and in the matrix. Accessory minerals are zircon, apatite, titanomagnetite, monazite, and very rare pyrite. Most rocks contain aggregates of epidote, chlorite, and opaque oxides replacing biotite. Rare myrmekitic rims on feldspars occur in this zone. Xenoliths of the Kodiak Formation, in parts as virtually unreacted slabs are distributed and show various stages of mechanical disaggregation and limited chemical reaction in the granitic matrix.

### *3.3 Central Zone of the Kodiak Batholith*

Rocks of the Central zone do not differ greatly from the Southern zone (Fig. 2), except that they have the highest content of mafic minerals for the batholith as a whole. In some cases the biotite-rich tonalites are composed of a finer-grained matrix of quartz and feldspar (~1mm), larger clusters of pseudo-hexagonal biotite (~1 cm) and somewhat more abundant fine-grained garnet. Fine-grained euhedral to subhedral garnet (< 3 mm) is disseminated in the matrix, as well as surrounded by and interleaved with, biotite and quartz. Sparse euhedral quartz microphenocrysts (~3mm), and small clusters of muscovite are also found. Most rocks are hypidiomorphic-granular and contain distinctly interleaved mixtures of biotite and epidote, and small, very fine-grained brecciated pods and clusters. Kyanite xenocrysts are more abundant toward the northeast end of the batholith. Locally, the granitic rocks contain abundant xenoliths of Kodiak Formation (up to 0.75 m) armored by narrow reaction rims, and also contain quartz-rich pods, and small fibrolitic (?) clusters surrounded by reaction rims.

### *3.4 Northern Zone of the Kodiak Batholith*

The Northern zone (Fig. 2) is highly fractured, locally contains abundant country-rock inclusions, including stoped blocks (up to ~1 m) and rafts (up to ~30 m?), and some aplite dikes (most <10 cm). Coarse quartz agglomerations and nodules, coarse thick books of hexagonal brown biotite, and composite nodules of aluminosilicate minerals, quartz, and muscovite are also found. Anhedral biotite precipitated late, occupying irregular spaces in the granitic matrix. Fine-grained subhedral to euhedral garnet is common, particularly associated with clusters of biotite (with quartz and feldspar).

The Northern zone rocks are fine to medium grained and vary from biotite-rich (>20%) to biotite poor (<5%) at the scale of outcrops. Mechanical disaggregation of country-rock inclusions is common. As a group, the rocks have relatively high contents of K-feldspar (Fig. 2). Biotite granodiorites contain sparse garnet and muscovite and textures vary from medium grained, hypidiomorphic granular to seriate. In a few cases, biotite foliation (~N70°E, steeply dipping N) parallels the axis of the batholith. Plagioclase phenocrysts (up to ~1 cm) and clusters of quartz (~1 cm) are more common than in rocks to the south, as are the quartz pods (up to ~10cm) enveloped by reaction bands. K-feldspar forms a fine-grained, anhedral, interstitial, interconnecting network. Color index is high where mechanical disaggregation and hybridization are prevalent, but generally lower than that of rocks to the south. Combinations of xenocrystic kyanite, garnet, muscovite, K-feldspar, and quartz form small agglomerates in the matrix. Small pods of dominant poikilitic fine-grained K-feldspar intergrown with plagioclase and quartz may represent residual melts.

### *3.5 Satellite Groups Adjacent to the Kodiak Batholith*

The tonalite-granodiorite plutons of the Western satellite group intruded the Kodiak Formation and closely resemble the granodioritic rocks of the Northern zone. In general, granitic rocks of the Northern and the Eastern satellite groups are muscovite-bearing, hypidiomorphic to aplitic, porphyritic to granular leucotonalites (Fig. 2). Plagioclase and K-feldspar mega-phenocrysts (< 5 mm) may be common. The rocks generally have low biotite abundance (<1%), and a remarkable network of interlocking, fine-

grained anhedral K-feldspar and rare garnet. Biotite can be found as part of fine-grained clusters with garnet and quartz, and as fine grained inclusions in plagioclase cores. Thin aplitic dikes (<10 cm) and muscovite are locally abundant, particularly near the margins of the bodies.

Part of the Eastern satellite group consists of granodioritic to gabbroic plutons (Fig. 1) that intruded the Ghost Rocks Formation near or on the Contact fault about 30 km east of the main mass of the batholith. Volumetrically minor pillow basalts and dikes may also be part of the igneous sequence. The mafic rocks range from fine to medium grained (pillow basalt) to very coarse grained (quartz diorite and quartz gabbro). Other Eastern satellite bodies are small granodioritic to dioritic bodies that intruded the Kodiak Formation west of the Contact fault, about 5-20 kilometers from the Central zone of the batholith. The felsic rocks from the Eastern satellites are similar to the granular, medium grained, biotite-rich tonalitic rocks in the Central zone of the batholith. Garnet and muscovite are not abundant. A few small miarolitic cavities (with quartz and tourmaline) were found in the more felsic rocks. The medium-grained leucogranite is muscovite-bearing and K-feldspar rich. Although the plutons from the Eastern and Western satellites are possibly cogenetic and part of the Kodiak batholith on the basis of field and petrographic similarities, age and geochemical information are not sufficient to link all of these plutonic rocks.

#### **4. Analytical Methods**

Representative whole-rock samples were collected from all rock types, and from all exposed parts of the pluton. A total of 60 samples were analyzed for major and trace elements (Tables 1-4). Analytical techniques included X-ray fluorescence, instrumental neutron activation, inductively coupled plasma-atomic emission spectrometry, and classical wet-chemistry methods. Most of the samples were analyzed by Activation Laboratories Ltd., Ancaster, Ontario by multiple techniques. International rock standards were used to monitor data accuracy and details are available from Activation Laboratories Ltd. Many elements were analyzed in duplicate in order to select the most precise data available. A subset of these

whole-rock samples ( $n = 42$ ) was analyzed for Nd, Sr, and Pb isotopic compositions (Tables 5-6) using a multicollector, automated Finnigan-MAT 262 mass spectrometer at the U.S. Geological Survey, Reston, VA. Detailed analytical techniques for Pb, Nd, and Sr isotopes are given in Ayuso et al. (2005), and Ayuso and Schulz (2003). Long-term reproducibility of the Nd isotopic work was monitored using the La Jolla standard: average value of  $^{143}\text{Nd}/^{144}\text{Nd} = 0.511845 \pm 5$  ( $n = 35$ ); for the Sr isotopic analyses, SRM 987 yielded an average value of  $^{87}\text{Sr}/^{86}\text{Sr} = 0.710245 \pm 5$  ( $n = 29$ ). Pb isotopic ratios of the whole rocks were corrected for mass fractionation by about  $0.12\% \text{ amu}^{-1}$  according to replicate measurements of NBS 981 ( $n = 25$ ). Total blanks during the course of this study were  $<20 \text{ pg}$  for Nd,  $<50 \text{ pg}$  for Sr, and  $< 50 \text{ pg}$  for Pb; thus they are insignificant relative to the Nd, Sr, and Pb abundances. Depleted mantle model ages were calculated as in the model of DePaolo (1981). The average crustal Pb evolution curve is from Stacey and Kramers (1975).

## 5. Results

### 5.1 Kodiak batholith: Major Elements

Samples of the Kodiak batholith lie in the medium-K (calc-alkaline series) field of the  $\text{K}_2\text{O}$  vs.  $\text{SiO}_2$  and the total alkalis vs.  $\text{SiO}_2$  diagrams (e.g.,  $\text{Na}_2\text{O} + \text{K}_2\text{O} < 6 \text{ wt. \%}$  and  $\text{K}_2\text{O} < 3 \text{ wt. \%}$  for  $\text{SiO}_2 = 66 \text{ wt. \%}$ ; Table 1, Fig. 3). Granitic rocks also plot along the calc-alkaline trend on a Na-Ca-K diagram (not shown) and distinguish the zonal variations within the batholith (particularly the Southern and Central zones as a group in comparison with the Northern zone). The AFM plot ( $\text{Na}_2\text{O} + \text{K}_2\text{O} - \text{Fe}_2\text{O}_3 - \text{MgO}$ ) (not shown) also indicates that the granitic rocks dominantly follow a calc-alkaline differentiation trend and become less alkalic (less sodic) in a trend from the Northern satellite group to the Northern zone, Central zone, and Southern zone. A general trend of  $\text{FeO}_{\text{total}}$  depletion characterizes the batholith, but some of the granitic rocks from the Central zone, and mafic rocks from the Eastern satellites (basalt to dacite:  $\text{SiO}_2 \sim 46-66 \text{ wt. \%}$ ) overlap the tholeiitic field. The degree of  $\text{FeO}_{\text{total}}/\text{MgO}$  enrichment as a function of  $\text{SiO}_2$  (Arculus, 2003) shows that the majority of the rocks belong to a low-Fe suite. Granitic rocks from the main mass of the batholith are compositionally distinct, plotting as a field shifted from the mafic rocks

from the Eastern satellite group, and showing compositional gaps compared to the leucogranites from the adjacent satellite bodies. The granitic rocks lie in the peraluminous to strongly peraluminous fields (alumina saturation index, ASI= molecular  $[Al_2O_3/K_2O+Na_2O+CaO]$ ), and show a wide range of ASI (1.08–1.37). Most have ASI values higher than 1.1 (Fig. 3). For the batholith as a whole, values of ASI do not increase consistently with silica content. The Southern and Central zones have generally higher values of  $Al/(Na+K)$  (~1.6–2.3) than the Northern zone, and Western and Northern satellites (1.2–1.8). Granitic rocks from the Eastern satellites are also more diverse and more aluminous (ASI ~1.46) than the main mass of the batholith. In contrast, mafic igneous rocks in the Eastern satellites are metaluminous  $[Al/(Ca+Na+K) \sim 0.7-0.9]$ .

Major element compositions are plotted against  $SiO_2$  in Figure 4. Variation diagrams illustrate inverse correlations of abundances of several oxides (e.g.,  $Fe_2O_3$ , MgO, CaO,  $TiO_2$ , and MnO) with increasing  $SiO_2$ . Figure 4 shows that the tonalitic to granitic rocks from the Southern, Central, and Northern zones span a wide range in  $SiO_2$  (57.31–72.02%), have high  $Al_2O_3$  (13.97–18.23%), low to moderate iron (total iron as  $Fe_2O_3$ : 0.79–7.57%), as well as  $TiO_2$  (0.20–0.94%),  $P_2O_5$  (0.13–0.25%), MgO (0.60–4.65%), and CaO (1.98–6.02%) contents (Table 1). These rocks also have generally high  $Na_2O$  (2.71–4.27%), and moderate  $K_2O$  (1.19–3.13%) so that the average value of  $Na_2O/K_2O$  is ~1.39 and  $Na_2O/(Na_2O+K_2O) > 0.5$ . Thus, the batholith is largely sodic and the Southern and Central zones constitute a compositional group, distinct from the Northern zone, which is grouped with the Northern and Western satellites. Plutonic rocks of the Northern ( $SiO_2$ : 70.89–75.75%), Eastern ( $SiO_2$ : 54.21–67.34%, one silicified sample at 80.41%, intruding the Kodiak Formation;  $SiO_2$ : 45.92–66.01%, intruding the Ghost Rocks Formation), and Western satellites ( $SiO_2$ : 68.05–69.16%) indicate compositional contrasts. The granitic satellite rocks have less  $TiO_2$ ,  $Fe_2O_3$ , MgO, and CaO, somewhat lower  $Al_2O_3$  and higher  $SiO_2$  and alkali element contents than granitic rocks from the Northern, Central, and Southern zones. In the Eastern satellite group, volumetrically minor quartz gabbro and diorite contain higher CaO and ferromagnesian elements than the batholith (Table 1).

### 5.2 Kodiak batholith: Minor and Trace Elements

Minor and trace element variations discussed below also show that granitic rocks from the Southern, Central, and Northern zones of the Kodiak batholith, as well as from the satellite groups, have overlapping trends. In some cases, the plutons from the Eastern satellites, and Northern satellites occupy distinct compositional fields (Fig. 5). Minor and trace element abundances plotted in multi-element (Fig. 6; primitive mantle-normalized, Sun and McDonough, 1989) and rare-earth element (REE) chondrite-normalized diagrams illustrate remarkable compositional homogeneity within each zone (Fig. 7), and especially in the granodiorites and tonalites of the Southern zone. The granitic rocks are enriched in large-ion lithophile elements (Ba, Rb, K, Cs, and Sr), other fluid-soluble elements (e.g., U, Pb, etc., Tatsumi et al., 1986) and light REEs (Fig. 6) compared to N-MORB. Such distinct trace element distributions result in high values of ratios involving the large-ion lithophile (LIL) elements relative to the high field strength elements (Nb, Ta, Zr, Hf, Ti) and Th (HFS). Commonly, these high values of LIL/HFS elements are taken as characteristic of volcanic arc signatures (Davidson, 1996).

The ferromagnesian elements (Sc, Cr, Co, Ni, and Zn) together with V and Ge generally decrease in abundance relative to  $\text{SiO}_2$ , consistent with compatible element behavior during evolution of the granitic magmas (Table 2; Fig. 5). Sc and V abundances are diagnostic, and the Southern and Central zones have higher abundances of these metals (Sc~12-25 ppm, V~51-139 ppm, respectively) than the Northern zone and Northern satellite group (~2-14 ppm, ~13-61 ppm) (Table 2). Evidence for significant hydrothermal alteration and sulfide mineral deposition associated with the granitic rocks has not been found. Most samples contain low abundances of Cu (up to ~50 ppm), Pb (up to ~40 ppm, one sample at ~70 ppm), Mo (up to ~6 ppm), Sn (up to ~5 ppm), and W (up to ~2 ppm). The batholith, moreover, is not enriched in Li, Be, B, and P, elements whose contents are known to be enhanced in rocks associated with granite-related mineralization.

For every zone in the batholith, the multielement diagrams show a relatively tight bundle of lines characterized by spiked patterns, small to large troughs for Th, large to moderate troughs for Nb and Ti,

and large spikes for Pb (Fig. 6). The positive Pb anomaly is somewhat larger in the leucogranites of the Northern zone. Also, although some scatter is evident for Ti, the heavy rare-earth elements and Y, the deepest troughs for these elements are in the Northern satellites (Fig. 6-7). Granitic rocks of the Western satellites resemble rocks of the Northern zone (Fig. 6). The Eastern satellite group shows no trend (Fig. 6).

The mantle-normalized diagrams for the granodioritic to tonalitic rocks show troughs for Nb and Ti that could be attributed to the effects of fractionation of titanomagnetite, ilmenite, and titanite during magma evolution and transport, or to the effects of such minerals remaining as residues after partial melting of the source rocks. Depletions and wide variations in the abundances of Nb, Ta and Th (2.98-9.58 ppm, 0.39-1.26 ppm, 1.23-8.12 ppm, respectively) are also key features of the Kodiak batholith that result in highly variable ratios of incompatible elements such as Nb/Ta = 2.59-19.21, Th/U = 0.38-4.16, and Th/Hf = 0.7-2.7 (Table 2). Such ratios, again, distinguish the different zones of the batholith, vary widely over very narrow ranges of silica or other indices of differentiation, and plot as broad bands instead of lines, even within individual zones. Notably, plots involving incompatible and compatible minor elements, for example, Th/Ta vs. TiO<sub>2</sub> (Fig. 8), highlight the zonal distinction within the batholith (Southern and Central zones as a group: Th/Ta = 5-14, TiO<sub>2</sub> = 0.5-0.9%; Northern zone: Th/Ta = 4-18, TiO<sub>2</sub> = 0.2-0.6%) and the broad variability within individual zones.

Small troughs for Rb, Sr, and P may also be evident in multielement plots of a few of the felsic rocks, and, these troughs likely reflect fractionation of feldspars and apatite. Generally, the troughs are deeper in the granodioritic and granitic rocks than in the tonalitic rocks (Fig. 6). The plots show moderate abundances for lithophile elements Rb, Sr and Ba (31-124 ppm, 35-261 ppm, 394-1100 ppm, respectively) and relatively enriched contents of Pb (2-72 ppm) in many granitic rocks. Moreover, abundances of Rb, Sr and Ba do not change methodically with increasing SiO<sub>2</sub> (Fig. 4) but show offsets and gaps separating the fields of granitic rocks of the combined Southern and Central zones (Rb = 41.3-92.8 ppm, Sr = 158.9-258.7 ppm, Rb/Sr ~0.2-0.6 at SiO<sub>2</sub> ~57-65%), from the Northern zone (Rb = 56.4-102.7 ppm, Sr = 159.7-261.5 ppm, Rb/Sr ~0.2-0.6, at SiO<sub>2</sub> ~ 64-72%) (Table 2). Granitic rocks from the

Northern and Western satellites are also distinct from the main mass, and in the case of the Northern satellites, they are characteristically enriched in Rb and depleted in Sr ( $Rb/Sr \sim 0.6-3.7$ , and  $SiO_2 \sim 74-76\%$ ).

Rare-earth element chondrite-normalized patterns show that as a group the Kodiak batholith is characterized by moderately steep light REEs and by gently sloping to flat heavy REEs (Fig. 7). Within individual zones in the batholith, REE patterns are generally coincident. Variations in the total abundance of REEs and silica uniquely distinguish the different zones (Southern and Central zones from the Northern zone). The most distinctive patterns are in the leucogranites from the Northern satellites which tend to have large negative Eu anomalies and are the most silicic (Fig. 7). The leucogranites also have generally lower total REE contents ( $\sim 30$  ppm) than the tonalitic and granitic rocks from the main zones of the batholith ( $\sim 50-150$  ppm). Quartz gabbro and diorite from the Eastern satellite group (intruding the Ghost Rocks Formation) have higher total REE ( $\sim 50-110$  ppm; Table 2; Fig. 7) abundances with increasing silica. Granitic rocks in this group, however, show no predictable trend. Values of  $Ce_N/Yb_N$  vary from  $\sim 5-10$  for the Southern and Central zones, and from  $\sim 7-11$  for the Northern zone. Most granitic rocks have small to moderate Eu negative anomalies ( $Eu/Eu^* \sim 0.45-1.0$ ) but a few have small positive Eu anomalies. The negative Eu anomalies are deeper ( $Eu/Eu^* \sim 0.15-0.40$ ) in the most felsic rocks from the Northern satellites, which also contain the lowest contents of Sr (and a narrow range of  $SiO_2 = 70.89-75.75\%$ ). Both features (Eu and Sr) are consistent with the effects of residual plagioclase. These felsic rocks are also characterized by lower abundances and flatter slopes of the light REEs and depletion in the heavy REEs compared to main batholith ( $Gd_N/Yb_N = 1.24-6.31$ ,  $Yb_N \sim 1-5$  in the satellite bodies, and  $Gd_N/Yb_N = 1.07-2.06$ ,  $Yb_N \sim 6-15$  in the main batholith zones). Granitic rocks of the Eastern satellite group in the Kodiak Formation have widely variable REE patterns, from flat (sample 01PH107B) to gently sloping (Fig. 7). These rocks also have moderate negative Eu anomalies and include a silica-rich sample with an U-shaped REE pattern associated with a moderate positive Eu anomaly (01PH107B). Granitic rocks from the Western satellite group overlap the compositions of tonalite and granodiorite in the main batholith (Fig. 7).

Trace element abundances of mafic and intermediate rocks of the Eastern satellite group (Table 2) scatter and cannot be used to precisely characterize this group (Fig. 4). Some samples are broadly enriched in Ba, Rb, Th, and K (fluid-mobile elements), have troughs for Nb, Sr, P and Ti, and spikes for Pb. Other samples, however, have deep Th and Nb troughs and small to moderate Pb and Sr spikes (Fig. 6). Samples with small troughs for Th, however, are also found. All these features suggest that various types of mantle were involved, including contributions from continental crustal sources as a result of sediment recycling in the source or contributions from crustal contamination. Gabbroic and dioritic rocks mostly have REE patterns with flat slopes at about ~20-40x chondrites for the light REEs, flat slopes for the heavy REEs, and small positive or negative Eu anomalies (Fig. 7). One sample of pillow basalt overlaps the other mafic rocks and has a distinctly negative Ce anomaly. None of the gabbros and quartz diorites, and few granodiorites of the Eastern satellite group show a reasonable match to the patterns of the granitic rocks in the main mass of the batholith (Fig. 7). Notably, all mafic rocks are quartz-bearing (sparse, resorbed quartz in the more mafic rocks), have elevated K<sub>2</sub>O contents, and differ from N- MORB (Table 2; Fig. 4). They show geochemical features like those of calc-alkaline tholeiitic rocks (e.g., enriched in the light REEs and other fluid-soluble elements, Nb troughs, etc). The mafic rocks also have moderate to low contents of Co (up to 22 ppm), Cr (up to 253 ppm), and Ni (up to 135 ppm) distinct from unevolved mafic rocks (Table 2). Gabbro and diorite of the Eastern satellites have values of diagnostic ratios (Nb/U~1.8-5.7, Ce/Pb = 0-30, Ba/Ta=1280-3368, and La/Th~2.6-12.9) that generally resemble mafic orogenic rocks (Nb/U=1-7, Ce/Pb = >10, Ba/Ta >450, La/Th=2-7; Gill, 1981; Hawkesworth et al., 1991). Low La/Yb values (~1.5-6.0), and elevated Th contents relative to Hf and Ta (Hf/Th= 1-10, Ta/Th= 0.1-0.2), again are akin to those from orogenic basaltic rocks.

### 5.3 Kodiak batholith: Nd, Sr, and Pb Isotopes

The Nd, Sr, and Pb isotopic compositions of representative samples are given in Table 5 and Fig. 9.  $\epsilon_{Nd}$  values calculated for 59 Ma (crystallization age) are plotted for all the zones in the batholith (Fig.

9A). The total range in  $\epsilon_{\text{Nd}}$  is -3.7 to +4.7 and in depleted-mantle model ages ( $T_{\text{DM}}$ ) from 517 Ma to 1110 Ma ( $T_{\text{DM}}$  ages calculated from LREE-enriched rocks with high  $^{147}\text{Sm}/^{144}\text{Nd} = 0.1117$  to  $0.2042$ ). The Northern, Central, and Southern zones in the batholith have ranges that overlap for  $\epsilon_{\text{Nd}}$ , but the lowest  $\epsilon_{\text{Nd}}$  value is in the Northern zone (-3.7) and the highest is in the Central zone (+4.7). Most  $\epsilon_{\text{Nd}}$  values in the Southern and Central zones are negative and all  $T_{\text{DM}}$  values in the batholith as a whole are older (Ayuso et al., 2005) than the crystallization age at ~59 Ma (Farris et al., 2006). From SW to NE within the main body of the batholith two general isotope groups can be discerned on the basis of values of  $\epsilon_{\text{Nd}}$  (Table 5). One group consists of most granitic rocks in the Southern and Central zones and is characterized by negative  $\epsilon_{\text{Nd}}$  values of -3.7 to -0.3 and  $T_{\text{DM}}$  ages ~ 838 Ma to 1011 Ma. Another group consists of other granitic rocks from the Central zone and Northern zone with higher  $\epsilon_{\text{Nd}}$  values of -0.4 to +4.7 and younger  $T_{\text{DM}}$  ages of ~ 450 Ma to 797 Ma. Granitic rocks from the Central zone appear to be transitional, intermediate between the Southern and Northern zones. Granitic plutons, diorite, and quartz gabbro from the Eastern satellite group have a wide range of  $\epsilon_{\text{Nd}}$  values of -2.7 to +6.4, and  $T_{\text{DM}}$  ages from 204 Ma to 2124 Ma.

Granitic rocks from the Southern, Central and Northern zones show ranges in initial  $^{87}\text{Sr}/^{86}\text{Sr}$  values from 0.703716 to 0.706358 (Fig. 9). Most values overlap those of granitic and mafic igneous rocks from the Eastern satellites, which have a range of initial  $^{87}\text{Sr}/^{86}\text{Sr}$  of 0.703457 to 0.706364. Initial  $^{87}\text{Sr}/^{86}\text{Sr}$  values of the Southern and Central zone intrusions tend to be slightly more radiogenic ( $^{87}\text{Sr}/^{86}\text{Sr} > 0.70426$ ) than the Northern zone ( $^{87}\text{Sr}/^{86}\text{Sr} < 0.70472$ ).  $^{87}\text{Sr}/^{86}\text{Sr}$  isotopic values of granitic rocks in the Kodiak-Shumagin shelf range widely, from ~0.70544-0.71500 (Hill et al., 1981). Our new data for the Kodiak batholith overlap the lower part of this range but extend to lower isotopic values.

Initial Pb isotopic values at 59 Ma are shown as histograms (Fig. 9) and standard  $^{207}\text{Pb}/^{204}\text{Pb}$  and  $^{208}\text{Pb}/^{204}\text{Pb}$  plotted against  $^{206}\text{Pb}/^{204}\text{Pb}$  (Fig. 10). Granitic rocks within the main mass of the batholith and from the Northern satellites show a range of  $^{206}\text{Pb}/^{204}\text{Pb}$  of 18.850-18.960,  $^{207}\text{Pb}/^{204}\text{Pb}$  of 15.575-15.694, and  $^{208}\text{Pb}/^{204}\text{Pb}$  of 38.350-39.039. Values for these rocks mostly overlap those of granitic rocks and

gabbro from the Eastern satellites, which have a range of  $^{206}\text{Pb}/^{204}\text{Pb}$  of 18.854-19.054,  $^{207}\text{Pb}/^{204}\text{Pb}$  of 15.543-15.587, and  $^{208}\text{Pb}/^{204}\text{Pb}$  of 38.322-38.610. In a transect from SW to NE along the axis of the batholith, the  $^{206}\text{Pb}/^{204}\text{Pb}$  values of the Southern and Central zones overlap and tend to be slightly more radiogenic ( $^{206}\text{Pb}/^{204}\text{Pb} > \sim 18.9$ ) than the values of the Northern zone and Northern satellites ( $^{206}\text{Pb}/^{204}\text{Pb} < \sim 18.9$ ). The  $^{207}\text{Pb}/^{204}\text{Pb}$  and  $^{208}\text{Pb}/^{204}\text{Pb}$  values are about the same for all the granitic rocks regardless of their zone. As in the case of the  $\epsilon_{\text{Nd}}$  values, granitic rocks of the Eastern satellites plot within the fields of the Southern and Central zones (Fig. 10).

#### 5.4 Geochemistry of Country rocks: Kodiak Formation and Ghost Rocks Formation

Major and trace element analyses of the Kodiak Formation, an inclusion of Kodiak Formation in granite of the Central zone, and the Ghost Rocks Formation are given in Tables 3 and 4. Compositional variations of the Kodiak Formation resemble those in orogenic rocks and show small to moderate ranges for  $\text{SiO}_2$  (~61.7-63.8%),  $\text{Al}_2\text{O}_3$  (~14.3-17.7%),  $\text{Fe}_2\text{O}_3$  (~6.4-7.3%),  $\text{MgO}$  (~1.9-2.6%),  $\text{CaO}$  (~1.1-1.9%),  $\text{Na}_2\text{O}$  (~1.9-2.6%),  $\text{K}_2\text{O}$  (~2.1-3.0%), and  $\text{TiO}_2$  (~0.8-0.9%). A country rock xenolith of Kodiak Formation falls in this range and lies in the field of the granitic rocks from the Central zone. The major element abundances of the Kodiak Formation and the xenolith broadly resemble the Kodiak batholith, although the flysch is generally higher in  $\text{Fe}_2\text{O}_3$  and lower in  $\text{CaO}$  and  $\text{Na}_2\text{O}$ . More importantly, all ASI values of the Kodiak Formation (1.60-1.84, one sample at 2.22) are also significantly higher than the Kodiak batholith (1.08-1.37). None of the metasediment samples overlap the granitic rocks. The only exception is the ASI value for the xenolith of Kodiak Formation. On multielement and rare earth element plots (Fig. 6, 7), the Kodiak Formation generally overlaps the batholith and shows coincidence in some trace element compositions with the granitic rocks, including the characteristic Nb and Ti troughs and the large Pb spike.

The Kodiak Formation shows a range of  $^{206}\text{Pb}/^{204}\text{Pb}$  of 18.978-19.057,  $^{207}\text{Pb}/^{204}\text{Pb}$  of 15.567-15.588, and  $^{208}\text{Pb}/^{204}\text{Pb}$  of 38.484-38.725 (Fig. 9). These values mostly overlap those of the Kodiak batholith (Fig. 10).  $\epsilon_{\text{Nd}}$  values of the Kodiak Formation range from about -6.7 to -1.5 at 59 Ma and

overlap the least evolved values of the Kodiak batholith ( $\epsilon_{Nd} = -3.7$  to  $+4.7$ ) (Fig. 9). The new data for the Kodiak Formation also extend to significantly more negative values than previous data for volcanoclastic sandstones and quartzose sandstones on Kodiak Island,  $\epsilon_{Nd}$  about  $-2$  to  $+5$  (Sample and Reid, 2003). One group of granitic rocks in the Kodiak batholith has  $\epsilon_{Nd}$  values ( $-3.7$  to  $-0.3$ ) that coincide with the volcanoclastic sandstones ( $-2$  to  $0$ ), and another group has  $\epsilon_{Nd}$  values ( $-0.4$  to  $+4.7$ ) that are significantly more juvenile ( $\epsilon_{Nd(t)} > 0$ ) and that overlap the quartzose sandstones ( $+2$  to  $+5$ ). Initial  $^{87}Sr/^{86}Sr$  values of the Kodiak Formation ( $0.705715$  to  $0.707118$ ) resemble the Kodiak batholith ( $0.703716$  to  $0.706358$ ) (Fig. 9, 11), and are less radiogenic than previously reported values for argillite and greywacke of the Kodiak Formation ( $0.70738$  to  $0.71088$ , Hill et al., 1983).

Sandstone- and argillite-rich sedimentary units of the Ghost Rocks Formation are different than the Kodiak Formation because they are higher in  $Fe_2O_3$  and  $MgO$ , and lower in  $CaO$  (Fig. 4; Table 3). Moreover, the Ghost Rocks Formation has considerably higher values of ASI ( $2.15$ - $2.21$ ) than most samples of the Kodiak Formation (ASI =  $1.60$ - $1.84$ , one sample at  $2.22$ ), and particularly higher than the Kodiak batholith (ASI =  $1.08$ - $1.37$ ) (Fig. 3). On multielement (Fig. 6) and REE plots (Fig. 7), the Ghost Rocks Formation overlaps the Kodiak Formation and Kodiak batholith. The Ghost Rocks Formation has values of  $^{206}Pb/^{204}Pb$  of  $19.029$ - $19.165$ ,  $^{207}Pb/^{204}Pb$  of  $15.588$ - $15.640$ , and  $^{208}Pb/^{204}Pb$  of  $38.636$ - $38.814$ , in the range of the Kodiak Formation (Fig. 9, 10).  $\epsilon_{Nd}$  values range from about  $-2.4$  to  $-1.2$  at  $59$  Ma, and initial  $^{87}Sr/^{86}Sr$  values from  $0.706593$  to  $0.706803$  (Fig. 11). These isotope values overlap the Kodiak Formation ( $\epsilon_{Nd} = -6.7$  to  $-1.5$ ;  $^{87}Sr/^{86}Sr = 0.705715$  to  $0.707118$ ) and the Kodiak batholith ( $\epsilon_{Nd} = -3.7$  to  $+4.7$ ;  $^{87}Sr/^{86}Sr = 0.703716$  to  $0.706358$ ). Overlap in  $T_{DM}$  values also characterize the Ghost Rocks Formation ( $959$  to  $1062$  Ma), Kodiak Formation ( $981$  to  $1489$  Ma), and the Kodiak batholith ( $517$  to  $1110$  Ma).

## 6. Discussion: Source and Origin of the Kodiak Batholith

### 6. 1 General Statement

The scale and extent of the Kodiak batholith, coupled with the distribution of satellite plutons of similar age and composition intruded southwest and northeast of Kodiak Island, suggest a magmatic event of considerable magnitude related to offscraping and underplating of the Chugach accretionary prism. Precise identification of the heat source required for melting cold, deep-water turbidites akin to the Kodiak Formation in the Chugach accretionary prism is an important feature bearing on the origin of the granitic rocks. A wide variety of heat sources in the forearc environment have been proposed: 1) basalt leaking from transform faults during subduction (Tysdal et al., 1977; Barker et al., 1992), 2) underthrusting of a ridge-trench-trench triple junction of oceanic plates under the accretionary prism (Marshak and Karig, 1977), 3) subduction of the Kula-Farallon ridge under the accretionary prism (Byrne, 1979), 4) thermal surge from the subducting plate (Hudson et al., 1979), 5) conduction of heat and advection of fluids from the hot, young subducting slab (Sisson et al., 1989), and heating in the forearc environment resulting in combinations of MORB-type mafic rocks associated with peraluminous felsic rocks (e.g., Groome et al., 2003), 6) upwelling of hot asthenosphere associated with decompressive melting and generation of MORB-like melts that pond under, and intrude, the forearc (“blow-torch effect” of DeLong et al., 1979; Plafker et al., 1989), and 7) intersection of the northern trench-ridge-trench triple junction of the Resurrection plate (Haeussler et al., 2003b; Bradley et al., 2003). Our favored interpretation for forming the Sanak-Baranof near-trench intrusives generated from 61 to 50 Ma, including the Kodiak batholith at about 58 Ma is a heat source(s) in the forearc environment generated by the intersection of the triple junction of the Resurrection plate. This forms the basis for our proposed model.

Physical interaction between basaltic magmas and flysch in some regions of the accretionary prism is well established (e.g., Hudson, 1994; Barker et al., 1992; Lytwyn et al., 2000; Kusky et al., 2003; Sisson et al., 2003a, b), but determining the relative chemical contributions of contemporaneous or older mantle-derived rocks to the magmatic source of the granitic rocks has been difficult. The role attributed

to mafic magmas varies widely. For example, ~10% of the Cordova granodiorites in the eastern Gulf of Alaska (Prince William Sound) may reflect mantle-derived contributions (Barker et al., 1992; Farmer et al., 1993), but a tonalite-trondhjemite suite in the eastern Chugach Mountains requires involvement of > 75% mantle-derived material (Sisson et al., 2003b, Harris et al., 1996).

In the Shumagin and Sanak Islands in the Kodiak-Shumagin shelf, southwest of Kodiak Island, Hill et al. (1981) and Hill and Morris (1982) considered MORB-like magmas to have been the most likely heat and mass source of granitic plutons on the basis of geochemical and isotopic data ( $^{87}\text{Sr}/^{86}\text{Sr}$  and  $\delta^{18}\text{O}$ ). In this interpretation, the granitic intrusives were derived from a MORB-type magma that rose through the accretionary prism and assimilated partial melts of the quartzofeldspathic and pelitic flyschoid source (greywacke of the Shumagin Formation, which is considered correlative to the Kodiak Formation).

On Kodiak Island, voluminous and cogenetic mafic rocks associated with the main mass of the Kodiak batholith are not known. In the Ghost Rocks Formation, adjacent to the batholith, Moore et al. (1983) described small mafic bodies associated with granitic plutons that in our subsequent work were assigned to the Eastern satellite group of the Kodiak batholith. Trace element signatures of these mafic rocks were summarized in the preceding section and show volcanic arc signatures. The rocks have high values of LIL/HFS ratios and enrichment in fluid-soluble elements characteristic of a mantle-wedge source (Elliott, 2003). We take the chemical features as consistent with the suggestion that calc-alkaline rocks on Kodiak Island reflect subduction under southern Alaska (Haeussler et al., 1995; 2003b), and that compositionally similar rocks likely underplated the prism shortly before the generation of the Kodiak batholith. Farris et al. (2006) demonstrated an internally consistent southwest to northeast trend toward younger crystallization ages along the axis of the batholith. The age trend was attributed to the effects of ridge subduction. In the following section, we similarly invoke thermal input to the forearc a result of the intersection of the northern trench-ridge-trench triple junction of the Resurrection plate in southern Alaska, and assess the extent of chemical contributions of such a thermal source to explain the compositional features of the Kodiak batholith.

## 6. 2 *Crustal and Mantle-derived Magmatic Sources of the Kodiak Batholith*

Buoyant tonalitic to granodioritic melts derived from thermal erosion of slab window margins have been linked to shallow melting of young subducted igneous oceanic crust (Thorkelson and Breitsprecher, 2005). The melts have been proposed to rise from their shallow melting site (~5 km?) and leave a residue of garnet-free amphibolite to pyroxenite (Thorkelson, 1996). In this view, mafic magmas produced as a result of decompression melting of asthenospheric mantle upwell into the opening gap during ridge subduction and are progressively replaced by other mantle sources. As a slab window is transported deeper into the mantle, calc-alkaline volcanism typical of an orogenic margin is replaced by tholeiitic to alkalic volcanism. Accordingly, the forearc crust may enclose both MORB-type mafic and peraluminous intermediate to felsic magmas, a magmatic association that would differ from the typical combination of calc-alkaline basalts and metaluminous granitic rocks in orogenic margins (Thorkelson and Breitsprecher, 2005).

Young lithospheric mantle beneath newly-created crust (possibly underlying the accretionary prism) is likely to be compositionally highly variable, in contrast to old lithospheric mantle (Zartman et al., 1991). Also, the composition of the shallow asthenospheric mantle in continental margins has been difficult to constrain, but studies focused on Neogene slab-window rocks from British Columbia to Baja California suggest that shallow asthenospheric mantle resembles rocks derived from E-MORB-type sources (Thorkelson and Taylor, 1989; Luhr et al., 1995; Gorrington and Kay, 2001, and references therein).

The Kodiak batholith probably accounts for less than 10% of the exposed area on Kodiak Island, but the granitic rocks are of sufficiently large volume (~2500 km<sup>3</sup>) to suggest that the magmas were derived from a sizeable source region, perhaps in the order of a cube ~15 km on a side (assuming partial melting of ~50%). Assuming that such a large source region is implicated by the partial melting events, it is reasonable to speculate that Kodiak batholith genesis involved protoliths that had both continental and mantle origins. In the discussion that follows we highlight problems distinguishing which geochemical signatures are derived from contemporaneous or from older mantle-derived rocks, which of the sources

known to be associated with subduction zones (e.g., depleted mantle wedge, subducted sediment, and altered mafic oceanic crust) may have been involved, and to what extent such sources included in the accretionary prism contributed to the granitic magmas. Within the accretionary prism, potential sources of the granitic rocks are: (1) previously generated or contemporaneous mantle-derived MORB-type magmas from ridge subduction that ponded at the bottom of or intruded into the turbidite fan, (2) calc-alkaline magmas derived from metasomatized mantle-wedge (originally represented by depleted upper mantle, Elliott, 2003) and from melting and devolatilization of subducted oceanic crust (altered MORB and oceanic sediments) that accreted or were injected into the accretionary prism, and (3) compositionally diverse flysch and various other older igneous rocks in the accretionary prism.

Recognizing diagnostic contributions from each of these sources in the granitic rocks on Kodiak Island is a challenging undertaking, especially because several potential sources may have been involved, and because the original chemical signatures of the mafic and felsic rocks could have been drastically modified by fractional crystallization and assimilation fractional crystallization reactions during emplacement. In the next section, we assess to what extent the observed compositional variations in the batholith have been affected by emplacement processes before evaluating the contributions of mantle-versus crustally-derived source rocks.

### *6.3 Chemical Variations within the Batholith*

The oxide and trace element abundances of the Kodiak batholith are generally characterized by a lack of orderly chemical variations as a function of  $\text{SiO}_2$ , Rb/Sr,  $\text{Na}_2\text{O}/\text{K}_2\text{O}$ , ASI, light REE or any other index of fractionation within each zone, and from zone to zone within the batholith. Certain geochemical features in the granitic rocks (e.g., negative anomalies for Eu, Sr, and Ti), however, suggest that fractional crystallization (FC) or assimilation and fractional crystallization reactions (AFC) may have affected the rocks.

For the purposes of illustration, we tested various residual assemblages and illustrate one that best fits the compositional variations of the granitic rocks in the Southern and Central zones (Fig. 12). The

assemblage is dominated by plagioclase and clinopyroxene, and includes a limited contribution of hornblende (although hornblende was not observed at this level of intrusion). This assessment is a first step in establishing the processes that affected the evolution of the granitic rocks because many of the detailed geological variables, such as the nature and proportions of the residual mineral assemblage, are imperfectly known. Fractional crystallization (FC, Rayleigh fractionation or crystal surface-liquid equilibrium model, Hanson 1978) and assimilation-fractional crystallization (AFC, DePaolo, 1981) paths are summarized in Fig. 12 using elements having contrasting degrees of compatibility (e.g., Sc, K<sub>2</sub>O, and Th). Partition coefficients were taken from compilations (Arth, 1976; Hanson, 1978; Henderson, 1986). Bulk distribution coefficients calculated for fractionating assemblages that approximate the chemical variations in the batholith for the Southern zone and Central zone, and for the Northern zone, respectively: Sc (1.5; 2.55), K<sub>2</sub>O (0.16; 0.16), Rb (0.2; 0.4), Th (0.17; 0.17), Ta (0.1; 0.1), Ce (0.7; 0.01). Fractional crystallization (FC) and assimilation-fractional crystallization (AFC) paths assume that parental compositions are represented by 01PH-116A for the Southern and Central zones and RAAK-41 for the Northern zone (starting compositions from each zone are represented by rocks with the lowest SiO<sub>2</sub> contents). The assimilant is the Kodiak Formation, sample RAAK-34. The ratio of mass of assimilant/mass fractionated ( $r$ ) is 0.35 in the Southern and Central zones and 0.10 in the Northern zone. Rock compositions from the Southern and Central zones show no optimal fits, but generally point to a crystallizing residual assemblage consisting of plagioclase (~50-57%) and clinopyroxene (~35-40%) along with some hornblende (up to 2%?). For the Northern zone, the assemblage consists of plagioclase (~40-45%), K-feldspar (~12-15.1%), hornblende (~25-30.0%), biotite (~5-9.2%), and trace amounts of accessory minerals (allanite ~ 0.2%; zircon ~ 0.1%; and sphene ~0.1%) (Figs. 12A, B).

The fractional crystallization trend fails to systematically connect the compositions of all the granitic rocks. The discrepancies may reflect uncertainties in geological variables such as choice of starting compositions, or selection of distribution coefficients that may not reflect magmatic evolution during melting and transport to the upper crust (Fig. 12A, 12B). In contrast to the Southern and Central zones, the Northern zone shows fractional crystallization trends that could reflect a residual assemblage

composed of plagioclase, K-feldspar, biotite, and perhaps include a contribution of hornblende, as well as trace amounts of allanite, zircon, and sphene. This mineral assemblage would broadly link the compositions (for Sc and K<sub>2</sub>O, but not for Sc and Th) in the Northern zone and Northern satellites and requires about 50% crystallization by weight for the Northern zone, and ~80% for the Northern satellites (Fig. 12). The REE patterns preclude the presence of significant amounts of garnet in the residue. In addition, our results suggest that there is no unique mineral assemblage capable of linking all the granitic rocks for the batholith as a whole.

The differences among the zones, however, could be the result of combined effects of assimilation and fractional crystallization reactions (AFC; DePaolo, 1981) involving the Kodiak Formation. The impact of such AFC reactions can be illustrated by assuming that selected samples represent compositions of end-member components (Fig. 12). The residual assemblage used in the calculation was the same as that applied in our fractional crystallization model. At low to moderate ratios of mass assimilated to mass fractionated ( $r < 0.35$ ), as expected from the high level of intrusion of the composite batholith, the compositional paths for FC and AFC do not differ greatly. AFC paths that cover the entire range of compositions in the Southern and Central zones as a group ( $r \sim 0.35$ , fraction crystallized  $F \sim 10-50\%$ ), and for the Northern zone can be devised ( $r \sim 0.10$ ,  $F \sim 20-50\%$ ). Compositional offsets and diverging trends of the granitic rocks, however, again argue that the variations for the batholith as a whole cannot be the result of AFC reactions involving this single continental crustal contaminant or a simple mineral assemblage. We concede that other rocks deeper in the crust could have been more important contaminants and could have compositions that would make the AFC curves link the zones within the batholith more exactly. It is also possible that the batholith was affected by varying degrees of fragmentation and assimilation, as suggested by petrographic variations, depending on whether the host granitic magmas are in the main mass of the batholith or in the flanking belts. Petrographic observations, for example, show that the batholith locally has abundant xenoliths armored by narrow reaction rims, as well as quartz-rich pods and biotite (plus aluminosilicate and garnet) clusters (Ayuso et al., 2005). Some of these areas indicate that  $>50\%$  of the mode is derived from mechanical

disaggregation of xenocrysts, and is thus locally consistent with an enhanced degree of reaction between the granitic magma and the Kodiak Formation. Moreover, recent studies of fractal fragmentation of xenoliths together with a survey of oxygen isotopic variations in plutons of the Eastern satellite belt, and in parts of the main mass of the batholith, also suggest that assimilation was an important local process (Farris and Paterson, 2007; Tangalos et al., 2003). We think, however, that the extent and effects involving major and trace elements and radiogenic isotopes compositions between the magmas and country rocks were locally controlled, and not extensive enough to account for the batholith as a whole.

We conclude that the absence of a continuum of rock compositions linking all the batholith zones and adjacent granitic and mafic satellite groups indicates that granitic rocks on Kodiak Island formed from distinct magmas. These magmas were unlikely to be mutually related simply by *in situ* FC (or AFC) during transport from their heterogeneous source region at the bottom of the accretionary prism and during emplacement higher in the continental crust. Also, plots involving compatible element variations in the mafic to granitic rocks scatter and do not produce mixing lines indicative of simple mixing of felsic melts and contemporaneous mafic mantle-derived magmas, making simple two-component mixing unlikely. All of these processes would have produced coherent elemental trends linking cogenetic rocks, as well as trace element ratios correlated with isotopic values of Pb, Sr, and  $\epsilon_{Nd}$ . Offsets, compositional gaps, and the heterogeneity in isotopic compositions in the Kodiak batholith can thus be taken as evidence that the batholith and its satellites did not evolve from a common, more mafic parent.

#### 6.4 Mantle and Crustal Contributions

Granitic rocks of the Kodiak batholith display an orogenic signature that is reflected in spidergram patterns with large negative spikes at Nb (and Th?), positive spikes at Pb, and  $T_{DM}$  ages older than 59 Ma (Figs. 6, 9). The near-chondritic values of many samples ( $\epsilon_{Nd} \sim 0$ ), and especially, the positive values in the main mass of the batholith (most samples have  $\epsilon_{Nd} = -3.7$  to  $+2.4$ , one sample at  $+4.7$ ) and even higher values in the Eastern satellites ( $\epsilon_{Nd} = +4.2$ , one silica-rich sample at  $+6.4$ ), closely link the

granite source region on Kodiak Island to rocks with volcanic arc compositions. The  $^{87}\text{Sr}/^{86}\text{Sr}$  values of granitic rocks in the main mass of the batholith ( $^{87}\text{Sr}/^{86}\text{Sr} = 0.704705\text{-}0.706923$ ) are also consistent with an orogenic arc setting in which mafic magmas were derived from depleted mantle (MORB) that had previously reacted with anatectic melts from the continental crust (hybridization), or alternatively, originated as melts from the mantle wedge overlying a subduction zone enriched in fluid-soluble elements and silica-rich fluids (Ba, Rb, K, Cs, Sr, Pb, Th, La, etc.) from sediment dehydration and fluid enrichment (Hawkesworth et al., 1991) during subduction (e.g., Bebout, 1996; Ryan et al., 1996).

Although the ultimate origin of components that produced the observed elemental and isotopic variations is difficult to establish, isotopic trends are consistent with mixing of source rocks originally derived from the mantle wedge (MORB-type basalt enriched by fluid-soluble elements) as one compositional end-member, together with melts and fluids derived from flysch (Fig. 13). The isotopic variations of the Kodiak batholith are thus intermediate between the mantle wedge source that was enriched by fluids ( $^{87}\text{Sr}/^{86}\text{Sr} < 0.7030$ ;  $\epsilon_{\text{Nd}} \sim +9$ ;  $^{206}\text{Pb}/^{204}\text{Pb} < 18.8$ ), and fluids and/or melts from flysch ( $^{87}\text{Sr}/^{86}\text{Sr} > 0.7065$ ;  $\epsilon_{\text{Nd}} \sim -4$ ;  $^{206}\text{Pb}/^{204}\text{Pb} > 19$ ) of the Kodiak Formation. The overall homogeneity of the Pb isotopes indicates that all of the Kodiak batholith rocks had a mantle end member plus a flysch end member. A rough estimate of the isotopic contribution of a mantle-derived end member can also be obtained by assuming a starting composition. For example, granitic samples suggest that at least 40%, and for many samples up to 80%, of the Nd isotopic variations reflect a mantle-type component. Samples having higher mantle contributions also have the youngest  $T_{\text{DM}}$  ages and high values of  $\epsilon_{\text{Nd}}$ . The balance of the Nd isotopic variation is derived from a recently recycled crustal component represented by the Kodiak Formation, which has the oldest  $T_{\text{DM}}$  ages and lowest values of  $\epsilon_{\text{Nd}}$ .

The batholith does not owe its origin to direct melting of MORB or simple fractional crystallization of such mafic magmas. Most major and trace element ratios (LILE/HFS) that are predicted to correlate with  $\epsilon_{\text{Nd}}$ , Pb, or Sr isotope compositions generated by subduction are generally decoupled. A few exceptions are notable, for example, Cs/Ta ratios show moderate positive correlations with isotopic

systems within the batholith zones (higher Cs/Ta and  $^{206}\text{Pb}/^{204}\text{Pb}$ ) (Fig. 13). Generally, the Northern zone is isotopically unique (e.g., lower  $^{206}\text{Pb}/^{204}\text{Pb}$  and  $\epsilon_{\text{Nd}}$  as low as -3.7) (Fig. 10). In addition, a plot of Nb/U versus Ce/Pb (Klein, 2003) shows all samples of the Kodiak batholith and flanking igneous groups intermediate between a predominant calc-alkaline end-member (having low values of Nb/U and Ce/Pb, similar to volcanic arc lavas) and a minor contribution from an altered oceanic crust end-member (having low values of Nb/U but high values of Ce/Pb) (Fig. 8). A contribution of altered oceanic crust as a component in the source of the granitic magmas is consistent with the interpretation of Thorkelson and Breitsprecher (2005) who described the nature of melts derived from thermal erosion of margins of slab windows. The transitional range of trace element compositions of the granitic rocks, however, indicates they are not simply direct melts of altered oceanic crust but likely include considerable recycled material, possibly as old as ~1 Ga to 1.5 Ga (based on an estimate of the average crustal residence or  $T_{\text{DM}}$  age of the Kodiak Formation sources). No clear evidence exists for direct chemical contributions from a depleted mantle reservoir (MORB), likely to represent ridge magma and invoked here as a possible heat source under the prism. Such MORB-like magmas would be expected to show trace element and isotope features intermediate between a depleted mantle source (e.g., high values of Nb/U and volcanic arc lavas with low values of Nb/U) (Fig. 8). Ratios of Ba/Th and La/ $\text{Sm}_{\text{N}}$  (Elliott, 2003) that characterize the mafic rocks on Kodiak Island (Eastern sateelite group) overlap the field of volcanic arc rocks and plot between contributions from altered mafic oceanic crust and sediment (Table 2). The calc-alkalic nature of the mafic rocks resembles island-arc tholeiitic basalt found at shallow depths of the Wadati-Benioff zone (e.g., Japan, Kuno, 1966) and resembles standard sources of continental arcs that include MORB and sediments (subducted oceanic crust), the mantle wedge, and the continental crust (Kay, 1978, 1980).

Pb isotopic values of the Kodiak batholith fall to the right of both the geochron and average Pb evolution curve (orogene,  $\mu = 9.74$ ; Zartman and Doe, 1981), at relatively higher ratios of  $^{206}\text{Pb}/^{204}\text{Pb}$  for a given value of  $^{207}\text{Pb}/^{204}\text{Pb}$  (Fig. 10). Most granitic rocks ( $\mu = 9.44$ – $9.71$ , one sample at 9.97) thus show lower values of  $\mu$  than the orogene model curve, consistent with Pb isotope ratios characteristic of

immature island arcs and active continental margins, as well as sub-continental lithospheric mantle that has been previously enriched by subduction (e.g., Zartman et al., 1991). The relatively radiogenic  $^{206}\text{Pb}/^{204}\text{Pb}$  values of the granitic rocks, for a given  $^{207}\text{Pb}/^{204}\text{Pb}$  value, imply that the time-integrated average composition of the source has evolved since at least ~1-1.5 Ga with U/Pb ratios consistently lower (more mantle-like) than the average continental crust. The  $^{207}\text{Pb}/^{204}\text{Pb}$  values of the granitic rocks, however, also extend toward more radiogenic compositions than island arc lavas, falling in fields along broad and steep slopes when compared to the  $^{206}\text{Pb}/^{204}\text{Pb}$  ratios. The fields are intermediate between depleted mantle-derived basalts (e.g., N-MORB and EMII of Zindler and Hart, 1986) and terrigenous sediments. This feature is consistent with the occurrence of kyanite, biotite (containing fibrolite? remnants), garnet, and muscovite in the granitic rocks and supports the idea that continental crustal rocks were also involved with the genesis of the Kodiak batholith if these minerals represent equilibrium residua produced during the generation of the primary peraluminous melts. However, the mineral clusters show no conclusive petrographic evidence for melting and there is no geochemical evidence that they represent refractory restitic material (see for example review by Clarke, 1981). Instead, at this time, we favor the idea that the mineral clusters are likely remnants of wall rock xenoliths mechanically dispersed during transport of the granitic magmas through the middle continental crust (~6 kb; Richardson et al., 1969). Values of  $^{207}\text{Pb}/^{204}\text{Pb}$  for the mafic rocks that are higher than typical MORB-derived rocks, together with small to moderate Pb and Sr spikes in spidergrams highlight the contributions of recycled continental crust in the accretionary prism (terrigenous or continental sediments in the flysch) that evolved at high U/Pb ratios (higher than the mantle model curve at  $\mu = \sim 9.5$ ). The steep slope of the Pb isotopic variations thus reflects source mixing and cannot be used to estimate the timing of the recycling event.

The foregoing geochemical data support a model for the genesis of the Kodiak batholith from partial melting of a mixed source consisting of diverse lithologic units. Mixing in the source region of the granitic magmas helps to explain the lack of covariations of major and trace element abundances and isotope compositions. Also, partial melting of a mixed source is consistent with decoupling of elemental

abundances and ratios of the LILE/HFS from the isotope signatures and can be explained if the zonal compositional differences within the batholith reflect the influx of different melts and the effects of mixing isotopically different magma sources.

### *6.5 Melting in the Accretionary Prism*

Next we will explore the notion that the granitic magmas owe their genesis to melting of a heterogeneous source that included flysch and amphibolites. Major-element compositions of melts produced by dehydration melting of felsic pelites, metagreywackes, and amphibolites (Fig. 3, 4) have been reported by Patino Douce (1999). The major element abundances of the Kodiak batholith overlap the fields for dehydration melting of amphibolites and metagreywackes (Fig. 3), and as suggested above, may be considered to represent melts from the bottom of the accretionary prism. A small volume of leucogranites in the Northern satellite bodies overlaps the compositions attributed to melts derived from felsic pelites. In contrast, the mafic and intermediate igneous rocks in the Ghost Rocks Formation do not consistently plot in a unique field. In addition, the Kodiak Formation and the Ghost Rocks Formation do not plot always in any one field as defined by Patino Douce (1999) or exactly match the compositions of large portions of the Kodiak batholith.

### *6.6 Flysch Melting*

The thick and rapidly deposited turbidite sequence of the Kodiak Formation is reported by Sample and Reid (2003) to be a voluminous turbidite fan derived from recycled orogen (volcaniclastic sandstones) with a marked Proterozoic contribution. The fan also includes input (quartzose sandstones) from a continental margin volcanic arc. The Kodiak Formation adjacent to the batholith is not enriched in  $\text{Al}_2\text{O}_3$  (14.3-17.7%) or depleted in the alkali elements (total  $\text{Na}_2\text{O}+\text{K}_2\text{O}$ : 4.4-4.7%). The flysch compositions fall within the range of the Paleocene Orca Group (largely quartzofeldspathic turbidites, Dumoulin, 1988), which is also thought to represent deposits derived from a magmatic arc developed near a continental margin (Winkler, 1976; Plafker et al., 1989). However, comparison of the average

compositions of the Kodiak Formation and the Orca Group flysch shows that they are not exact analogues. For example, they are similar for SiO<sub>2</sub> (Kodiak Formation: ~63.8%, Orca Group: 67.6%), Al<sub>2</sub>O<sub>3</sub> (~15.9%, and 16.0%, respectively), MgO (~2.4%, and 2.4%), and K<sub>2</sub>O (~2.6%, and 2.3%), but the Kodiak Formation is higher in FeO<sub>total</sub> (~6.2%, and 4.2%), and lower in CaO (~1.4%, and 2.0%), and Na<sub>2</sub>O (~2.2%, and 3.1%)

The general coincidence of the major and trace element data and the overlap in  $\epsilon_{Nd}$ , Sr and Pb isotopic values of the Kodiak batholith with those of metasediments representing the Chugach accretionary prism, however, may be used as evidence that the batholith was derived by partial melting of metasedimentary rocks that generally resemble the Kodiak Formation. For example, the Kodiak Formation ( $\epsilon_{Nd} = -6.7$  to  $-1.5$ ) is broadly similar to argillite ( $\epsilon_{Nd} = -3.8$  to  $-0.6$ ) and greywacke ( $\epsilon_{Nd} = -3.3$  to  $-2.0$ ) in the Orca Group, as well as phyllite and metagreywacke ( $\epsilon_{Nd} = -3.3$  to  $-2.3$ ) in the Valdez Group from the eastern Gulf of Alaska. Also, nearly the same range of  $T_{DM}$  values (0.84 to 1.01 Ga) characterizes the Kodiak batholith, quartzose sandstones of the Kodiak Formation, and flysch from eastern Gulf of Alaska. The Kodiak Formation has  $^{87}Sr/^{86}Sr$  values (0.705715 to 0.707118) that resemble the Orca and Valdez Groups (0.70602 to 0.70684, one sample at 0.70804). The Pb isotopic compositions, moreover, show convergence between the batholith and the Kodiak Formation (Fig. 10). There is no consensus on the source terrane for the Kodiak Formation, but, taken as a group, isotope signatures of the flysch closely resemble the composition of the Coast Plutonic Complex, the orogenic belt along the Coast Mountains of British Columbia and southeastern Alaska (Farmer et al., 1993; Sample and Reid, 2003). The Complex possibly corresponds to a Phanerozoic continental margin volcanic arc source and represents the best candidate for the recycled material in the accretionary flysch. In this case, the Chugach flysch may have been deposited and accreted south of its current latitude (Sample and Reid, 2003).

Considering the overall compositional correspondence between the Orca Group and the Kodiak Formation, the impact of a melting process affecting the flysch of the western Gulf of Alaska can be evaluated by comparison to experimental melts of greywacke and dacite (Conrad et al., 1988). Such a

comparison shows the following: (1) No exact match exists between the experimental greywacke and dacite melts and the average compositions of the Kodiak batholith. Comparison to other recent experimental melting studies of greywacke (e.g., Stevens et al., 1997) also show large compositional divergence compared to the batholith. (2) Greywacke glass (623B,  $X_{\text{H}_2\text{O}} = 0.25$ , 925°C) is generally a good match, except that  $\text{FeO}_{\text{total}}$ , MgO and  $\text{K}_2\text{O}$  abundances are higher in the granitic rocks. Plagioclase, orthopyroxene, ilmenite and a trace of garnet make up the residue ( $\pm$  quartz) for many of the runs done at 10 kbars. Notably, the estimated pressure at the bottom of the prism in the western Gulf of Alaska, however, is from at least 4 kbar to about 7-8 kbar (Sample and Reid, 2003), lower than the 10 kbar experimental conditions. More importantly, results of unpublished experimental work at 3-5 kbar have plagioclase, orthopyroxene, and ilmenite ( $\pm$  quartz) but no garnet in the residue (referenced in Conrad et al., 1988). Compositional discrepancies for  $\text{FeO}_{\text{total}}$  and MgO in the granitic rocks may also indicate that the peraluminous melts were in equilibrium with plagioclase (but not quartz) and were produced at moderate degrees of melting and high temperature ( $F = 70\text{-}85\%$ ,  $T > 900^\circ\text{C}$ ) (e.g., Miller et al., 1985). (3) The compositions of experimental glass from dacite (326A,  $X_{\text{H}_2\text{O}} = 0.5$ , 900°C, near the quartz-fayalite-magnetite buffer) of Conrad et al. (1988) and the granitic rocks show good similarity for  $\text{SiO}_2$ ,  $\text{TiO}_2$ ,  $\text{Al}_2\text{O}_3$ ,  $\text{Na}_2\text{O}$ , and  $\text{P}_2\text{O}_5$ . Other oxide abundances differ, in that the granitic rocks are somewhat enriched in MgO and  $\text{K}_2\text{O}$ , and depleted in  $\text{FeO}_{\text{total}}$  and CaO. (4) Dacite glass, however, has orthopyroxene and clinopyroxene in the residue but no plagioclase. Other dacite glasses (samples 623A, 625A) produced at higher temperatures (925 to 950 °C,  $X_{\text{H}_2\text{O}} = 0.25$ ) have residual plagioclase and no garnet, and are also similar to the average granitic rock from the Kodiak batholith. The bulk of the observations above suggest that some of the compositional features of the Kodiak batholith, especially of the Northern zone granitic rocks, can be explained by 70-85% melting of greywacke (and/or dacite) within the accretionary prism at conditions of  $X_{\text{H}_2\text{O}} = 0.25\text{-}0.50$ , 925 to 950°C,  $f_{\text{O}_2}$  near the QFM buffer.

### 6.7 Amphibolite Melting

Several geochemical attributes of the Kodiak Formation suggest that dehydration melting of greywacke is insufficient to explain the geochemistry of the granitic rocks and that more mafic components, for example, amphibolite, are needed in the source: (1) the batholith and the Kodiak Formation show moderate overlap in major element abundances but significant differences in average contents of  $\text{FeO}_{\text{total}}$ ,  $\text{MgO}$ , and  $\text{CaO}$  among others. The Kodiak Formation is also generally depleted in the alkali elements, and as a group, has much higher ASI values ( $>1.5$ ) than the granitic rocks ( $\text{ASI} < 1.5$ ). (2) The Kodiak Formation and the experimental greywacke melt compositions do not show matches for  $\text{SiO}_2$ ,  $\text{CaO}$  and  $\text{Na}_2\text{O}$  (Kodiak Formation is too low), and for  $\text{FeO}_{\text{total}}$  and  $\text{MgO}$  (Kodiak Formation is too high). Significantly, the granitic rocks have lower  $\text{SiO}_2$  (and higher  $\text{FeO}_{\text{total}}$ ,  $\text{MgO}$  and  $\text{K}_2\text{O}$  abundances) than the melts of greywacke used by Conrad et al. (1988), suggesting that other non-greywacke sources were involved. The Ghost Rocks Formation samples show even greater differences compared to the experimental compositions (and the Kodiak batholith), as they are measurably lower in  $\text{SiO}_2$ ,  $\text{CaO}$ , and  $\text{Na}_2\text{O}$ , and higher in  $\text{Al}_2\text{O}_3$ ,  $\text{MgO}$ , and  $\text{FeO}_{\text{total}}$  than the Kodiak Formation. (3) Comparison of experimental melts of greywacke and amphibolite by Patino-Douce (1999) with the Kodiak batholith (Fig. 3, 4) shows that most of the granitic rocks overlap the field of amphibolite (e.g., the granitic rocks show high abundances for the sum of  $\text{Al}_2\text{O}_3$ ,  $\text{FeO}_{\text{total}}$ ,  $\text{MgO}$ , and  $\text{TiO}_2$  compared to the field of metagreywacke melts).

The compositional features listed above for the Kodiak batholith reflect a mixture of sources that included greywacke, but which also had significant contributions from a more mafic component. General similarity of elemental abundances of the calc-alkaline mafic volcanic and intrusive rocks from the Eastern satellite group and experimental melting studies of amphibolites provide the means to estimate fractions of melting, temperature, water activity, and mineral assemblages controlling the evolution of granitic melts that closely resemble the compositions of the Kodiak batholith. Sisson et al. (2005) studied melting of moderately hydrous high-K shoshonitic high-alumina basalt, medium-K high-alumina basalt, and medium-K basaltic andesite that characterized the mafic liquids present during the evolution of the Sierra Nevada batholith. Except for the high-K shoshonitic high-alumina basalt, the other basalts used for

the experimental work show notable similarities to the mafic rocks adjacent to the Kodiak batholith. Experimental glasses were made at 700 MPa (about 20-25 km or ~ 6-8 kbar), which approximates the pressure at the bottom of the accretionary prism. Gabbro from the Eastern satellite group (02-KD-31B; Table 1) resembles the medium-K basaltic andesite of the experimental studies in SiO<sub>2</sub> (55.57% and 53.95%), TiO<sub>2</sub> (0.91% and 1.03%), Al<sub>2</sub>O<sub>3</sub> (17.99% and 17.85%), MnO (0.12% and 0.15%), MgO (5.60% and 5.43%), and K<sub>2</sub>O (1.10% and 1.19%). Moderate differences exist for CaO (8.22% and 9.33%), FeO<sub>total</sub> (6.78% and 8.11%), and Na<sub>2</sub>O (3.55% and 2.74%).

Comparison of the experimental melts of Sisson et al. (2005) with the average composition of the granitic rocks from the Kodiak batholith shows: (1) no exact match exists between the experimental melts and the average compositions of the granitic rocks. Moreover, other detailed experimental melt studies of amphibolite also lack exact compositional convergence with the batholith (e.g., Rapp and Watson, 1995). Glasses obtained at 900±25°C by Sisson et al. (2005), however, are a fair match to the entire range of granitic compositions, from the least silicic and presumably least evolved, to the most silicic rocks. The solidus assemblage for the amphibolites at 700 MPa included intermediate plagioclase (consistent with small negative Eu anomalies in the Kodiak granitic rocks), amphibole, biotite, and quartz (±pyroxene, and K-feldspar?); no garnet formed in the residue.

## 7. Summary and Petrogenetic Model

The large volume of granitic magma represented by the Kodiak batholith, together with plutons of similar age and composition near Kodiak Island, suggests that they correspond to a regional magmatic event derived from a sizeable source region. The batholith is dominantly composed of tonalite to granodiorite. Small granodiorite-granite plutons outcrop to the north, and others, ranging from granitic to quartz diorite and quartz gabbro flank the main body. The batholith encloses country rock xenoliths and contains widely disseminated coarse clusters of biotite, muscovite, plagioclase, and quartz closely associated with fine-grained garnet. Fine-grained kyanite is disseminated in the matrix and occurs as distinctly zoned megacrysts, especially in the Northern zone of the batholith. Very fine-grained fibrolite

(?) may also occur as inclusions in clusters of biotite and quartz. Mafic enclaves are generally absent. Aplites, pegmatites, and miarolitic cavities are uncommon. The batholith contains zonal distinctions discerned on the basis of petrographic variations, major and trace element abundances, and Nd-Sr-Pb isotopic ratios along a trend from SW to NE (Southern zone, Central zone, and Northern zone). Plutons flanking the main body of the batholith are assigned to the Northern, Western and Eastern satellite groups.

The Kodiak batholith is calc-alkalic (medium-K) and shows increases in  $\text{SiO}_2$  (~61 wt. %–73 wt. %) and decreases in  $\text{TiO}_2$  (~0.9 wt. %–0.3 wt. %) in a trend from SW to NE. The zonal distinctions identified above distinguish mainly between the Southern and Central zones taken as a group, in comparison to the Northern zone. The least alkalic (less sodic) rocks are in the Southern zone.  $\text{FeO}_{\text{total}}/\text{MgO}$  values show that the batholith belongs to a low-Fe suite. The batholith is peraluminous to strongly peraluminous (alumina saturation index,  $\text{ASI} = 1.08\text{--}1.37$ ). The Southern and Central zones have generally higher values of  $\text{Al}/(\text{Na}+\text{K})$  (~1.6–2.3) than the Northern zone, and Western and Northern satellites (1.2–1.8). Granitic rocks from the Eastern satellites are also more diverse and more aluminous ( $\text{ASI} \sim 1.46$ ) than the main mass of the batholith. Quartz gabbro and diorite are metaluminous [ $\text{Al}/(\text{Ca}+\text{Na}+\text{K}) \sim 0.7\text{--}0.9$ ]. The batholith shows no significant evidence for hydrothermal alteration and sulfide mineral deposition.

The batholith is enriched in large-ion lithophile elements (Ba, Rb, K, Cs, and Sr), other fluid-soluble elements (e.g., U, Pb, etc.) and light REEs compared to N-MORB. Trace element distributions result in high values of ratios involving large-ion lithophile elements and Nb, Ta, Zr, Hf, Ti, and Th. Generally, high values of such ratios are taken as characteristic of volcanic arc signatures. Relative depletions and wide variations in the abundances of Nb, Ta and Th are also key features of the Kodiak batholith. Highly variable ratios of Nb/Ta, Th/U, Th/Ta, and Th/Hf, among others, over narrow ranges of silica or other indices of differentiation characterize the different zones. Sc, Cr, Co, Ni, Zn, V and Ge contents generally decrease in abundance relative to  $\text{SiO}_2$ , and the Southern and Central zones have higher abundances of Sc and V than the Northern zone and Northern satellite group.

The zonal distinctions are also expressed by the isotope ratios of the granitic rocks. Two groups exist on the basis of  $\epsilon_{\text{Nd}}$  values. One group consists of the Southern and Central zones and is characterized by negative  $\epsilon_{\text{Nd}}$  values of -3.7 to -0.3 and  $T_{\text{DM}}$  ages  $\sim$  838 Ma to 1011 Ma. Another group consists of granitic rocks from the Northern zone (and a few rocks from the Central zone) showing higher  $\epsilon_{\text{Nd}}$  values of -0.4 to +4.7 and younger  $T_{\text{DM}}$  ages of  $\sim$  450 Ma to 797 Ma. The Central zone thus appears to be compositionally transitional, between the Southern and Northern zones. Granite, diorite, and gabbro from the Eastern satellite group have a wide range of  $\epsilon_{\text{Nd}}$  values of -2.7 to +6.4, and  $T_{\text{DM}}$  ages from 204 Ma to 2124 Ma. Initial  $^{87}\text{Sr}/^{86}\text{Sr}$  values of the Southern and Central zone intrusions tend to be slightly more radiogenic ( $^{87}\text{Sr}/^{86}\text{Sr} > 0.70426$ ) than the Northern zone. In a transect from SW to NE along the axis of the batholith, initial  $^{206}\text{Pb}/^{204}\text{Pb}$  values of the Southern and Central zones overlap and also tend to be slightly more radiogenic ( $^{206}\text{Pb}/^{204}\text{Pb} > \sim 18.9$ ) than the values of the Northern zone and Northern satellites ( $^{206}\text{Pb}/^{204}\text{Pb} < \sim 18.9$ ). As in the case of the  $\epsilon_{\text{Nd}}$  values, granitic rocks of the Eastern satellites plot within the fields of the Southern and Central zones.

Precise identification of the chemical components in the source region of the near-trench intrusives in the Sanak-Baranof belt and their relative contributions has proven difficult. A general consensus exists that physical interaction involving basaltic magmas and flysch is a common mechanism involved with the genesis of the granitic intrusions (e.g., Barker et al., 1992; Hudson, 1994; Lytwyn et al., 2000; Kusky et al., 2003; Sisson et al., 2003a, b). However, the exact role attributed to mafic magmas, the type of mafic magmas involved during granite generation in the near-trench environment, and identification of diagnostic features distinguishing between contemporaneous and mantle-derived rocks involved with granite genesis remains imperfectly known.

Our previous geochemical studies of the Cordova granodiorites in the eastern Gulf of Alaska (Prince William Sound) suggested that the contribution of mantle-derived magma likely accounted for less than 10% of the granitic melts and that the bulk of the melts reflected anatexis of the flysch in the accretionary prism (Barker et al., 1992; Farmer et al., 1993). This mantle component was not precisely

identified but was consistent with N-MORB-like mantle associated with ridge subduction, and mantle associated with transform faults. Magmas associated with transform faults have a wide range in trace element and isotopic compositions, including those ranging from N-MORB to E-MORB (e.g., Langmuir and Bender, 1984; Kela et al., 2007). In contrast to the Cordova granodiorites, in the eastern Chugach Mountains, granitic rocks were thought to require involvement of > 75% mantle-derived material (N-MORB to E-MORB compositions) that underplated the base of the accretionary wedge during ridge subduction (Sisson et al., 2003b). Also, Lytwin et al. (2000) and Bradley et al. (2003) showed that near-trench felsic plutons and mafic to felsic dikes in the Chugach accretionary prism (Kenai Peninsula) have a wide range of geochemical signatures. The felsic plutons and felsic dikes are calc-alkaline, and the basaltic andesites range from MORB-like to E-MORB, but also include rocks that resemble island-arc volcanics. The geochemical variations thus suggest that both island arc and MORB-like compositions can exist in the same ridge system (Sisson et al., 2003b).

In the Kodiak-Shumagin shelf, Hill et al. (1981) and Hill and Morris (1982) considered MORB-like magmas to have been the most likely heat and mass source of plutons in the accretionary prism (particularly intrusions in Shumagin and Sanak Islands). The granitic rocks were thought to indicate reaction of MORB-type magma and assimilation of the Shumagin Formation. On Kodiak Island, Moore et al. (1983) conducted a survey of the geochemical features of the mafic to intermediate rocks in the Ghost Rocks Formation adjacent to the main mass of the Kodiak batholith and described them as MORB and andesite. Granodioritic rocks flanking the main mass of the Kodiak batholith were attributed to mixing of MORB and sediments. Our preliminary data for these and other volumetrically minor gabbros and diorites in the Eastern satellite group show, instead, that they are quartz-bearing, have elevated  $K_2O$  contents, and differ from typical N-MORB compositions. The mafic rocks resemble calc-alkaline tholeiitic rocks, and display many trace element features including enrichment in the light REEs and fluid-soluble elements, relative depletion in Nb, and values of diagnostic ratios (Nb/U, Ce/Pb, Ba/Ta, and La/Th) that generally bear a similarity to mafic orogenic rocks.

Assuming that the small volume of mafic magma adjacent to the main mass of the batholith is cogenetic and has been characterized adequately, our favored interpretation is that the mafic rocks that underplated (and evolved to more intermediate compositions) and were stored in the deeper levels of the accretionary prism. The mafic rocks could represent magmatism in a continental arc setting if conditions for melting of the mantle wedge were appropriate as a result of rising fluids liberated from the subducting slab into the mantle wedge in forearc regions. In this scenario, metasomatizing fluids enrich the wedge in water and fluid-soluble elements (Bebout, 1996) prior to ridge subduction under the arc. Transfer of fluid-soluble elements conveys components to the sources of arc magmas by metasomatizing the mantle wedge, and is a flux for partial melting leading to arc magmatism (Ryan et al., 1996).

An alternative origin for the volumetrically minor mafic rocks flanking the Kodiak batholith is that they resemble underplated mafic magmas produced by the slab window. In this case, the observed trace element and isotopic compositions of the mafic magmas reflect hybridization, crustal assimilation, and mixing of N-MORB mantle and the metasedimentary rocks in the accretionary prism, or slab window magma related to E-MORB type magma (from transform faults?). Our trace element data are not conclusive, but elements such as Cs, Rb, Ba, Th, and Pb are significantly enriched relative to E-MORB, and light REE contents are also considerably higher than N-MORB and E-MORB. If the mafic rocks in the Eastern satellite group originally represented N-MORB mantle, their trace element and isotopic signatures have been disturbed, and their exact magma type cannot be identified compellingly. Regardless of the ultimate origin of the mafic rocks in the Kodiak batholith, however, our interpretation suggests that ridge-trench interaction (northern trench-ridge-trench triple junction of the Resurrection plate) intersected the southern Alaskan margin producing hot, dense MORB-type basaltic magmas generated by decompression melting of asthenospheric mantle that upwelled into the opening gap, interacted with peridotite in the mantle wedge underlying the volcanic arc forming compositionally transitional MORB-like to arc magmas, and triggered partial melting of a heterogeneous source region.

Ridge subduction, thus, acted predominantly as a migrating (SW to NE) thermal trigger beneath the accretionary prism, which sequentially partially melted a mixture of mantle-derived material and

recycled continental crustal source rocks. Melt production and migration of the subducting ridge under the prism is reflected in a trend from SW to NE along the axis of the batholith, resulting in younger granite crystallization ages. The age trend suggests that the thermal/igneous event related to the Kodiak batholith was relatively brief, in contrast to the typical metaluminous to peraluminous and relatively long-lived orogenic batholiths (for example, Sierra Nevada Batholith, Peninsular Ranges Batholith of the Californias, and Coast Batholith of Peru).

The Kodiak batholith overlaps the major and trace element compositions and  $\epsilon_{Nd}$ , Sr and Pb isotopic values of metasedimentary rocks in the Chugach accretionary prism. The metasedimentary rocks may represent the protoliths that provided granitic melts from the bottom of the accretionary prism. Major and trace element analyses of the Kodiak Formation and the Ghost Rocks Formation show that they resemble orogenic rocks. Both formations, however, differ in  $Fe_2O_3$ , CaO,  $Na_2O$ , or MgO contents, and are more aluminous than the Kodiak batholith. Comparison of trace element abundances (Nb, Ti, and Pb) and ratios of  $^{206}Pb/^{204}Pb$ ,  $^{207}Pb/^{204}Pb$ , and  $^{208}Pb/^{204}Pb$ , as well as all Sr and  $\epsilon_{Nd}$  shows that the flysch mostly overlaps the Kodiak batholith. The overall major- and trace element and isotopic similarity between the flysch and the batholith support the idea that the granitic rocks could have been formed by anatexis of the metasedimentary rocks. Support for this notion is also provided by experimental studies of greywacke (Conrad et al. 1988) that has a bulk composition matching that of the Kodiak Formation. Results show that greywacke melts closely replicate the composition of the Northern zone granites, but fail to produce melts equivalent to the Southern and Central zones of the batholith. Instead, we suggest that the source region in the accretionary prism undergoing melting likely included a more mafic lithology. We suggested above that the mafic rocks (and intermediate evolutionary products) underplated and were intercalated at the bottom of the prism prior to the arrival of the ridge. If this suggestion is reasonable, experimental melting studies of amphibolites (Sisson et al., 2005) that have notable bulk chemical similarities to the calc-alkaline mafic volcanic and intrusive rocks from the Eastern satellite group are appropriate for comparison, and can be used to test whether the melt products match the compositions of

the Southern and Central zones of the batholith. As reviewed above, the solidus assemblage for the amphibolites is a fair match to the entire range of granitic compositions in the Southern and Central zones of the batholith.

The preceding geochemical data support a model for the genesis of the Kodiak batholith from partial melting of a mixed source consisting of a lithologically diverse sequence that included the Kodiak Formation, and amphibolites in the source region. Estimates of mantle contributions to the batholith on the basis of Nd isotopic compositions suggest a wide range, from 40%-80%. Samples having high mantle contributions also have the young  $T_{DM}$  ages and high values of  $\epsilon_{Nd}$ . The balance of the Nd isotopic budget is thought to reflect a recently recycled crustal component represented by the Kodiak Formation, which has the oldest  $T_{DM}$  ages and lowest values of  $\epsilon_{Nd}$ . Partial melting of a mixed source is consistent with decoupling of elemental abundances and ratios of the LILE/HFS from the isotope signatures in the granitic rocks from the various zones. Mixing in the source region is also suggested by the lack of covariations of major and trace element abundances and isotope compositions.

Geochemical observations summarized above support the idea that zonal compositional differences represent incursion of different melts and the effects of mixing isotopically different magma sources stored in the accretionary prism. These magmas were unlikely to be mutually related simply by *in situ* fractional crystallization and assimilation and fractional crystallization reactions during transport from their heterogeneous source region at the bottom of the accretionary prism and during emplacement higher in the continental crust. Also, plots involving compatible element variations in the mafic to granitic rocks scatter and do not produce mixing lines indicative of simple mixing of felsic melts and contemporaneous mafic mantle-derived magmas, making simple two-component mixing unlikely. All of these processes would have produced coherent elemental trends linking cogenetic rocks, as well as trace element ratios correlated with isotopic values of Pb, Sr, and  $\epsilon_{Nd}$ . Offsets, compositional gaps, and the heterogeneity in isotopic compositions in the Kodiak batholith can thus be taken as evidence that the batholith and its satellites did not evolve directly from a common, more mafic parent.

Significant recent advances have been made in the understanding of the petrogenesis of the near-trench intrusives from the Sanak-Baranof belt (e.g., Bradley et al., 2003; Kusky et al., 2003, Sisson et al., 2003a; Groome et al., 2003; Farris et al., 2006). In particular, based on an overview of ridge-trench interactions in modern and ancient settings, Sisson et al. (2003b) suggested that although no unique geological signature of ridge subduction events has been found, a combination of features that includes igneous rock sequences and associated processes, records of thermal events, and changes in plate kinematics can be diagnostic. Our study of the Kodiak batholith specifically highlights the need for detailed documentation of diagnostic geochemical features of mantle-derived magmas and continental sources implicated with granite genesis. In addition, we find that a more complete comprehension of the evolution of mantle properties as a result of ridge subduction processes would better constrain models of crustal evolution along the Sanak-Baranof belt, magmatism inboard from the slab window (back arc), and crust-mantle interaction processes associated with changes in plate kinematics and deformation regimes.

### **Acknowledgements**

The original manuscript was greatly improved through constructive reviews by Carter Hearn and Jeffrey Grossman (both at the U.S. Geological Survey). We also thank two reviewers for their comments made for the journal. For technical and laboratory assistance in the Radiogenic Isotope Laboratory, we thank Anna Colvin, Jeremy Dillingham, Giuseppe Grezzi, John Jackson, Ann Lyon, and Jennifer Murphy. We also extend our gratitude to P. McCrory and D. Wilson, guest editors of the special issue, for their advice and comments in preparing the final document.

### **References**

- Arth, J.G., 1976. Behavior of trace elements during magmatic processes-A summary of theoretical models and their applications. U.S. Geol. Survey, J. Res., 4, 41-47.
- Arth, J.G., Barker, F., and Stern T.W., 1988. Coast batholith and Taku plutons near Ketchikan, Alaska: Petrography, geochronology, geochemistry and isotopic character. Am J. Sci., 288-A,

- 461-489.
- Arculus, R.J., 2003. Use and abuse of the terms calcalkaline and calcalkalic. *J. Petrol.*, 44, 929-935.
- Ayuso, R.A., Schulz, K.J., 2003. Nd-Pb-Sr isotope geochemistry and origin of the Ordovician Bald Mountain and Mount Chase massive sulfide deposits, northern Maine. In: Goodfellow, W.D., McCutcheon, S.R., Peter, J.M. (Eds.), *Volcanogenic Massive Sulfide Deposits of the Bathurst District and Northern Maine. Economic Geology Monograph 11*, pp. 611-630.
- Ayuso, R.A., Wooden, J.N., Foley, N.K., Seal, R., II, Sinha, A.K., 2005. U-Pb zircon ages and Pb isotope geochemistry of gold deposits from the Carolina slate belt of South Carolina. *Eco. Geol.*, 100, 225-252.
- Ayuso, R.A., Haeussler, P.J., Bradley, D.C., Farris, D.W., Colvin, A.S., 2005. The effects of ridge subduction on chemical and isotopic zoning of the Kodiak batholith, southern Alaska (abs.). *Geol. Soc. Am. (abs.)* 37, 80.
- Barker, F., Farmer, G.L., Ayuso, R.A., Plafker, G., Lull, J.S., 1992. 50-Ma granodiorite of the Eastern Gulf of Alaska: Melting in an accretionary prism in the forearc. *J. Geophys. Research*, 97, 6757-6778.
- Bebout, G., 1996. Volatile transfer and recycling at convergent margins: mass balance and insights from high-P/T metamorphic rocks: In: Bebout, G.E., Scholl, D.W., Kirby, S.H., Platt, J.P. (Eds.), *Subduction: Top to Bottom, Geophysical Monograph 96*, Am. Geophys. Union, 179-193.
- Bevier, M.L., Anderson, R.G., 1990. New U-Pb and K-Ar ages for igneous rocks, Iskut River map area, B.C. *Geol. Assoc. Can. Abst. Prog.*, 15, A-10.
- Bradley, D.C., Kusky, T.M., 1992. Deformation history of the McHugh Complex, Seldovia quadrangle, south central Alaska: *U.S. Geological Survey Bulletin* 1999, 17-32.
- Bradley, D.C., Haeussler, P.J., and Kusky, T.M., 1993. Timing of Early Tertiary ridge subduction in southern Alaska: *U.S. Geological Survey Bulletin* 2068, 163-177.
- Bradley, D., Kusky, T., Haeussler, P., Goldfarb, R., Miller, M., Dumolin, J., Nelson, S.W., Karl, S., 2003. Geologic signature of early Tertiary ridge subduction in Alaska: In: Sisson, V.B., Roeske,

- S.M., Pavlis, T.L. (Eds.), *Geology of a Transpressional Orogen Developed during Ridge-Trench Interaction along the North Pacific Margin*. Geol. Soc. Am. Special Paper 371, 19-50.
- Byrne, T., 1979, Late Paleocene demise of the Kula Pacific spreading center. *Geology*, 10, 191-196.
- Clarke, D.B., 1981. The mineralogy of peraluminous granites; a review. *Can. Mineral.*, 19, 3-17.
- Class, C., Miller, D.M., Goldstein, S.L., and Langmuir, C.H., 2000. Distinguishing melt and fluid subduction components in Umnak Volcanics, Aleutian Arc. *Geochem. Geophys. Geosyst.*, 1, paper number 1999GC000010.
- Conrad, W.A., Nicholls, I.A., Wall, V.J., 1988. Water-saturated and undersaturated melting of metaluminous and peraluminous crustal compositions at 10 kb: Evidence for the origin of rhyolites in the Taupo Volcanic Zone, New Zealand, and other granitoids. *J. Petrol.*, 29, 765-803.
- Davidson, J.P., 1996. Deciphering mantle and crustal signatures in subduction zone magmatism. In: Bebout, G.E., Scholl, D.W., Kirby, S.H., Platt, J.P. (Eds.), *Subduction: Top to Bottom*, Geophys. Monograph 96, pp. 251-262.
- Debaille, V., Doucelance, R., Weis, D., and Schiano, P., 2006. Multi-stage mixing in subduction zones: Application to Merapi volcano (Java island, Sunda arc). *Geochim. Cosmochim. Acta*, 70, 723-741.
- Delong, S.E., Schwarz, W.M., Anderson, R.N., 1979. Thermal effects of ridge subduction. *Earth Planet. Sci. Lett.*, 44, 239-246.
- DePaolo, D.J., 1981. Trace element and isotopic effects of combined wall-rock assimilation and fractional crystallization. *Earth Planet. Sci. Lett.*, 53, 189-202.
- Dumoulin, J. A., 1988. Sandstone petrographic evidence and the Chugach-Prince William terrane boundary in southern Alaska. *Geology*, 16, 456-460.
- Dusel-Bacon, C., Csejtev, B., Jr., Foster, H.L., Doyle, E.O., Nokleberg, W.J., Plafker, G., 1993. Distribution, facies, ages, and proposed tectonic associations of regionally metamorphosed rocks in east- and south-central Alaska: U.S. Geological Survey Professional Paper 1497-C, 1-72.

- Elliott, T., 2003. Tracers of the slab: In: Eiler, J. (Ed.), *Inside the Subduction Factory*. Geophys. Monograph 138, Am. Geophys. Union, 23-46.
- Engebretson, D.C., Cox, A.V., Gordon, R.G., 1985. Relative motions between oceanic and continental plates in the Pacific Basin. *Geol. Soc. Am. Sp. Paper* 206, 59p.
- Farmer, G.L., Ayuso, R.A., Plafker, G., 1993. A Coast Mountains provenance for the Valdez and Orca Groups, southern Alaska, based on Nd, Sr, and Pb isotopic evidence. *Earth Planet. Sci. Lett.*, 116, 9-21.
- Farris, D.W., and Paterson, S.R., 2007. Contamination of silici magmas and fractal fragmentation of xenoliths in Paleocene plutons on Kodiak Island, Alaska. *Canadian Mineral.*, 45, 107-129.
- Farris, D.W., Haeussler, P., Friedman, R., Paterson, S.R., Saltus, R.W., and Ayuso, R., 2006. Emplacement of the Kodiak batholith: A consequence of slab-window migration. *Geol. Soc. Am. Bull.*, 118, 1360-1376.
- Fisher, D., Byrne, T., 1987. Structural evolution of underthrust sediments, Kodiak Islands, Alaska. *Tectonics*, 6, 775-793.
- Gill, J., 1981. *Orogenic Andesites and Plate Tectonics*. Springer, New York, 190.
- Godwin, C.I., Gabites, J.E., and Andrew, A., 1988. A galena lead isotope data base for the Canadian Cordillera, Province of British Columbia. *Mineral. Res. Div. Pap.* 1988-4.
- Gorring, M.L., Kay, S.M., 2001. Mantle processes and sources of Neogene slab window magmas from southern Patagonia, Argentina. *J. Petrol.*, 42, 1067-1094.
- Groome, W.G., Thorkelson, D.J., Friedman, R.M., Mortensen, J.K., Massey, N.W.D., Marshall, D.D., Layer, P.W., 2003. Magmatic and tectonic history of the Leech River Complex, Vancouver Island, British Columbia: Evidence for ridge-trench intersection and accretion of the Crescent Terrane: In: Sisson, V.B., Roeske, S.M., Pavlis, T.L. (Eds.), *Geology of a Transpressional Orogen Developed during Ridge-Trench Interaction along the North Pacific Margin*. *Geol. Soc. Am. Special Paper* 371, p. 327-354.

- Haeussler, P.J., Bradley, D.C., Goldfarb, R.J., 2003a. Brittle deformation along the Gulf of Alaska margin in response to Paleocene-Eocene triple junction migration: In: Sisson, V.B., Roeske, S.M., Pavlis, T.L. (Eds.), *Geology of a Transpressional Orogen Developed during Ridge-Trench Interaction along the North Pacific Margin*. Geol. Soc. Am. Special Paper 371, p. 119-140.
- Haeussler, P.J., Bradley, D.C., Wells, R., Miller, M.L., 2003b. Life and death of the Resurrection plate: Evidence for an additional plate in the northeastern Pacific in Paleocene-Eocene time. *Geol. Soc. Am. Bull.*, 115, 867-880.
- Haeussler, P.J., Bradley, D.C., Goldfarb, R., Snee, L., 1995. Link between ridge subduction and gold mineralization in southern Alaska. *Geology*, 23, 995-998.
- Hanson, G.N., 1978. The application of trace elements to the petrogenesis of igneous rocks of granitic composition. *Earth Planet. Sci. Lett.*, 38, 26-43.
- Harris, N.R., Sisson, V.B., Wright, J.E., Pavlis, T.L., 1996. Evidence for Eocene mafic underplating during fore-arc intrusive activity, eastern Chugach Mountains, Alaska. *Geology*, 24, 263-266.
- Hart, S.R., 1984. A large-scale isotope anomaly in the Southern Hemisphere mantle. *Nature*, 309, 753-757.
- Hawkesworth, C.J., Hergt, J.M., McDermott, F., Ellam, R.M., 1991. Destructive margin magmatism and the contributions from the mantle wedge and subducted crust. *Australian J. Earth Sci.*, 38, 577-594.
- Henderson, P. 1986. *Inorganic Geochemistry*. Pergamon Press, 356 p.
- Hill, M., Morris, J., 1982. Source rocks for Paleocene granitic intrusives of the Kodiak-Shumagin shelf, southwest Alaska: Evidence from Pb and Nd isotopes. *EOS, Trans. Am. Geophys. Union*, 63, 462.
- Hill, M., Morris, J., Whelan, J., 1981. Hybrid granodiorites intruding the accretionary prism, Kodiak, Shumagin, and Sanak Islands, southwest Alaska. *J. Geophys. Res.*, 86, 10569-10590.
- Hudson, T., 1994. Crustal melting events in Alaska. In: Plafker, G., Berg, H.C. (Eds.), *The Geology of Alaska: Geol. Soc. Am., Geology of North America*, v. G-1, 657-670.

- Hudson, T., Plafker, G., Peterman, Z.E., 1979. Paleogene anatexis along the Gulf of Alaska margin. *Geology*, 7, 573-577.
- Jones, D.L., Siberling, N.J., Coney, P.J., Plafker, G., 1987. Lithotectonic terrane map of Alaska (west of the 141<sup>st</sup> meridian). U.S. Geological Survey Misc. Field Studies Map, MF-1874-A.
- Karsten, J.L., Klein, E.M., Sherman, S.B., 1996. Subduction zone geochemical characteristics in ocean ridge basalts from the southern Chile Ridge: Implications of modern ridge subduction systems for the Archean. *Lithos*, 37, 143-161.
- Kay, R.W., 1978. Aleutian magnesian andesites: melts from subducted Pacific ocean crust. *J. Volc. Geoth. Res.*, 4, 117-132.
- Kay, R.W., 1980. Volcanic arc magmas: implications of a melting-mixing model for element recycling in the crust-upper mantle system. *J. Geol.*, 88, 497-522.
- Kela, J.M., Stakes, D.S., Duncan, R.A., 2007. Geochemical and age constraints on the formation of the Gorda Escarpment and Mendocino Ridge of the Mendocino transform fault in the NE Pacific. *Geol. Soc. Amer. Bull.*, 119, 88-100.
- Klein, E.M., 2003. Geochemistry of the igneous oceanic crust. *Treatise on Geochemistry*, 3-13, 433-463.
- Kuno, H., 1966. Lateral variation of basalt magma across continental margins and island arcs. *Bull. Volcan.*, 29, 195-222.
- Kusky, T.M., Bradley, D.C., Donley, D.T., Rowley, D, Haeussler, P.J., 2003. Controls on intrusion of near-trench magmas of the Sanak-Baranof belt, Alaska, during Paleogene ridge subduction, and consequences for forearc evolution: In: Sisson, V.B., Roeske, S.M., Pavlis, T.L. (Eds.), *Geology of a Transpressional Orogen Developed during Ridge-Trench Interaction along the North Pacific Margin*. *Geol. Soc. Am. Special Paper 371*, 269-292.
- Langmuir, C.H., Bender, J.F., 1984. The geochemistry of oceanic basalts in the vicinity of transform faults: observations and implications. *Earth Planet. Sci. Lett.*, 69, 107-127.

- Luhr, J.F., Aranda-Gomez, J.J., Housh, T.B., 1995. San Quintin volcanic field, Baja California Norte, Mexico: geology, petrology and geochemistry. *J. Geophys. Res.*, 100, 10353-10380.
- Lytwyn, J., Lockhart, S., Casey, J., Kusky, T., 2000. Geochemistry of near-trench intrusives with ridge subduction, Seldovia quadrangle, southern Alaska. *J. Geophys. Res.*, 105, 27,957-27,978.
- Marshak, R.S., Karig, D.E., 1977. Triple junctions as a cause for anomalously near-trench igneous activity between the trench and volcanic arc. *Geology*, 5, 233-236.
- Miller, C.F., Watson, E.B., Rapp, R.P., 1985. Experimental investigation of mafic mineral-felsic liquid equilibria: preliminary results and petrogenetic implications (abs.). *EOS, Trans. Am. Geophys. Union*, 66, 1130.
- Moore, J.C., Byrne, T., Plumley, P.W., Reid, M., Gibbons, H., Coe, R.S., 1983. Paleogene evolution of the Kodiak Islands, Alaska: Consequences of ridge-trench interaction in a more southerly latitude. *Tectonics*, 2, 265-293.
- Nilsen, T.H., Moore, G.W., 1979. Reconnaissance study of Upper Cretaceous to Miocene stratigraphic units and sedimentary facies, Kodiak and adjacent islands, Alaska. *U.S. Geological Survey Professional Paper 1093*, 1-34.
- Patino Douce, A.E., 1999. What do experiments tell us about the relative contributions of crust and mantle to the origin of granitic magmas? In: Castro, A., Fernandez, C., Vigneresse, J.L., (Eds.), *Understanding Granites: Integrating New and Classical Techniques*, Geol. Soc. London, Special Publication, 168, 55-75.
- Pavlis, T.L., Sisson, V.B., 1995. Structural history of the Chugach metamorphic complex in the Tana River region, eastern Alaska: A record of Eocene ridge subduction. *Geol. Soc. Am. Bull.*, 107, 1333-1355.
- Plafker, G., Jones, D.L., Pessagno, E.A., Jr., 1977. A Cretaceous accretionary flysch and mélangé terrane along the Gulf of Alaska margin: *U.S. Geological Survey Circular 751B*, 41-43.

- Plafker, G., Nokleberg, W.J., Lull, J.S., 1989. Bedrock geology and tectonic evolution of the Wrangellia, Peninsular, and Chugach terranes along the Trans-Alaska Crustal Transect in the Chugach Mountains and souther Copper River Basin, Alaska. *J. Geophys. Res.*, 94, 4255-4295.
- Rapp, R.P., Watson, E.B., 1995. Dehydration melting of metabasalt at 8-32 kbar: Implications for continental growth and crust-mantle recycling. *J. Petrol.*, 36, 891-931.
- Richardson, S.W., Gilbert, M.C., Bell, P.M., 1969. Experimental determination of kyanite-andalusite and andalusite-sillimanite equilibria: the aluminum silicate triple point. *Am. J. Sci.*, 267, 259-272.
- Ryan, J., Morris, J., Bebout, G., Leeman, B., 1996. Describing chemical fluxes in subduction zones: insights from “depth-profiling” studies of arc and forearc rocks. In: Bebout, G.E., Scholl, D.W., Kirby, S.H., Platt, J.P., (Eds.), *Subduction: Top to Bottom*, Geophysical Monograph 96, Am. Geophys. Union, 263-276.
- Sample, J.C., Fisher, 1986. Duplexes and underplating in an ancient accretionary complex, Kodiak islands, Alaska. *Geology*, 14, 160-163.
- Sample, J.S., Moore, J.C., 1987. Structural style and kinematics of an underplated slate belt, Kodiak and adjacent islands, Alaska. *Geol. Soc. Am. Bull.*, 99, 7-20.
- Sample, J.C., Reid, M.R., 2003. Large-scale, latest Cretaceous uplift along the northeast Pacific Rim: Evidence from sediment volume, sandstone petrography, and Nd isotope signatures of the Kodiak Formation, Kodiak Island, Alaska: In: Sisson, V.B., Roeske, S.M., Pavlis, T.L. (Eds.), *Geology of a Transpressional Orogen Developed during Ridge-Trench Interaction along the North Pacific Margin*. *Geol. Soc. Am. Special Paper 371*, 51-70.
- Samson, S.D., Patchett, P.J., McClelland, W.C., Gehrels, G.E., 1991. Nd and Sr isotopic constraints on the petrogenesis of the west side of the northern Coast Mountains batholith, Alaskan and Canadian Cordillera. *Can. J. Earth Sci.*, 28, 939-946.
- Sisson, T.W., Ratajeski, K., Hankins, W.B., Glazner, A.F., 2005. Voluminous granitic magmas from basaltic sources. *Contrib. Mineral. Petrol.*, 148, 635-661.

- Sisson, V.B., Pavlis, T.L., Roeske, S.M., Thorkelson, D.J., 2003a. Introduction: An overview of ridge-trench interactions in modern and ancient settings: In: Sisson, V.B., Roeske, S.M., Pavlis, T.L. (Eds.), *Geology of a Transpressional Orogen Developed during Ridge-Trench Interaction along the North Pacific Margin*. Geol. Soc. Am. Special Paper, 1-18.
- Sisson, V.B., Poole, A.R., Harris, N.R., Burner, H.C., Pavlis, T.L., Copeland, P., Donelick, R.A., McLelland, W.C., 2003b. Geochemical and geochronologic constraints for genesis of a tonalite-trondhjemite suite and associated mafic intrusive rocks in the eastern Chugach Mountains, Alaska: A record of ridge-transform subduction: In: Sisson, V.B., Roeske, S.M., Pavlis, T.L. (Eds.), *Geology of a Transpressional Orogen Developed during Ridge-Trench Interaction along the North Pacific Margin*. Geological Society of America Special Paper 371, p. 293-326.
- Sisson, V.B., Hollister, L.S., Onstott, T.C., 1989. Petrologic and age constraints on the origin of a low-pressure/high-temperature metamorphic complex, southern Alaska. *J. Geophys. Res.*, 94, 4392-4410.
- Stacey, J.D., Kramers, J.N., 1975. Approximation of terrestrial lead isotope evolution by a two-stage model. *Earth Planet. Sci. Lett.*, 36, 207-222.
- Stevens, G., Clemens, J.D., Droop, G.T.R., 1997. Melt production during granulite-facies anatexis: experimental data from "primitive" metasedimentary protoliths. *Contrib. Mineral. Petrol.*, 128, 352-370.
- Sun, S.S., McDonough, W.F. Chemical and isotopic systematics of oceanic basalts: implications for mantle composition and processes. In: Saunders, A.D., Norry, M.J., (Eds.), *Magmatism in the Ocean Basins*, Geol. Soc. Special Pub. 42, 313-345.
- Tangalos, G.E., Farris, D.R., Valley, D.W., Haeussler, P.J., Haileab, B. 2003. Genesis and contamination of the Kodiak batholith, Kodiak Island, Alaska: using O18 to quantify the assimilated component of the batholith. *Geol. Soc. Am. Abstr. Programs* 35, 325.

- Tatsumi, Y., Hamilton, D.L., Nesbitt, R.W., 1986. Chemical characteristics of fluid phase released from a subducted lithosphere and the origin of arc magmas: evidence from high pressure experiments and natural rocks. *J. Volc. Geoth. Res.*, 29, 293-309.
- Taylor, S.R., and McLennan, S.M., 1985. *The Continental Crust: its Composition and Evolution*. Blackwell Scientific Publications, 312 p.
- Thorkelson, D.J., 1996. Subduction of diverging plates and the principles of slab window formation. *Tectonophysics*, 255, 47-63.
- Thorkelson, D.J., Taylor, R.P. 1989. Cordilleran slab windows. *Geology*, 17, 833-836.
- Thorkelson, D.J., Breitsprecher, K., 2005. Partial melting of slab window margins: genesis of adakitic and non-adakitic magmas. *Lithos*, 79, 25-41.
- Tysdal, R.G., Case, J.E., Winkler, G.R., Clark, S.H.B., 1977. Sheeted dikes, gabbro, and pillow basalt in flysch of coastal southern Alaska. *Geology*, 5, 377-383.
- Vrolijk, P. Meyers, G., and Moore, J.C., 1988. Warm fluid migration along tectonic mélanges in the Kodiak accretionary complex, Alaska. *J. Geophys. Res.*, B9, 10313-10324.
- Winkler, G.R., 1976. Deep sea fan deposition of the Lower Tertiary Orca Group, eastern Prince William Sound, Alaska, in *Recent and Ancient Sedimentary Environments in Alaska*: In: Miller, T.P. (Ed.), 1975 Symposium Proceedings, R1-R20, Alaska Geological Society, Anchorage.
- Zartman, R.E., Doe, B.R., 1981. Plumbotectonics - the model. *Tectonophysics*, 75, 135-162.
- Zartman, R.E., Futa, K., Peng, Z.C. 1991. A comparison of Sr-Nd-Pb isotopes in young and old continental lithospheric mantle: Patagonia and eastern China, *Australian J. Earth Sci.*, 38, 545-557.
- Zindler, A., Hart, S.R., 1986. Chemical geodynamics. *Ann. Rev. Earth Planet. Sci.*, 14, 493-571.

### Figures

Figure 1. Map of the Kodiak batholith showing internal subdivisions and sample locations: Southern zone, Central zone, and Northern zone; groups of igneous rocks flanking the batholith: Northern

satellites, Western satellites, and Eastern satellites; and country rocks shown in gray (the Uppermost Cretaceous Kodiak Formation, and the Paleocene Ghost Rocks Formation; Sample and Moore, 1987; Sample and Read, 2003). The Kodiak Formation outcrops east of the Uganik thrust (landward boundary) and west of the Contact fault (seaward boundary). The Kodiak Formation was intruded by the main mass of the Kodiak batholith (Southern, Central and Northern zones) and the Northern and Western satellite plutons. The Ghost Rocks Formation outcrops east of the Contact fault and was intruded by some of the Eastern satellite plutons. Map also shows location of samples used for zircon geochronology (Farris et al., 2006). Inset map of Alaska shows the Chugach-Prince William accretionary wedge (Chugach-Prince William terrane), Sanak-Baranof near-trench intrusive rocks, and the Kodiak batholith (Bradley et al., 2003).

Figure 2. Modal compositions of the granitic rocks of the Kodiak batholith. The four modal components illustrated are quartz, plagioclase, alkali feldspar, and the sum of the mafic minerals. The Kodiak batholith follows a calc-alkaline trend as a whole, showing moderate internal differences that distinguish the relatively plagioclase- and mafic minerals-enriched (biotite) Central zone from the Northern zone. In the satellite rocks, those from the Eastern satellite group include quartz gabbro and diorite and consequently are also relatively enriched in plagioclase and mafic minerals.

Figure 3. A) Total alkalis vs.  $\text{SiO}_2$ ; B)  $\text{K}_2\text{O}$  vs  $\text{SiO}_2$ ; C) ASI (alumina saturation index) vs  $\text{SiO}_2$ ; D)  $\text{Al}_2\text{O}_3/(\text{MgO}+\text{FeO}_{\text{total}}+\text{TiO}_2)$  versus  $\text{Al}_2\text{O}_3+\text{MgO}+\text{FeO}_{\text{total}}+\text{TiO}_2$  for the Kodiak batholith, Kodiak Formation, and Ghost Rocks Formation (symbols as in Fig. 2). Generalized fields show experimental melt compositions of peraluminous leucogranites, metagreywacke, and amphibolite taken from Patino Douce (1999); experimental melt compositions also shown: sample 623B from Conrad et al. (1988), and sample 1649 from Sisson et al. (2005).

Figure 4. Major element variation diagrams for the Kodiak batholith: A)  $\text{Al}_2\text{O}_3$ ; B)  $\text{MgO}$ ; C)  $\text{FeO}_{\text{total}}$ ; D)  $\text{TiO}_2$ ; E)  $\text{Na}_2\text{O}$ ; F)  $\text{CaO}$ ; G)  $\text{K}_2\text{O}$ ; H)  $\text{P}_2\text{O}_5$ . Starting materials used for melting studies:

greywackes (sample #623, Conrad et al., 1988), open star symbols, and medium-K basaltic andesite (sample YOS-55A, Sisson et al., 2005), solid star symbols. The Kodiak batholith shows inverse correlations of  $\text{Al}_2\text{O}_3$ ,  $\text{MgO}$ ,  $\text{FeO}_{\text{total}}$ ,  $\text{TiO}_2$ , and  $\text{CaO}$  with increasing  $\text{SiO}_2$ ; the alkalis are generally directly correlated with  $\text{SiO}_2$ .

Figure 5. Trace element variation diagrams for the Kodiak batholith (symbols as in Fig. 2): A) Ba; B) Sr; C) Rb; D) Zr; E) V; F) Cr; G) Ni; H) Sc. Granitic rocks from the Southern, Central, and Northern zones of the Kodiak batholith, as well as from the satellite groups, generally have overlapping trends or in some cases occupy distinct compositional fields (e.g., Eastern satellite group, Northern satellite group). Contents of Sr, V, Ni, and Sc are inversely correlated with  $\text{SiO}_2$ , and Ba and Rb are directly correlated with  $\text{SiO}_2$ .

Figure 6. Multi-element primitive mantle-normalized plots (Sun and McDonough, 1989) of samples from the Kodiak batholith. Tonalite and granodiorite from: A) Southern zone ( $\text{SiO}_2 = 62.52\text{-}65.16$  wt.%); B) Central zone ( $\text{SiO}_2 = 57.31\text{-}65.42$  wt.%); C) Northern zone ( $\text{SiO}_2 = 64.18\text{-}72.02$  wt.%). D) Granodiorite and granite from the Western and Northern satellite groups ( $\text{SiO}_2 = 68.05\text{-}75.75$  wt.%). E) Mafic, intermediate, and felsic igneous rocks of the Eastern satellite group (outer trenchward belt), which intruded the Ghost Rocks Formation ( $\text{SiO}_2 = 45.92\text{-}66.01$  wt.%); granodiorite and granite from the Eastern satellite group (inner trenchward belt) adjacent to batholith, which intruded the Kodiak Formation and the Ghost Rocks Formation ( $\text{SiO}_2 = 54.21\text{-}80.41$  wt.%). F) Kodiak Formation ( $\text{SiO}_2 = 61.74\text{-}66.30$  wt.%), Ghost Rocks Formation ( $\text{SiO}_2 = 59.27\text{-}61.33$  wt.%), and country rock inclusion in the Kodiak batholith ( $\text{SiO}_2 = 58.24$  wt.%). Also shown for comparison are patterns for normal MORB (N-MORB), and enriched MORB (E-MORB), (Sun and McDonough, 1989) and upper continental crust (UCC) (Taylor and McLennan, 1985). The multi-element diagrams show a relatively tight bundle of lines characterized by spiked patterns for individual zones in the batholith, small to large troughs for Th, large to moderate troughs for Nb and Ti, and large spikes for Pb. The leucogranites of the

Northern zone show somewhat larger Pb spikes than granitic rocks elsewhere in the batholith, and consistently deep troughs for Ti, the heavy rare-earth elements and Y.

Figure 7. Chondrite-normalized rare-earth element diagrams of the Kodiak batholith. A) Southern zone. B) Central zone. C) Northern zone. D) Western and Northern satellite groups. E) Mafic, intermediate, and felsic igneous rocks of the Eastern satellite group, outer trenchward belt; granodiorite and granite from the Eastern satellite group, inner trenchward belt adjacent to batholith. F) Kodiak Formation, Ghost Rocks Formation, and country rock inclusion. Other patterns are as in Fig. 6. The Kodiak batholith is characterized by moderately steep light REEs and by gently sloping to flat heavy REEs. Individual zones have similar REE patterns.

Leucogranites from the Northern satellites generally have large negative Eu anomalies and lower total REE contents than the tonalitic and granitic rocks from the main zones of the batholith.

Figure 8. A) Th/Ta vs TiO<sub>2</sub>. B) Ce/Pb vs. Nb/U (symbols as in Fig. 2). Fields for island arc tholeiite, normal MORB and OIB, marine sediments, and the average composition of continental crust are from Klein (2003). The plot of Th/Ta vs. TiO<sub>2</sub> emphasizes the zonal distinction within the batholith (Southern and Central zones as a group compared to the Northern zone). Compositional fields for the batholith as a whole depart from each other and lack orderly trends even within individual zones. The plot of Nb/U versus Ce/Pb (Klein, 2003) shows the Kodiak batholith and flanking igneous groups plot between a calc-alkaline end-member (similar to arc lavas) and an altered oceanic crust end-member..

Figure 9. Histograms of isotopic values for samples from the Kodiak batholith and country rocks: A)  $\epsilon_{Nd}$ . B)  $T_{DM}$  or crustal residence ages. C) Initial  $^{87}Sr/^{86}Sr$ . D)  $^{206}Pb/^{204}Pb$ ; E)  $^{207}Pb/^{204}Pb$ ; F)  $^{208}Pb/^{204}Pb$ . Main batholith includes the Southern, Central, and Northern zones; satellites refer to the Northern, Western, and Eastern satellite groups; inclusion is Kodiak Formation in the granitic rocks of the Central zone.

Figure 10. A)  $^{206}Pb/^{204}Pb$  vs.  $^{207}Pb/^{204}Pb$ , and B)  $^{206}Pb/^{204}Pb$  vs.  $^{208}Pb/^{204}Pb$  for the Kodiak batholith, adjacent satellite groups, Kodiak Formation, and Ghost Rocks Formation (symbols as in Fig. 2).

Orca and Valdez Groups, basaltic tuffs, and granitic rocks (near Cordova) from the eastern Gulf of Alaska are from Barker et al. (1992) and Farmer et al. (1993). Data from Sanak pluton, and Sanak (argillite and greywacke) from the Kodiak-Shumagin shelf from southwest Alaska are from Hill and Morris (1982). The northern Coast Plutonic Complex (CPC) is shown for reference (Godwin et al., 1988; Bevier and Anderson, 1990; Farmer, unpub. data). Also illustrated are the model growth curve for average crust (S&K, tick marks at 250 m.y., Stacey and Kramers, 1974), which closely resembles the composition of the orogene model growth curve (arc rocks). Model growth curves for upper continental crust, orogene, and mantle (tick marks at 400 m.y.) are from Zartman and Doe (1981). The Northern Hemisphere Reference Line (NHRL) is from Hart (1984). A line representing an age of ~1 Byr ( $T_{DM}$  or crustal residence age of the flysch) is shown for reference.

Figure 11.  $\epsilon_{Nd}$  versus initial  $^{87}Sr/^{86}Sr$  for the Kodiak batholith, adjacent satellite groups, Kodiak Formation, and Ghost Rocks Formation (symbols as in Fig. 2). Granitic rocks from the Cordova area (Barker et al., 1992) and the Orca and Valdez Groups (flysch) from eastern Gulf of Alaska (Farmer et al., 1993) are shown for comparison. Nd and Sr isotopic data for the northern Coast Plutonic Complex (CPC, a possible source of recycled material into the accretionary flysch) is shown for reference (Arth et al., 1988; Samson et al., 1991; Farmer et al., 1993, and references therein).

Figure 12. Variation diagrams for A) Sc-K<sub>2</sub>O. B) Sc-Th for the Kodiak batholith (symbols as in Fig. 2) illustrating trends of models for fractional crystallization (FC) and assimilation-fractional crystallization (AFC). Abbreviations: FCSC, path of fractional crystallization of tonalite and granodiorite, Southern zone and Central zones; AFCSC, path of assimilation-fractional crystallization of tonalite and granodiorite, Southern and Central zones; FCN, fractional crystallization of tonalite and granodiorite, Northern zone; AFCN, path of assimilation-fractional crystallization of tonalite and granodiorite, Northern zone. Fractional crystallization and AFC

paths show the evolution of the liquids at 0.1 increments. The FC trend does not link all the granitic rocks. Compositional offsets and diverging trends indicate that the variations cannot be the result of AFC reactions involving a single crustal contaminant or a simple mineral assemblage. The extent and effects of chemical reactions between the magmas and country rocks were limited and AFC reactions did not produce significant and systematic changes in composition of the host granitic magmas. See text for more detailed explanation.

Figure 13. A)  $\epsilon_{\text{Nd}}$  versus  $^{206}\text{Pb}/^{204}\text{Pb}$  illustrating compositional trends in the Kodiak batholith (symbols as in Fig. 2) and possible mixing models relating the mantle wedge source (North Pacific MORB), MORB fluid (subducted altered basaltic crust), and flysch (Kodiak Formation). The fields and compositions representing mantle wedge plus MORB fluids, mantle wedge plus sediment melt or sediment fluid, and possible isotopic trends as a result of mixing were modified from Class et al. (2000), and Debaille et al. (2006). B)  $^{87}\text{Sr}/^{86}\text{Sr}$  versus  $^{206}\text{Pb}/^{204}\text{Pb}$ . C)  $^{206}\text{Pb}/^{204}\text{Pb}$  versus Nd/Pb. D)  $^{207}\text{Pb}/^{204}\text{Pb}$  vs. Ce/Pb. Isotopic and trace element trends are consistent with mixing of source rocks originally derived from the mantle wedge (MORB-type basalt enriched by fluid-soluble elements) as one compositional end-member, together with melts and fluids derived from flysch. Isotopic compositions are intermediate between the mantle wedge source ( $^{87}\text{Sr}/^{86}\text{Sr} < 0.7030$ ;  $\epsilon_{\text{Nd}} \sim +9$ ;  $^{206}\text{Pb}/^{204}\text{Pb} < 18.8$ ), and fluids and/or melts from flysch ( $^{87}\text{Sr}/^{86}\text{Sr} > 0.7065$ ;  $\epsilon_{\text{Nd}} \sim -4$ ;  $^{206}\text{Pb}/^{204}\text{Pb} > 19$ ) of the Kodiak Formation.

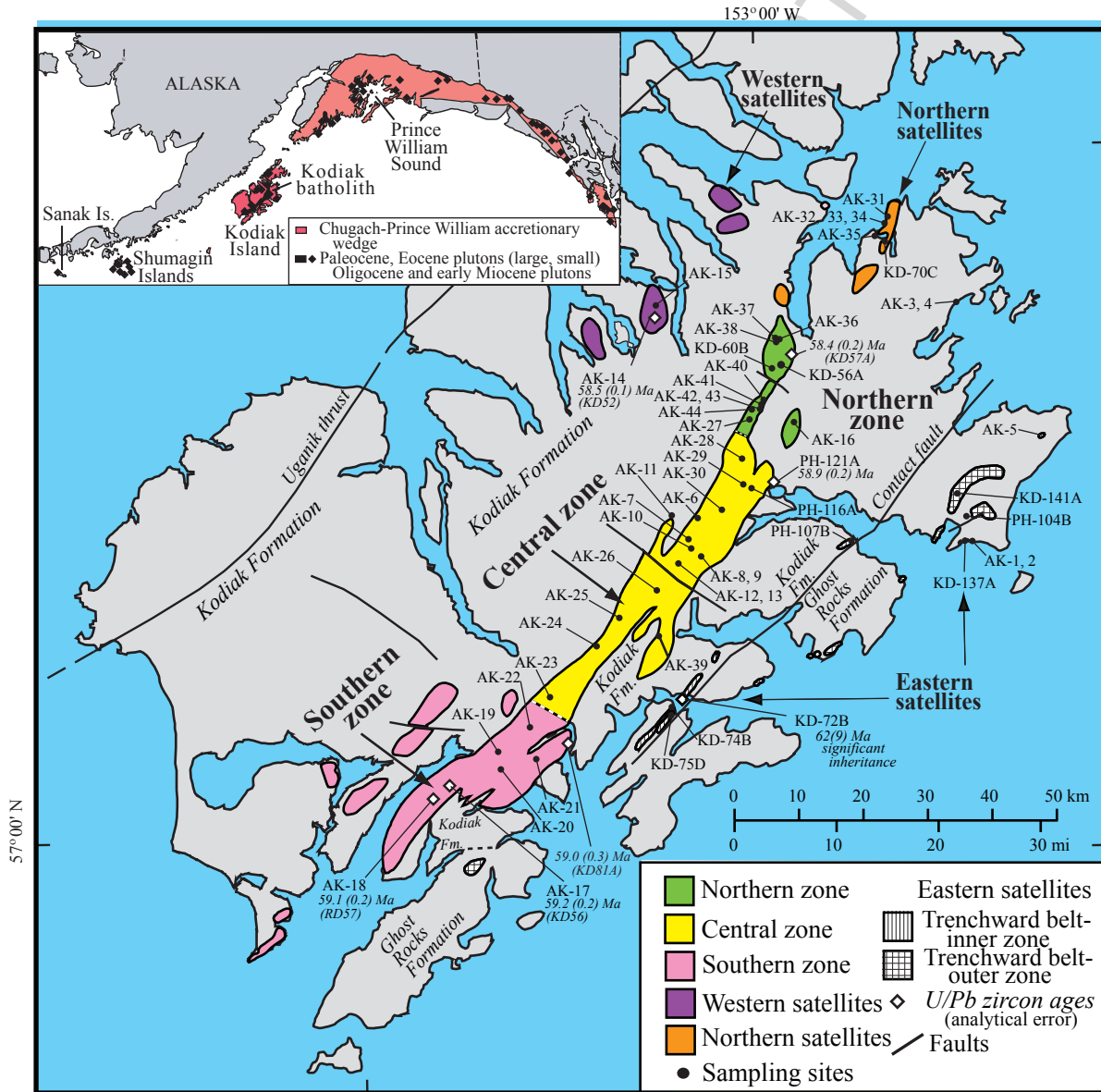
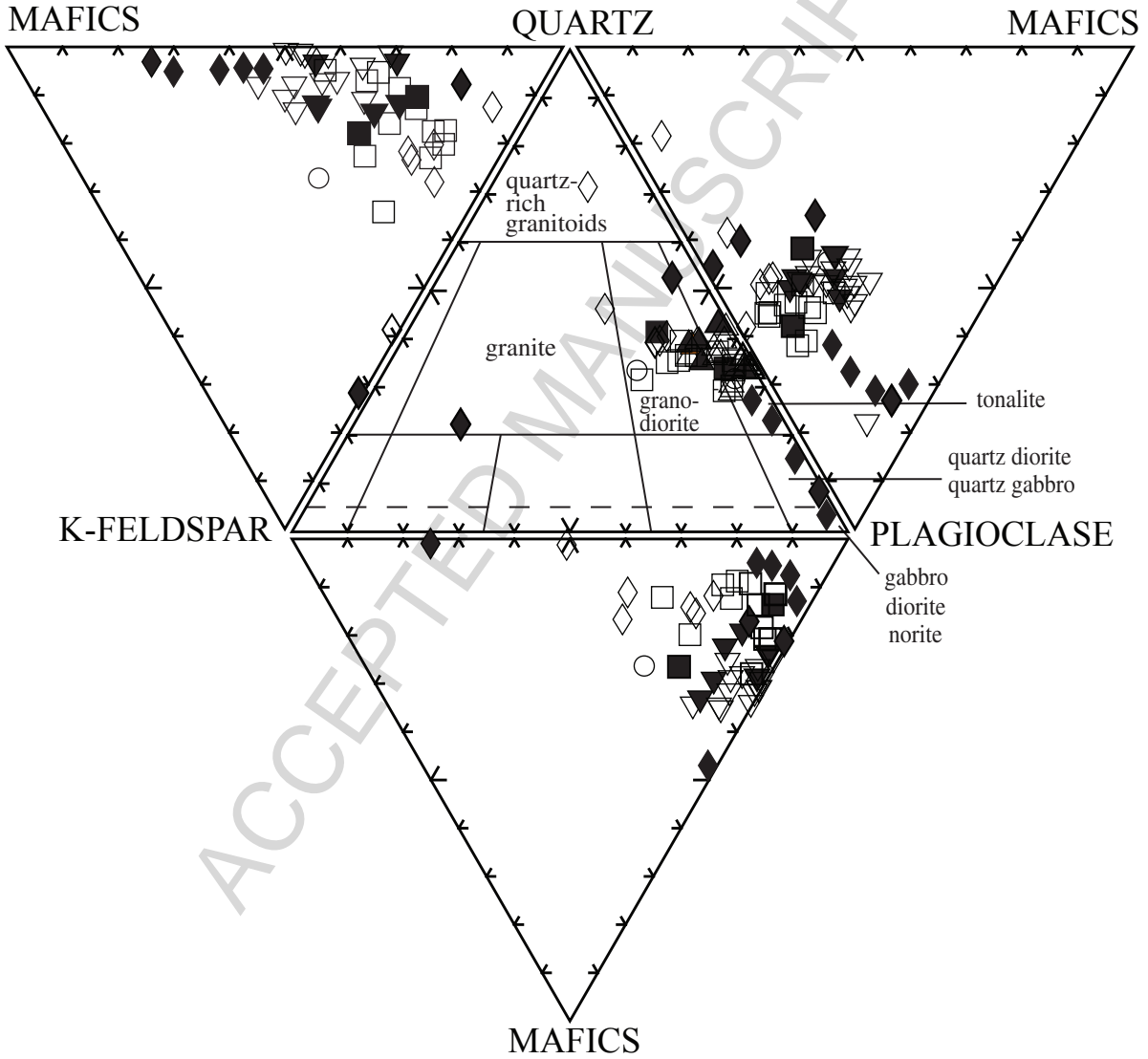


Figure 1



□ Northern zone	■ Western satellites	○ Eastern satellites/outer	* Inclusion
△ Central zone	◇ Northern satellites	● Ghost Rocks Formation	
▲ Southern zone	◆ Eastern satellites/inner	+ Kodiak Formation	

Figure 2

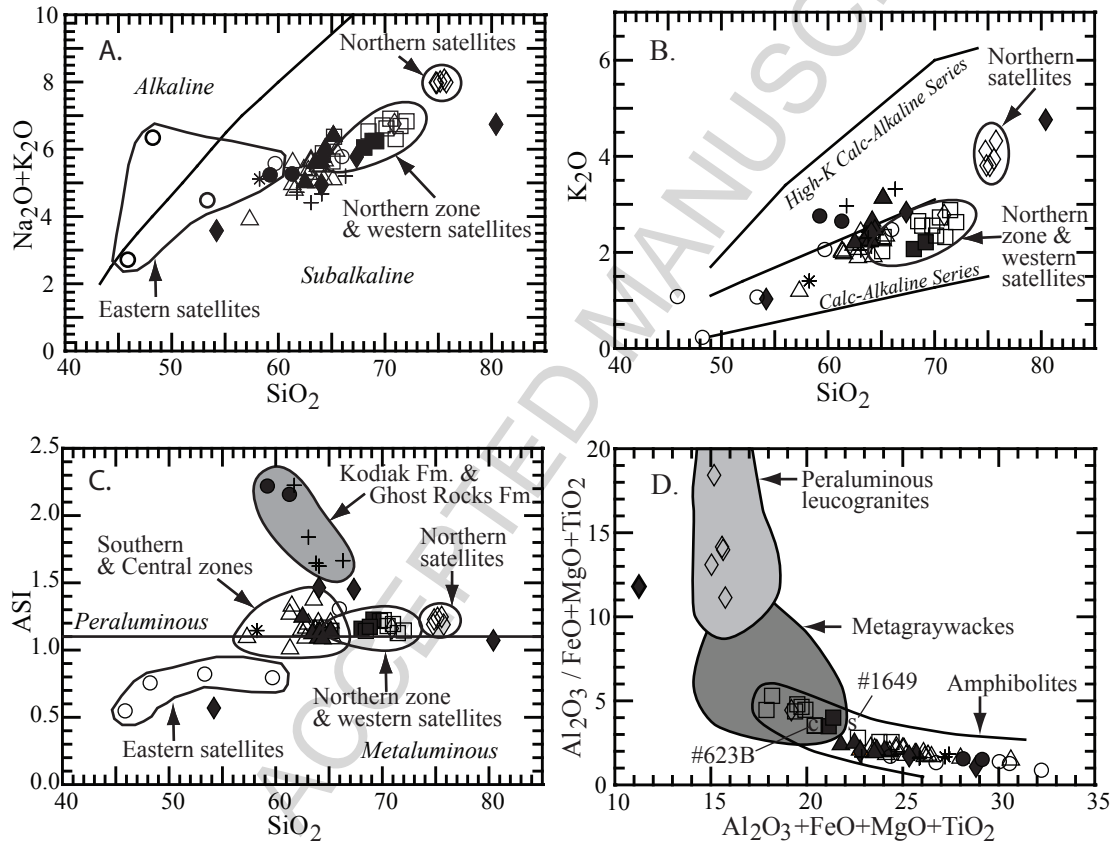


Figure 3

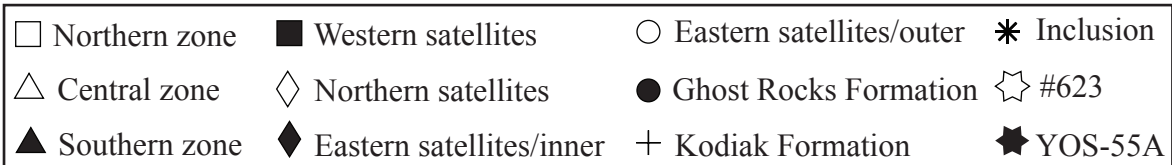
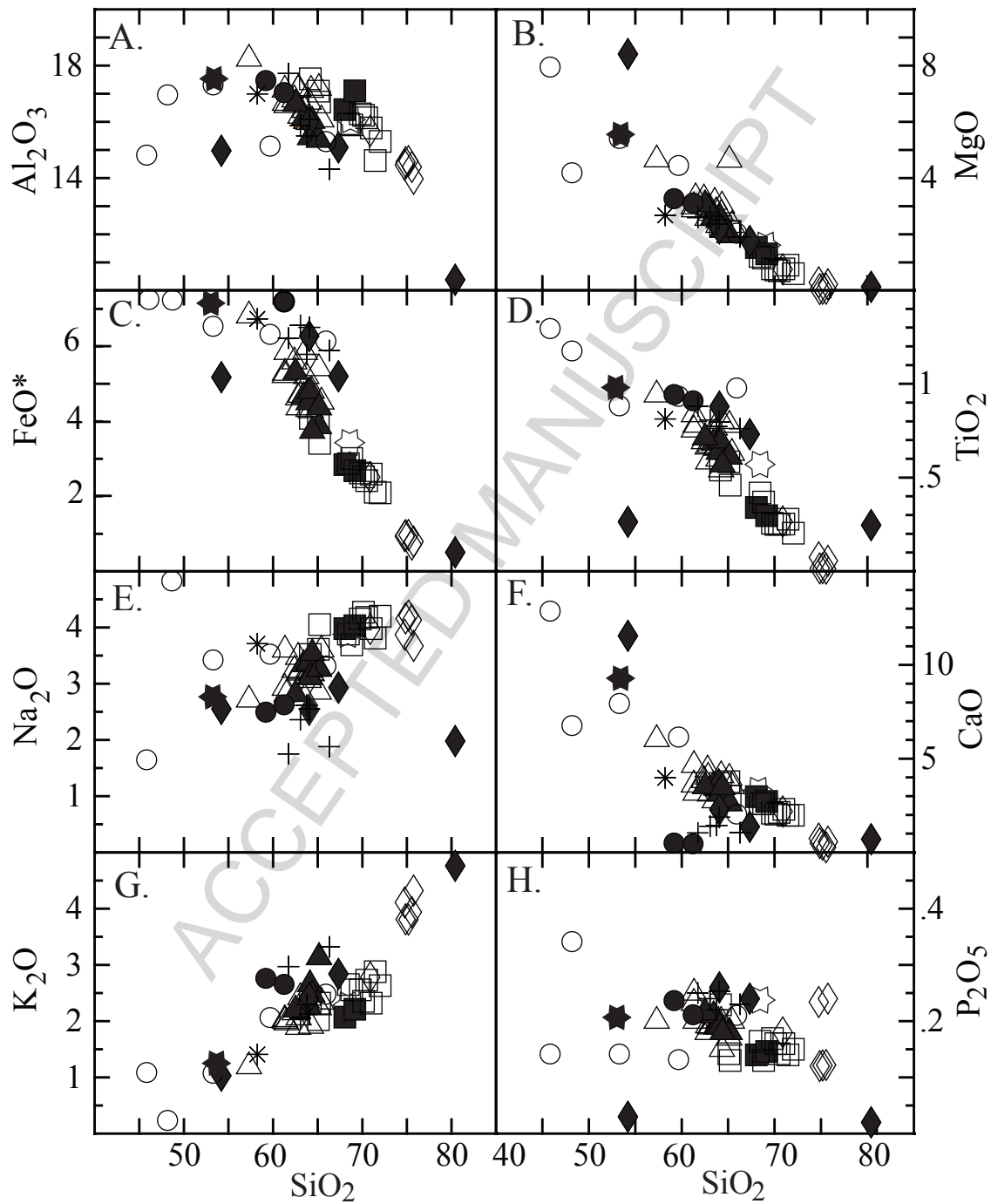


Figure 4

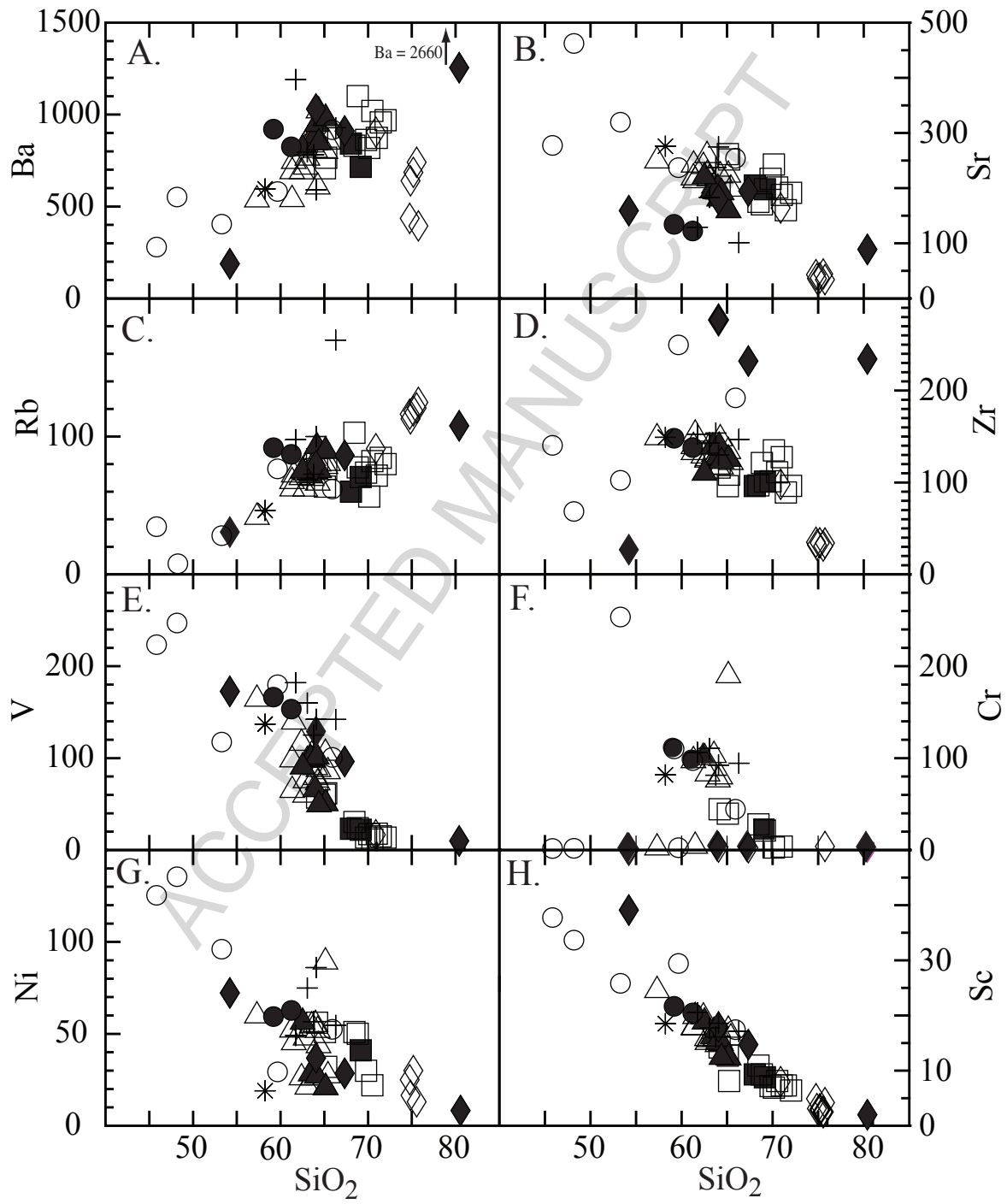


Figure 5

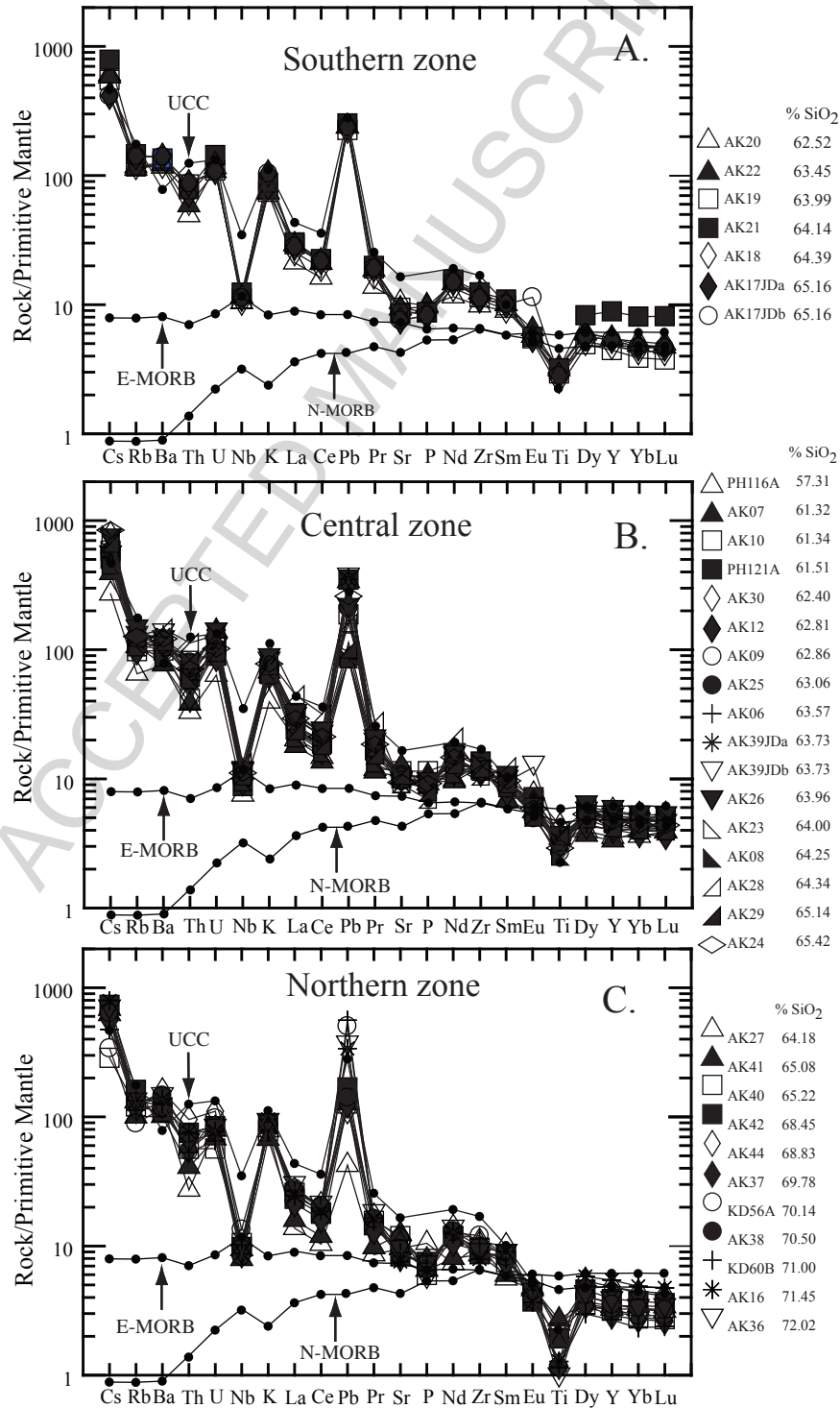


Figure 6

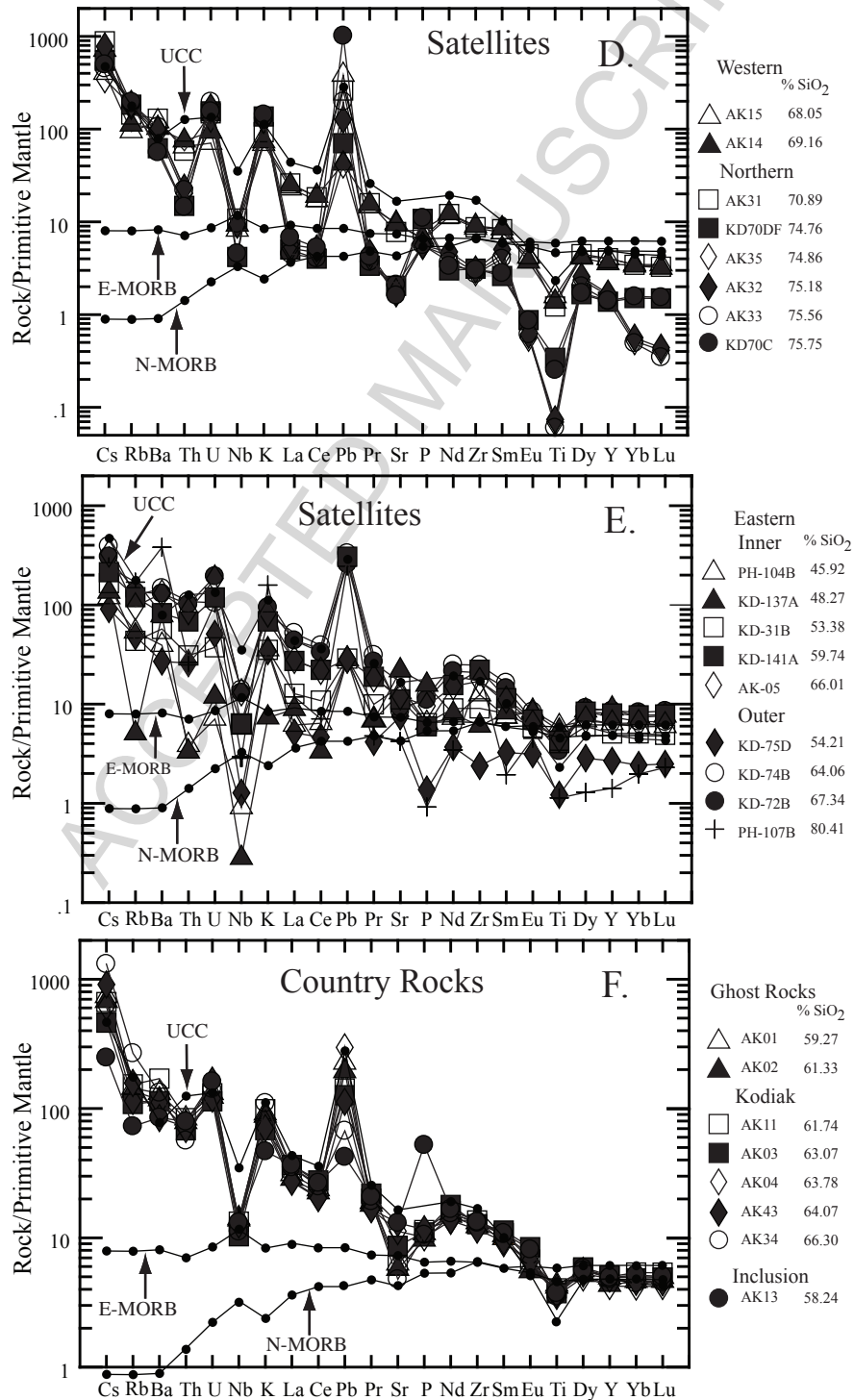


Figure 6 (continued)

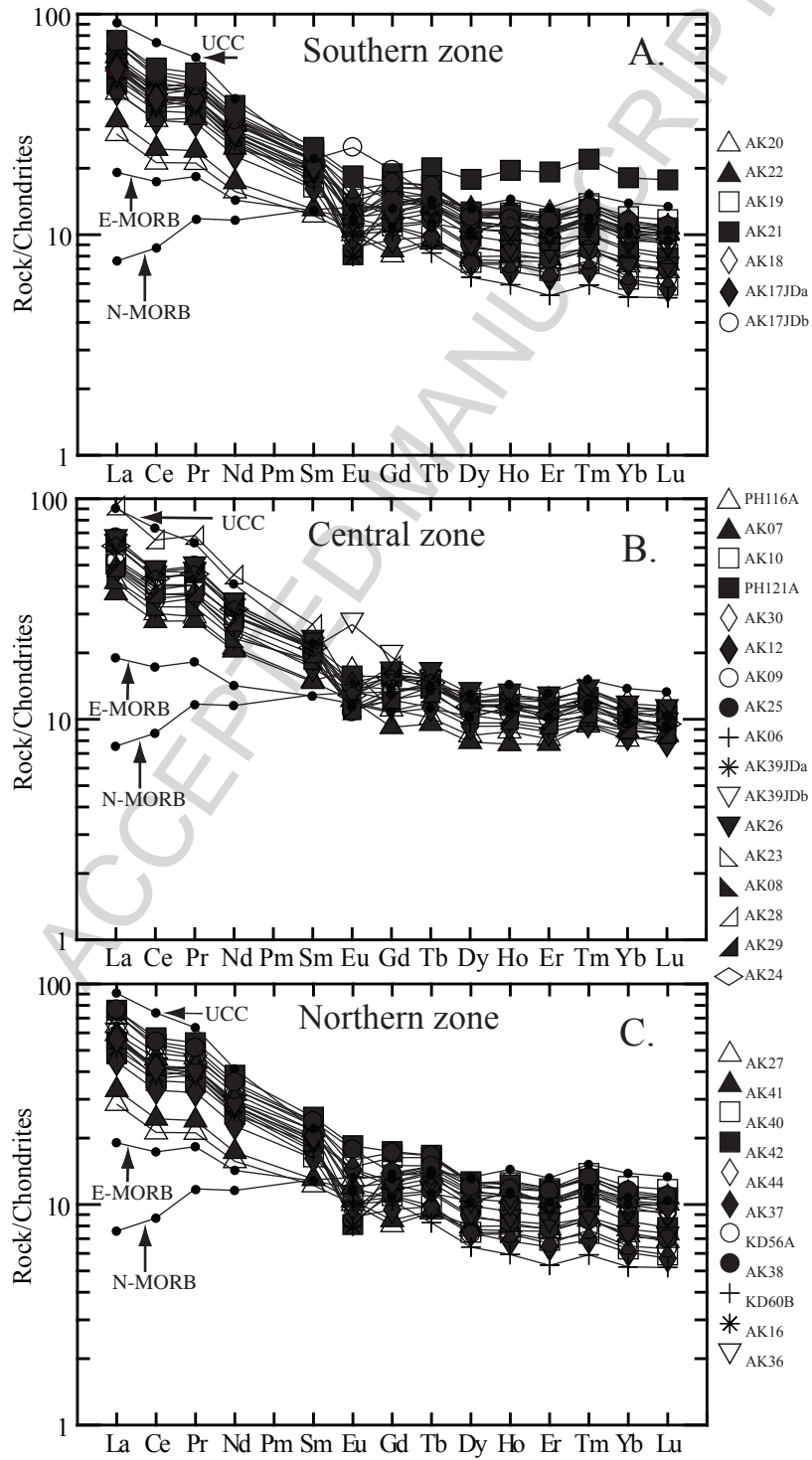


Figure 7

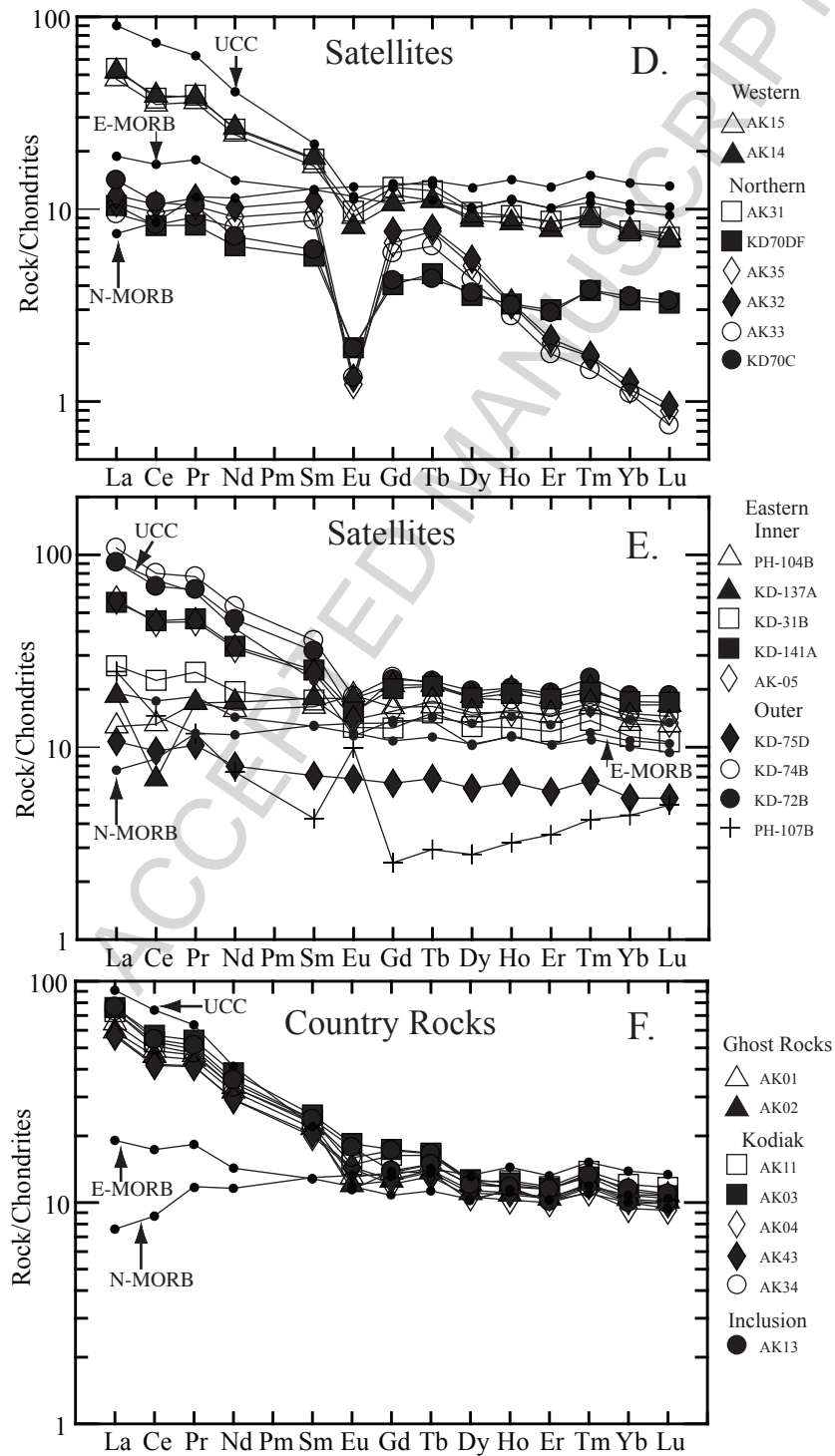


Figure 7 (continued)

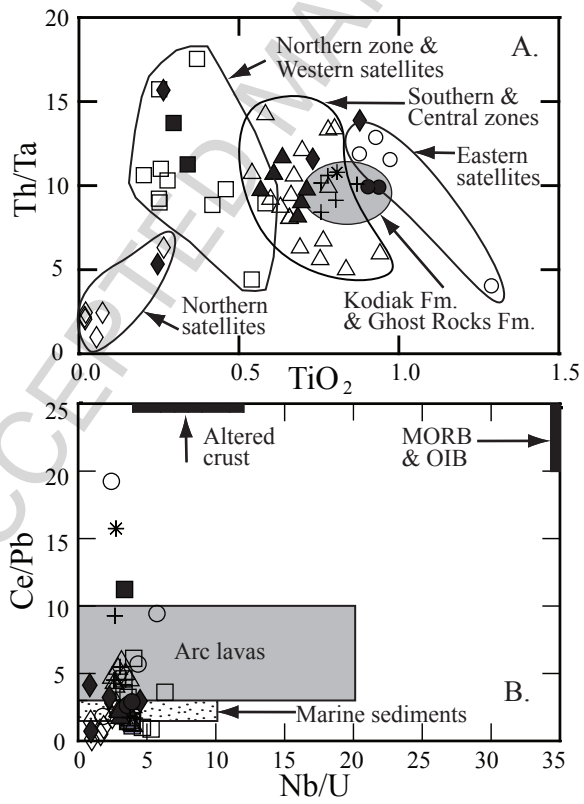


Figure 8

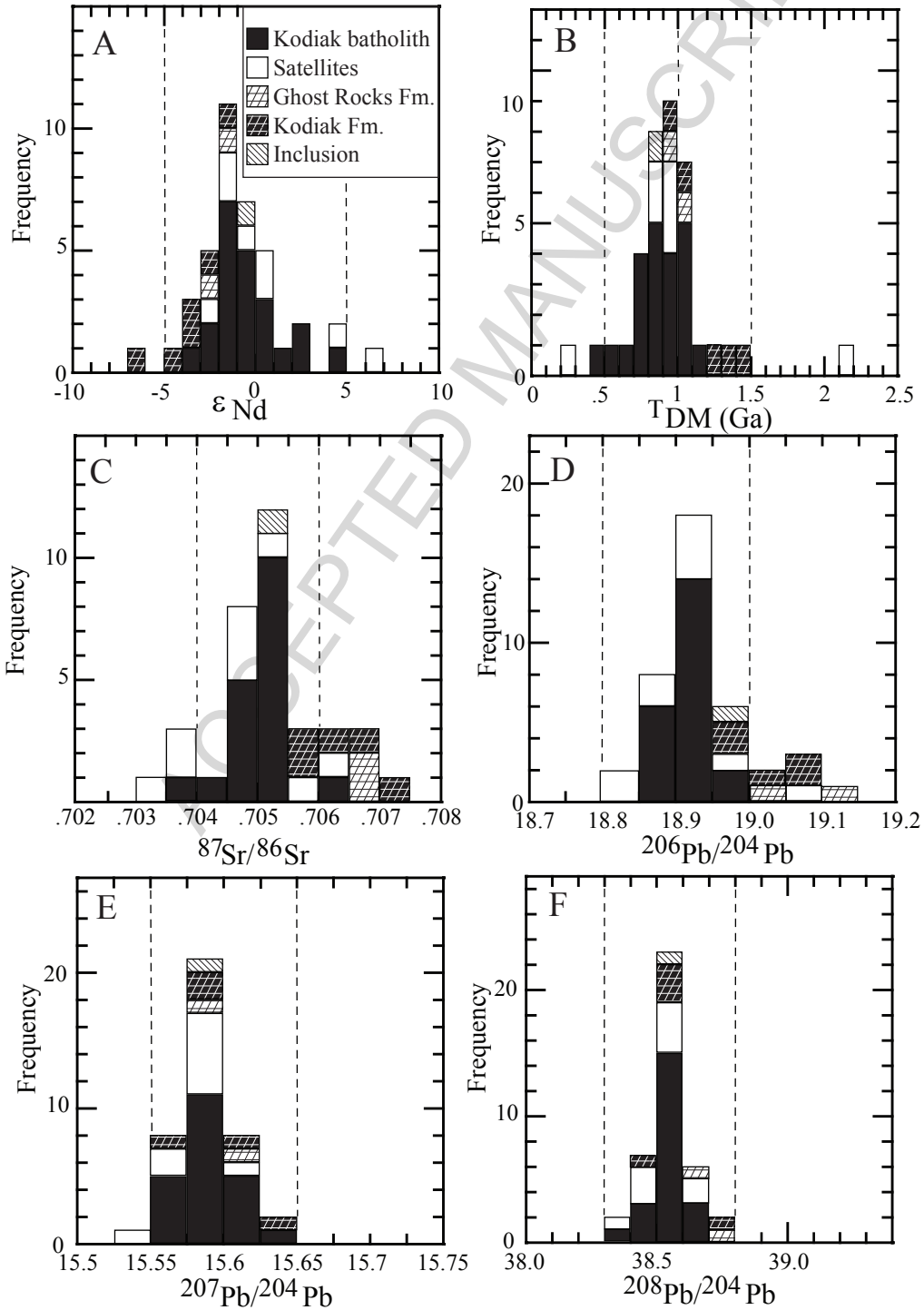


Figure 9

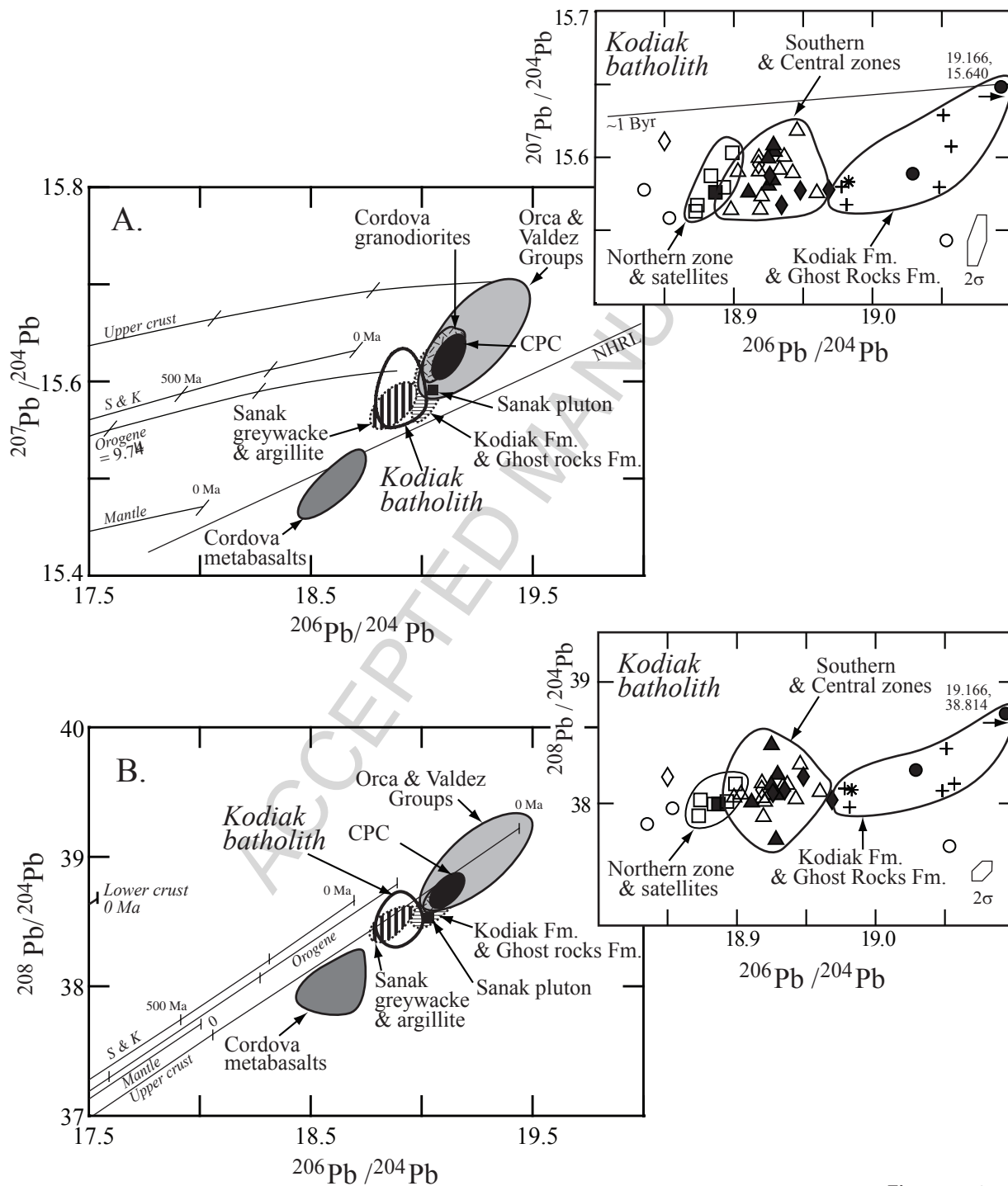


Figure 10

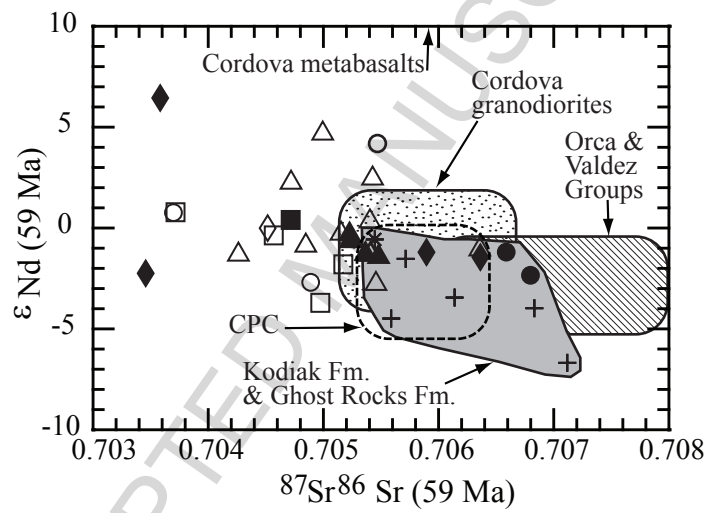


Figure 11

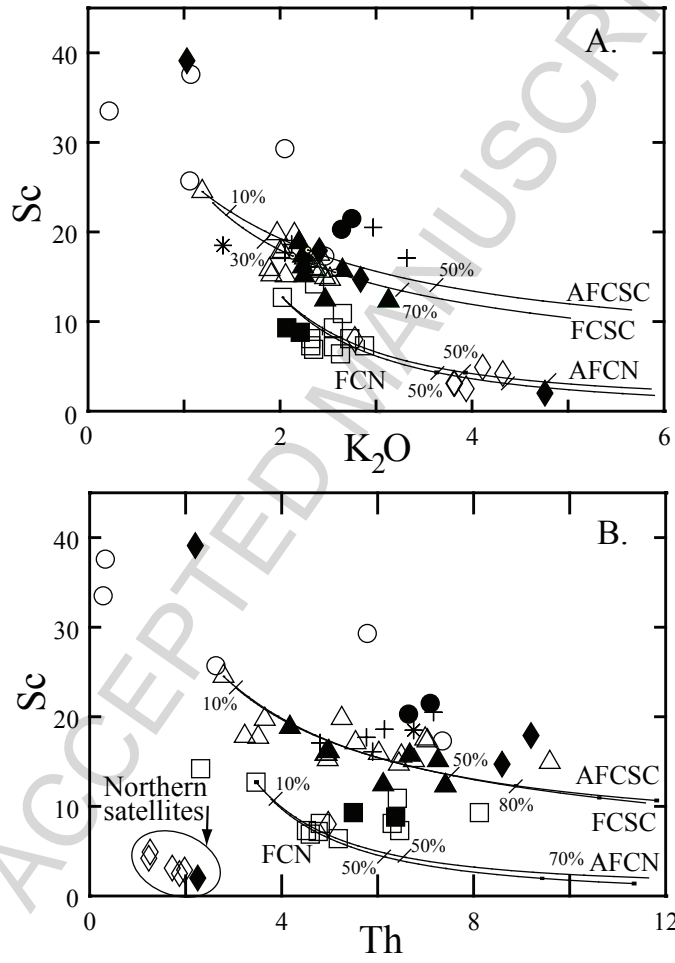


Figure 12

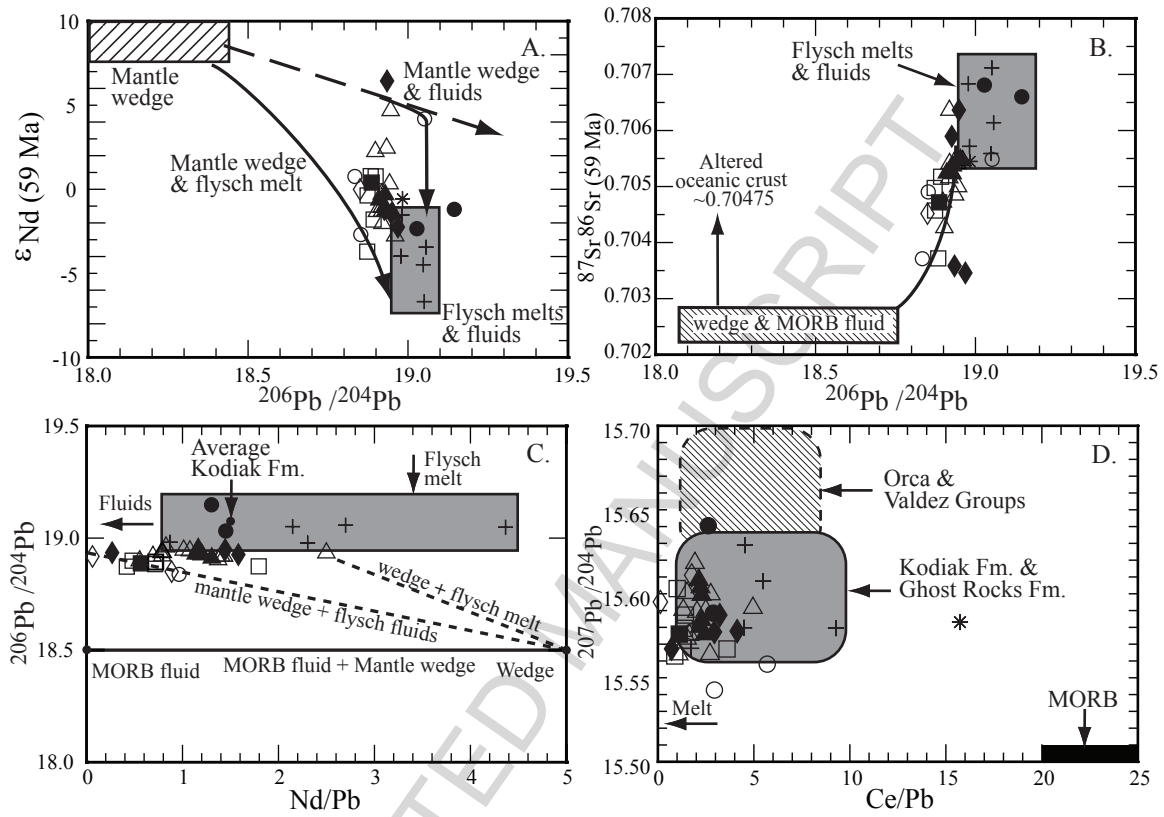


Figure 13

Table 1. Major element compositions (ppm) of representative samples from the Kodiak batholith, adjacent intrusive and volcanic rocks flanking the batholith, Kodiak Island, Alaska

Sample	Northern Satellite Group						Western Satellite Group		Northern Zone				
	RA02AK31	RA02AK32	RA02AK33	RA02AK35	01KD70DV	01KD70C	RA02AK15	RA02AK14	RA02AK37	RA02AK36	RA02AK38	01KD56A	01KD60B
Major elements (wt. %)													
SiO <sub>2</sub>	70.89	75.18	75.56	74.86	74.76	75.75	68.05	69.16	69.78	72.02	70.50	70.14	71.00
Al <sub>2</sub> O <sub>3</sub>	15.67	14.60	14.39	14.56	14.46	13.97	16.43	17.10	16.28	15.30	16.14	16.23	15.78
TiO <sub>2</sub>	0.27	0.02	0.01	0.02	0.07	0.06	0.34	0.30	0.26	0.20	0.25	0.25	0.25
Fe <sub>2</sub> O <sub>3</sub>	2.79	1.08	0.79	1.07	1.04	0.88	3.16	2.98	2.91	2.32	2.69	2.80	2.88
MgO	0.75	0.06	0.06	0.05	0.29	0.22	1.53	1.30	0.77	0.60	0.70	0.73	0.77
MnO	0.07	0.05	0.01	0.05	0.05	0.05	0.06	0.06	0.05	0.04	0.05	0.05	0.05
CaO	2.18	0.41	0.27	0.49	0.73	0.57	2.97	2.71	2.09	1.98	2.13	2.04	2.29
Na <sub>2</sub> O	3.97	4.21	4.13	4.16	3.87	3.67	3.98	4.03	4.15	4.20	4.18	4.27	3.98
K <sub>2</sub> O	2.78	3.80	3.94	3.81	4.11	4.32	2.07	2.21	2.56	2.63	2.73	2.35	2.32
P <sub>2</sub> O <sub>5</sub>	0.18	0.12	0.12	0.12	0.23	0.24	0.14	0.15	0.17	0.15	0.14	0.16	0.16
LOI	0.64	0.77	0.81	0.67	0.64	0.60	1.40	0.90	0.97	0.64	0.64	1.19	0.86
Total	100.18	100.29	100.09	99.85	100.26	100.32	100.13	100.89	99.98	100.09	100.14	100.21	100.35
S %	nd	0.005	0.046	0.009	0.004	nd	nd	<0.001	0.005	nd	0.005	nd	nd
ASI <sup>1</sup>	1.16	1.24	1.25	1.23	1.19	1.19	1.16	1.23	1.22	1.15	1.18	1.22	1.19
K <sub>2</sub> O+Na <sub>2</sub> O	6.75	8.01	8.07	7.97	7.98	7.99	6.05	6.24	6.71	6.83	6.91	6.62	6.30
Na <sub>2</sub> O/K <sub>2</sub> O	0.70	0.90	0.95	0.92	1.06	1.18	0.52	0.55	0.62	0.63	0.65	0.55	0.58

nd, not determined

<sup>1</sup>ASI= mol Al<sub>2</sub>O<sub>3</sub>/(K<sub>2</sub>O+Na<sub>2</sub>O+CaO)<sup>2</sup>Inner: trenchward belt of rocks adjacent to batholith; intruded the Kodiak Formation and the Ghost Rocks Formation<sup>2</sup>Inner: trenchward belt of rocks adjacent to batholith; intruded the Kodiak Formation and the Ghost Rocks Formation<sup>3</sup>Outer: trenchward belt of rocks; intruded the Ghost Rocks Formation

Northern Zone						Central Zone				Central Zone			
RA02AK40	RA02AK44	RA02AK42	RA02AK41	RA02AK27	RA02AK16	RA02AK28	01PH121A	RA02AK29	01PH116A	RA02AK30	RA02AK06	RA02AK07	RA02AK10
65.22	68.83	68.45	65.08	64.18	71.45	64.34	61.51	65.14	57.31	62.40	63.57	61.32	61.34
16.70	15.89	15.93	17.09	17.53	14.62	15.53	16.58	17.19	18.23	16.78	16.41	17.13	16.66
0.46	0.37	0.42	0.58	0.54	0.28	0.80	0.78	0.78	0.94	0.69	0.76	0.75	0.84
3.79	3.34	3.19	4.47	4.53	2.34	5.34	6.49	6.01	7.57	6.21	6.49	5.80	5.87
2.10	1.15	1.21	2.09	2.27	0.90	3.01	3.30	4.64	4.65	3.26	3.14	2.98	2.87
0.07	0.05	0.05	0.07	0.08	0.05	0.08	0.11	0.09	0.12	0.11	0.12	0.09	0.10
2.99	2.59	2.58	3.76	3.68	1.98	3.13	3.16	3.96	6.02	3.84	2.76	3.59	4.64
4.05	3.69	3.88	3.61	3.52	3.81	3.18	2.81	2.85	2.71	3.24	2.74	2.92	3.60
2.32	2.56	2.65	2.03	2.36	2.88	2.47	1.97	2.24	1.19	2.15	2.26	2.03	2.00
0.13	0.13	0.16	0.14	0.23	0.14	0.15	0.20	0.17	0.20	0.21	0.20	0.23	0.25
1.88	0.65	0.82	0.90	0.93	0.71	1.06	2.81	1.22	1.25	1.15	1.61	2.07	0.81
99.71	99.25	99.34	99.82	99.84	99.16	99.09	99.72	104.29	100.19	100.04	100.06	98.92	98.97
nd	0.006	0.005	0.006	0.004	nd	nd	nd	0.002	nd	nd	0.012	<0.001	nd
1.14	1.17	1.14	1.14	1.17	1.13	1.14	1.33	1.20	1.09	1.15	1.37	1.27	1.01
6.37	6.25	6.53	5.64	5.88	6.69	5.65	4.78	5.09	3.90	5.39	5.00	4.95	5.60
0.57	0.69	0.68	0.56	0.67	0.76	0.78	0.70	0.79	0.44	0.66	0.82	0.69	0.56

Central Zone			Central Zone			Central Zone			Southern Zone				
RA02AK08	RA02AK09	RA02AK12	RA02AK26	RA02AK25	RA02AK39A	RA02AK39B	RA02AK24	RA02AK23	RA02AK22	RA02AK19	RA02AK21	RA02AK20	RA02AK17A
64.25	62.86	62.81	63.96	63.06	63.73	63.73	65.42	64.00	63.45	63.99	64.14	62.52	65.16
17.12	17.18	17.14	16.10	16.20	16.02	16.02	16.07	16.70	16.11	15.98	15.44	16.64	15.35
0.54	0.58	0.66	0.60	0.67	0.66	0.66	0.63	0.70	0.68	0.64	0.70	0.71	0.61
4.76	4.85	5.14	4.80	5.22	5.22	5.22	5.02	5.30	5.18	5.00	5.33	5.90	4.29
2.72	2.93	2.57	2.32	2.75	2.80	2.80	2.32	2.49	2.60	2.53	2.58	3.05	1.96
0.09	0.08	0.08	0.09	0.08	0.09	0.09	0.09	0.09	0.09	0.09	0.09	0.10	0.07
4.09	4.02	4.40	3.39	3.12	3.44	3.44	3.51	3.44	3.55	3.68	3.12	3.51	2.60
3.19	3.19	3.47	3.24	3.22	3.12	3.12	3.60	3.06	3.34	3.37	3.11	2.81	3.26
1.91	2.06	1.89	2.52	2.42	2.37	2.37	2.34	2.41	2.24	2.25	2.65	2.20	3.13
0.20	0.19	0.18	0.20	0.19	0.19	0.19	0.20	0.19	0.21	0.19	0.19	0.22	0.18
1.03	1.32	1.12	1.80	2.27	1.31	1.31	0.71	1.03	1.41	1.05	1.38	1.63	2.21
99.90	99.26	99.46	99.01	99.21	98.94	98.94	99.91	99.41	98.86	98.76	98.72	99.29	98.82
0.022	0.007	nd	nd	nd	nd	nd	nd	0.008	nd	nd	nd	0.013	nd
1.16	1.16	1.09	1.13	1.19	1.15	1.15	1.08	1.20	1.12	1.09	1.13	1.24	1.14
5.10	5.25	5.36	5.76	5.64	5.49	5.49	5.94	5.47	5.58	5.62	5.76	5.01	6.39
0.60	0.65	0.54	0.78	0.75	0.76	0.76	0.65	0.79	0.67	0.67	0.85	0.78	0.96

Southern Zone		Eastern Satellite Group				Eastern Satellite Group				
RA02AK17B	RA02AK18	01PH107B <sup>2</sup>	01KD72B <sup>2</sup>	01KD74B <sup>2</sup>	01KD75D <sup>2</sup>	RA02AK05 <sup>3</sup>	01KD141A <sup>3</sup>	02KD31B <sup>3</sup>	01PH104B <sup>3</sup>	01KD137A <sup>3</sup>
65.16	64.39	80.41	67.34	64.06	54.21	66.01	59.74	53.38	45.92	48.27
15.35	16.02	10.38	15.09	15.98	14.97	15.27	15.11	17.28	14.79	16.93
0.61	0.57	0.25	0.73	0.88	0.26	0.97	0.93	0.88	1.29	1.17
4.29	4.15	0.56	5.78	6.97	5.75	6.80	7.00	7.24	9.17	9.25
1.96	2.16	0.13	1.76	2.21	8.41	2.01	4.42	5.38	7.92	4.16
0.07	0.07	0.01	0.09	0.10	0.11	0.11	0.12	0.12	0.21	0.19
2.60	3.46	0.70	1.37	2.28	11.55	2.00	6.11	7.90	12.83	6.72
3.26	3.54	1.98	2.93	2.53	2.55	3.30	3.51	3.41	1.63	6.11
3.13	2.47	4.76	2.84	2.41	1.03	2.47	2.05	1.06	1.07	0.22
0.18	0.18	0.02	0.24	0.26	0.03	0.21	0.13	0.14	0.14	0.34
2.21	1.63	0.54	2.15	2.18	1.41	1.91	1.27	3.04	4.16	5.75
98.82	98.64	99.74	100.32	99.86	100.28	101.06	100.39	99.83	99.13	99.11
nd	nd	nd	nd	nd	nd	0.036	nd	0.034	nd	nd
1.14	1.08	1.07	1.45	1.46	0.57	1.30	0.79	0.82	0.54	0.75
6.39	6.01	6.74	5.77	4.94	3.58	5.77	5.56	4.47	2.70	6.33
0.96	0.70	2.40	0.97	0.95	0.40	0.75	0.58	0.31	0.66	0.04

Table 2. Trace element compositions (ppm) of representative samples from the Kodiak batholith, adjacent intrusive and volcanic rocks flanking the batholith, Kodiak Island, Alaska

Sample	Northern Satellite Group						Western Satellite Group		Northern Zone			Northern Zor	
	RA02AK31	RA02AK32	RA02AK33	RA02AK35	01KD70DV	01KD70C	RA02AK15	RA02AK14	RA02AK37	RA02AK36	RA02AK38	01KD56A	01KD60B
Rb	91	119	121	113	116	125	60	71	74	80	82	56	72
Cs	7.0	6.1	3.6	2.7	4.3	3.9	3.2	5.6	4.4	5.2	5.0	2.7	3.8
Sr	164	37	44	36	43	34	205	198	217	191	201	243	188
Ba	905	686	740	639	435	394	842	715	862	969	1020	818	873
Rb/Sr	0.56	3.20	2.73	3.15	2.70	3.68	0.29	0.36	0.34	0.42	0.41	0.23	0.38
Cs/Ta	8.9	7.0	3.9	3.2	8.3	3.1	6.5	12.1	10.2	10.7	12.6	5.4	7.5
La	17.8	3.9	3.1	3.6	3.4	4.7	15.6	17.2	14.6	19.5	18.5	19.1	18.3
Ce	32.7	9.1	7.2	8.3	7.1	9.4	30.3	33.7	28.5	35.5	35.8	36.0	35.0
Pr	4.4	1.3	1.0	1.2	0.9	1.2	4.0	4.3	3.6	4.7	4.5	4.4	4.3
Nd	16.4	6.4	5.0	5.7	4.1	4.5	15.4	16.7	14.3	17.6	17.7	17.2	16.7
Sm	3.7	2.2	1.8	2.0	1.2	1.2	3.4	3.7	3.3	3.8	3.9	3.6	3.5
Eu	0.8	0.1	0.1	0.1	0.1	0.1	0.7	0.6	0.7	0.7	0.6	0.8	0.8
Gd	3.6	2.1	1.6	1.8	1.1	1.2	3.3	2.9	2.6	3.4	3.1	3.0	2.9
Tb	0.59	0.37	0.30	0.36	0.22	0.20	0.52	0.52	0.46	0.53	0.54	0.44	0.39
Dy	3.30	1.88	1.48	1.74	1.22	1.26	3.12	3.01	2.55	2.99	3.06	2.51	2.20
Ho	0.65	0.23	0.19	0.22	0.22	0.22	0.64	0.59	0.48	0.59	0.58	0.51	0.41
Er	1.95	0.48	0.40	0.45	0.67	0.65	1.93	1.75	1.45	1.83	1.73	1.50	1.19
Tm	0.27	0.05	0.04	0.05	0.11	0.11	0.28	0.27	0.21	0.26	0.25	0.23	0.18
Yb	1.69	0.28	0.24	0.25	0.74	0.77	1.71	1.66	1.33	1.56	1.64	1.42	1.15
Lu	0.24	0.03	0.03	0.03	0.11	0.11	0.26	0.24	0.19	0.24	0.24	0.21	0.18
Y	18	8	6	7	6	6	18	16	13	17	16	15	12
La/Yb	10.5	14.1	12.9	14.0	4.7	6.0	9.1	10.4	11.0	12.5	11.3	13.4	15.9
Total REE	88.0	28.5	22.5	25.8	21.2	25.7	81.2	87.2	74.3	93.3	92.1	91.0	87.2
Ce/Pb	10.5	2.5	1.7	3.0	2.2	2.9	20.4	17.2	16.8	21.4	20.2	17.6	25.6
Zr	98	34	31	32	35	34	96	101	101	96	111	135	127
Hf	3.2	2.1	1.9	1.9	1.8	1.4	3.1	3.4	3.4	3.2	3.5	3.5	3.4
Nb	8	7	7	7	3	3	6	7	6	6	6	10	7
Ta	0.79	0.87	0.91	0.84	0.52	1.26	0.49	0.46	0.43	0.49	0.40	0.50	0.50
Th	5.0	2.0	1.9	1.7	1.3	1.2	5.5	6.4	4.8	5.2	6.3	4.6	4.5
U	3.1	3.6	4.1	2.7	3.3	3.3	1.5	2.0	1.7	1.7	1.8	2.0	1.4
Nb/Ta	9.8	7.7	7.5	7.9	5.7	2.6	12.0	14.2	14.2	12.2	14.8	19.2	14.4
Zr/Hf	30.2	16.7	16.6	16.7	19.9	23.8	31.0	29.7	30.2	30.1	31.8	38.6	37.9
Th/U	13.0	19.3	33.8	41.4	27.0	31.7	18.9	12.6	16.7	15.3	16.3	21.0	19.1
Nb/U	2.5	1.9	1.6	2.5	0.9	1.0	3.9	3.4	3.6	3.6	3.3	4.7	5.3

Sc	8	3	3	3	5	4	9	9	7	6	8	7	7
Co	nd	<1	<1	<1	<1	nd	nd	5	3	nd	3	nd	nd
Ni	<20	30	13	16	25	<20	<20	41	30	<20	22	<20	<20
Au (ppb)	1.4	0.4	10.9	<0.2	<0.2	<2	<2	2.1	10.2	<0.2	3.8	0.4	<0.2
Ir	<5	<5	<5	<5	<5	<5	<5	<5	<5	<5	<5	<5	<5
Mo	4.0	<2	<2	<2	<2	<2	5.3	2.2	<2	5.0	<2	<2	<2
Ge	1.1	1.3	1.4	1.1	1.5	1.8	0.6	1.2	1.2	1.3	1.1	0.9	1.1
Sn	2.8	3.6	4.4	2.8	1.9	2.6	2.0	1.6	1.5	1.4	1.6	1.5	1.4
Cu	<10	8	25	15	1	<10	<10	8	6	<10	3	<10	<10
Ag	<0.2	0.4	10.9	<0.2	<0.2	<0.2	<0.2	2.1	10.2	<0.2	3.8	<0.2	<0.2
Zn	49.0	53.0	29.0	98.9	33.0	<30	53.2	76.0	82.8	47.9	82.0	40.0	46.5
Cd	nd	<0.5	<0.5	<0.5	<0.5	nd	nd	<0.5	0.9	<0.5	<0.5	nd	nd
Hg (ppb)	12	100	834	63	57	121	31	11	360	121	5	118	119
Pb	19	9	14	3	5	72	27	3	9	25	10	36	40
Ga	18	19	19	18	13	13	16	17	18	18	18	19	18
In	<0.1	<0.1	<0.1	<0.1	<0.1	<0.1	<0.1	<0.1	<0.1	<0.1	<0.1	<0.1	<0.1
Tl	0.39	0.65	0.72	0.47	0.52	0.69	0.17	0.44	0.50	0.60	0.46	0.25	0.38
As	11.6	33.6	355.0	<0.5	2.1	3.3	10.9	1.3	1.8	3.3	13.1	7.7	2.5
Sb	0.8	0.2	9.4	0.3	0.2	nd	0.6	0.2	0.3	0.5	<0.1		
Bi	0.14	0.11	0.17	0.91	<0.1	<0.1	<0.1	0.17	0.21	<0.1	0.52	0.11	<0.1
Se	0.13	0.15	0.38	0.28	0.14	0.12	0.12	0.24	0.15	<0.1	0.34	0.23	0.25
Te	<0.1	<0.1	<0.1	<0.1	<0.1	<0.1	<0.1	<0.1	<0.1	<0.1	<0.1	<0.1	<0.1
V	16.6	<5	<5	<5	<5	<5	23.1	22.1	13.4	13.5	11.3	17.2	17.8
Cr	14.0	6.0	8.0	6.0	9.0	3.9	33.0	21.2	19.0	8.0	10.0	2.7	3.8
W	<0.5	0.8	0.9	<0.5	<0.5	<0.5	<0.5	<0.5	<0.5	<0.5	<0.5	1.5	<0.5
Br	<0.5	<0.5	<0.5	<0.5	<0.5	<0.5	<0.5	<0.5	<0.5	<0.5	<0.5	<0.5	<0.5

nd, not determined

<sup>2</sup>Inner: trenchward belt of rocks adjacent to batholith; intruded the Kodiak Formation and the Ghost Rocks Formation

<sup>3</sup>Outer: trenchward belt of rocks; intruded the Ghost Rocks Formation

ie	Northern Zone					Central Zone				Central Zone				
	RA02AK40	RA02AK44	RA02AK42	RA02AK41	RA02AK27	RA02AK16	RA02AK28	01PH121A	RA02AK29	01PH116A	RA02AK30	RA02AK06	RA02AK07	RA02AK10
	77	78	103	64	83	84	80	72	78	41	70	70	67	62
	2.3	4.7	5.8	4.9	5.4	6.2	5.7	4.0	5.2	2.1	6.1	5.0	3.1	4.6
	252	170	175	261	203	160	191	213	223	249	239	204	218	241
	765	1100	830	707	866	957	1020	745	800	535	688	834	537	688
	0.30	0.46	0.59	0.24	0.41	0.53	0.42	0.34	0.35	0.17	0.29	0.34	0.31	0.26
	4.6	10.1	8.0	12.7	10.3	10.0	8.0	7.5	9.9	4.6	10.5	6.1	5.3	6.6
	17.8	18.4	15.9	10.9	9.4	16.8	30.6	20.9	16.0	13.8	15.5	16.5	12.3	16.6
	32.4	36.7	31.5	21.2	18.4	33.2	56.2	40.7	31.8	26.1	29.0	32.0	24.1	33.3
	4.3	4.7	4.0	2.7	2.4	4.5	7.6	5.2	4.2	3.3	4.0	4.1	3.1	4.6
	16.2	18.7	16.1	10.9	9.9	17.3	28.4	20.5	17.3	13.3	15.2	16.3	12.9	18.3
	3.3	4.4	3.8	2.6	2.5	4.4	5.5	4.4	4.0	3.0	3.6	3.7	3.0	4.2
	0.8	0.7	0.6	0.8	0.8	0.6	1.0	1.2	0.8	1.3	1.1	0.9	0.9	1.1
	3.0	3.7	3.2	2.3	2.2	4.1	4.8	4.3	3.4	3.1	3.8	3.0	2.5	4.4
	0.46	0.69	0.59	0.44	0.43	0.70	0.71	0.65	0.62	0.48	0.66	0.56	0.45	0.72
	2.56	3.96	3.39	2.73	2.64	4.28	3.84	3.96	3.58	2.90	4.11	3.30	2.70	4.28
	0.52	0.76	0.65	0.56	0.53	0.89	0.73	0.82	0.69	0.62	0.88	0.67	0.54	0.91
	1.55	2.33	1.98	1.75	1.70	2.67	2.23	2.52	2.12	1.83	2.73	2.04	1.74	2.70
	0.22	0.35	0.30	0.26	0.26	0.39	0.31	0.37	0.32	0.28	0.41	0.30	0.29	0.38
	1.38	2.14	1.85	1.70	1.60	2.40	1.96	2.38	1.98	1.78	2.59	2.01	1.95	2.38
	0.20	0.31	0.27	0.25	0.23	0.35	0.29	0.37	0.29	0.29	0.39	0.30	0.29	0.35
	14	22	18	16	15	25	20	23	19	16	26	18	15	24
	12.9	8.6	8.6	6.4	5.9	7.0	15.6	8.8	8.1	7.8	6.0	8.2	6.3	7.0
	84.8	97.9	84.2	59.1	52.9	92.4	144.1	108.3	87.1	72.1	83.9	85.8	66.8	94.3
	27.2	15.8	17.7	14.9	11.0	20.5	20.5	21.6	16.0	19.5	13.0	10.8	8.2	16.2
	109	121	97	96	116	89	117	153	134	149	129	131	139	132
	3.1	3.9	3.3	2.9	3.5	3.1	3.6	3.8	4.0	3.6	3.6	3.9	4.0	3.7
	8	8	7	6	7	6	9	6	7	5	8	9	8	8
	0.49	0.46	0.72	0.39	0.52	0.63	0.72	0.53	0.53	0.47	0.58	0.83	0.58	0.70
	4.8	8.1	6.4	3.5	2.3	6.5	9.6	5.3	7.0	2.8	3.6	5.5	3.2	3.5
	1.2	2.3	1.8	1.4	1.7	1.6	2.7	1.9	2.0	1.3	2.2	3.0	2.9	2.1
	15.4	16.7	9.7	14.5	12.8	10.0	13.2	11.8	14.1	11.4	14.0	10.4	13.7	11.6
	35.1	31.4	29.1	32.6	33.0	29.1	32.5	40.1	33.8	41.4	36.1	33.8	34.8	35.3
	33.8	16.6	17.6	12.9	15.4	13.5	14.0	18.1	15.0	19.3	11.5	13.9	21.8	13.4
	6.3	3.3	3.9	4.0	4.0	3.9	3.4	3.3	3.7	4.0	3.6	2.9	2.7	4.0



Central Zone			Central Zone			Central Zone			Southern Zone			
RA02AK08	RA02AK09	RA02AK12	RA02AK26	RA02AK25	RA02AK39A	RA02AK39B	RA02AK24	RA02AK23	RA02AK22	RA02AK19	RA02AK21	RA02AK20
66	74	62	89	80	79	79	80	80	71	75	93	75
3.5	4.5	3.9	5.6	4.3	4.1	4.1	6.7	6.0	4.6	4.3	6.2	4.8
222	225	259	199	217	194	194	198	193	196	199	180	221
605	714	816	804	762	910	910	850	870	854	882	946	815
0.30	0.33	0.24	0.45	0.37	0.41	0.41	0.41	0.41	0.36	0.37	0.51	0.34
7.7	9.4	7.5	8.0	7.1	6.7	6.7	9.6	10.4	7.5	7.0	8.4	11.2
14.1	17.1	15.8	21.2	21.9	20.2	20.2	20.1	17.6	20.1	20.2	20.9	14.5
28.0	34.6	30.6	40.2	40.7	37.9	37.9	37.5	35.2	37.3	39.2	40.0	28.6
3.6	4.5	4.1	5.4	5.5	5.1	5.1	5.1	4.6	5.1	5.3	5.5	3.8
14.7	18.5	16.0	20.9	21.1	19.7	19.7	19.9	18.5	19.8	20.9	21.1	15.6
3.7	4.4	3.5	4.6	4.5	4.2	4.2	4.3	4.9	4.5	4.4	4.9	4.0
0.9	0.8	1.0	1.0	1.0	1.1	2.1	1.0	0.9	1.1	0.9	0.9	1.0
3.3	3.6	3.4	4.5	4.3	4.3	5.3	4.2	3.6	4.5	4.3	5.2	3.8
0.66	0.67	0.53	0.76	0.71	0.69	0.69	0.69	0.69	0.76	0.65	0.94	0.71
3.99	3.83	3.19	4.47	4.09	4.00	4.00	3.92	4.17	4.39	3.64	6.11	4.48
0.80	0.74	0.65	0.90	0.85	0.81	0.81	0.80	0.85	0.90	0.73	1.37	0.92
2.49	2.25	1.97	2.80	2.51	2.51	2.51	2.36	2.71	2.72	2.12	4.33	2.81
0.38	0.34	0.29	0.40	0.36	0.35	0.35	0.36	0.41	0.39	0.30	0.66	0.42
2.33	2.09	1.84	2.49	2.11	2.21	2.21	2.18	2.51	2.40	1.91	3.98	2.55
0.34	0.30	0.27	0.37	0.32	0.32	0.32	0.32	0.37	0.35	0.28	0.60	0.37
21	20	18	25	23	22	22	21	23	25	20	40	25
6.1	8.2	8.6	8.5	10.4	9.2	9.2	9.3	7.0	8.4	10.6	5.2	5.7
79.3	93.8	83.0	109.9	110.2	103.5	105.5	102.8	96.4	104.2	104.7	116.5	83.5
10.3	13.7	16.9	14.4	19.7	17.9	17.9	17.5	13.9	16.5	17.1	13.2	11.8
147	126	124	116	139	127	127	122	127	139	128	140	110
4.5	3.7	3.6	3.5	4.1	3.8	3.8	4.1	3.8	4.0	3.7	4.2	3.3
7	7	7	8	8	8	8	8	8	8	8	9	7
0.46	0.48	0.52	0.70	0.61	0.61	0.61	0.69	0.58	0.61	0.62	0.74	0.43
5.0	6.8	4.9	6.4	6.5	4.9	4.9	6.0	7.0	5.0	7.3	6.7	4.2
2.7	2.5	1.8	2.8	2.1	2.1	2.1	2.1	2.5	2.3	2.3	3.0	2.4
14.4	14.1	13.0	11.1	13.1	13.0	13.0	11.4	13.8	13.4	12.8	11.9	17.3
32.9	34.0	34.4	32.9	33.8	33.5	33.5	29.8	33.0	35.0	34.7	33.5	33.7
18.7	16.4	15.8	15.9	18.5	19.1	19.1	12.1	13.2	15.5	17.1	14.9	15.6
2.5	2.7	3.7	2.8	3.9	3.8	3.8	3.7	3.2	3.6	3.5	2.9	3.1



Southern Zone			Eastern Satellite Group				Eastern Satellite Group				
RA02AK17A	RA02AK17B	RA02AK18	01PH107B <sup>2</sup>	01KD72B <sup>2</sup>	01KD74B <sup>2</sup>	01KD75D <sup>2</sup>	RA02AK05 <sup>3</sup>	01KD141A <sup>3</sup>	02KD31B <sup>3</sup>	01PH104B <sup>3</sup>	01KD137A <sup>3</sup>
89	89	75	108	86	79	31	61	76	28	34	3
3.3	3.3	3.3	1.9	2.4	3.1	0.7	2.6	1.7	1.3	0.9	1.1
159	159	192	89	195	179	159	253	236	318	276	461
978	978	846	2660	910	1030	188	913	577	399	275	547
0.56	0.56	0.39	1.21	0.44	0.44	0.19	0.24	0.32	0.09	0.12	0.01
4.7	4.7	5.2	4.5	3.3	4.7	5.1	4.1	3.7	5.9	11.5	110.0
19.3	19.3	17.5	8.1	30.1	35.8	3.5	19.2	18.7	8.7	4.2	6.1
38.5	38.5	34.2	12.6	59.2	69.3	8.3	38.5	39.3	19.3	11.4	5.9
5.3	5.3	4.6	1.3	7.4	8.6	1.1	5.0	5.2	2.7	1.9	1.9
20.3	20.2	18.3	4.7	29.1	34.0	5.0	20.2	21.1	12.3	9.8	10.8
4.5	4.5	4.1	0.9	6.4	7.3	1.4	4.9	5.1	3.6	3.3	3.6
0.9	1.9	0.9	0.8	1.1	1.4	0.5	1.1	1.2	1.0	1.4	1.4
4.4	5.4	4.1	0.7	6.2	6.4	1.8	4.2	5.6	3.5	4.5	5.8
0.70	0.70	0.65	0.14	1.04	1.01	0.32	0.82	0.97	0.71	0.77	0.99
4.17	4.17	3.80	0.95	6.73	6.17	2.10	5.18	6.19	4.38	5.03	6.32
0.87	0.87	0.79	0.22	1.42	1.22	0.46	1.06	1.33	0.88	1.09	1.41
2.59	2.59	2.37	0.79	4.30	3.61	1.32	3.34	4.01	2.71	3.27	4.11
0.37	0.37	0.35	0.13	0.69	0.54	0.20	0.51	0.58	0.41	0.48	0.61
2.31	2.31	2.15	0.97	4.07	3.29	1.20	3.18	3.80	2.50	2.90	3.64
0.34	0.34	0.32	0.17	0.63	0.49	0.18	0.45	0.58	0.36	0.44	0.56
24	24	22	6	39	34	12	29	37	23	29	41
8.4	8.4	8.2	8.4	7.4	10.9	3.0	6.0	4.9	3.5	1.5	1.7
104.5	106.5	94.1	32.4	158.5	179.1	27.5	108.0	113.5	63.0	50.5	53.2
16.9	16.9	13.5	5.8	14.5	31.4	7.7	9.9	15.7	24.5	76.5	23.7
125	125	123	234	232	277	27	191	249	102	139	67
3.8	3.8	3.8	6.7	5.8	6.6	0.9	5.8	5.9	3.0	3.1	1.9
8	8	8	2	9	10	1	9	4	4	1	0
0.69	0.69	0.63	0.42	0.74	0.66	0.14	0.64	0.45	0.22	0.08	0.01
7.4	7.4	6.1	2.3	8.6	9.2	2.2	7.3	5.8	2.6	0.3	0.3
2.3	2.3	2.5	2.2	4.1	2.2	1.1	3.9	2.5	0.8	0.1	0.2
11.6	11.6	11.9	4.9	12.5	15.0	6.5	14.7	10.0	20.3	8.0	20.0
32.9	32.9	32.0	34.7	39.9	41.8	31.0	32.9	42.1	33.9	44.3	35.3
27.4	27.4	22.9	56.5	35.6	25.5	42.7	23.6	45.1	21.1	36.3	3.0
3.5	3.5	3.0	0.9	2.3	4.5	0.8	2.4	1.8	5.7	4.4	nd



Table 3. Major element compositions of representative samples of the Kodiak Formation and Ghost Rocks Formation, Kodiak Island, Alaska

Sample	Ghost Rocks Formation		Kodiak Formation					
	RA02AK01	RA02AK02	RA02AK03	RA02AK04	RA02AK34	RA02AK43	RA02AK11	RA02AK13 <sup>1</sup>
Major elements (wt. %)								
SiO <sub>2</sub>	59.27	61.33	63.07	63.78	66.30	64.07	61.74	58.24
Al <sub>2</sub> O <sub>3</sub>	17.44	17.01	15.87	15.50	14.31	16.08	17.72	16.99
TiO <sub>2</sub>	0.94	0.91	0.81	0.77	0.76	0.80	0.88	0.81
Fe <sub>2</sub> O <sub>3</sub>	8.39	7.97	7.29	6.43	6.54	7.23	6.91	7.48
MgO	3.24	3.08	2.63	2.36	1.90	2.53	2.59	2.67
MnO	0.09	0.09	0.12	0.07	0.15	0.17	0.12	0.12
CaO	0.45	0.41	1.39	1.44	1.05	1.88	1.03	3.97
Na <sub>2</sub> O	2.48	2.61	2.36	2.62	1.88	2.55	1.75	3.71
K <sub>2</sub> O	2.75	2.64	2.05	2.30	3.32	2.12	2.97	1.41
P <sub>2</sub> O <sub>5</sub>	0.24	0.21	0.24	0.22	0.23	0.25	0.25	1.14
LOI	4.73	4.39	3.93	3.29	3.06	2.24	3.52	3.17
Total	100.01	100.64	99.75	98.78	99.50	99.91	99.48	99.71
S %	0.121	0.337	0.153	0.203	0.009	0.367	0.004	0.038
ASI <sup>2</sup>	2.2	2.2	1.8	1.6	1.7	1.6	2.2	1.1
K <sub>2</sub> O+Na <sub>2</sub> O	5.2	5.3	4.4	4.9	5.2	4.7	4.7	5.1
Na <sub>2</sub> O/K <sub>2</sub> O	1.1	1.0	0.9	0.9	1.8	0.8	1.7	0.4

<sup>1</sup>Country rock inclusion in Central zone of batholith

<sup>2</sup>ASI= mol Al<sub>2</sub>O<sub>3</sub>/(K<sub>2</sub>O+Na<sub>2</sub>O+CaO)

Table 4. Trace element compositions (ppm) of representative samples from the Kodiak Formation and Ghost Rocks Formation, Kodiak Island, Alaska

Sample	Ghost Rocks Formation		Kodiak Formation					
	RA02AK01	RA02AK02	RA02AK03	RA02AK04	RA02AK34	RA02AK43	RA02AK11	RA02AK13 <sup>1</sup>
Rb	91	87	69	73	170	100	98	46
Cs	5.8	5.3	3.6	4.9	10.4	7.2	5.3	2.0
Sr	133	121	183	237	101	275	129	276
Ba	917	820	797	781	928	590	1190	595
Rb/Sr	0.69	0.72	0.38	0.31	1.68	0.36	0.76	0.17
Cs/Ta	8.1	8.0	5.7	8.2	17.6	12.1	7.2	3.0
La	21.3	19.6	25.1	18.9	24.2	18.6	24.0	25.2
Ce	42.0	39.7	49.3	36.5	44.3	36.0	46.0	47.2
Pr	5.2	5.0	6.1	4.6	5.3	4.6	5.5	5.7
Nd	20.9	20.0	24.3	18.4	20.9	18.4	21.8	22.6
Sm	4.6	4.4	5.1	4.0	4.7	4.2	4.8	4.8
Eu	1.0	0.9	1.4	1.1	1.2	1.1	1.1	1.4
Gd	3.8	3.5	4.8	3.3	4.7	3.5	4.5	3.8
Tb	0.70	0.64	0.79	0.62	0.78	0.66	0.77	0.70
Dy	4.13	3.78	4.35	3.64	4.29	3.90	4.25	4.12
Ho	0.83	0.76	0.86	0.72	0.82	0.77	0.88	0.82
Er	2.59	2.34	2.60	2.25	2.28	2.38	2.65	2.58
Tm	0.40	0.37	0.39	0.34	0.35	0.36	0.41	0.40
Yb	2.48	2.28	2.39	2.07	2.20	2.25	2.66	2.54
Lu	0.37	0.34	0.36	0.31	0.34	0.34	0.40	0.37
Y	22	20	23	19	22	22	23	23
La/Yb	8.6	8.6	10.5	9.2	11.0	8.3	9.0	9.9
Total REE	110.3	103.6	127.7	96.9	116.4	97.0	119.8	122.3
Ce/Pb	15.3	15.4	20.6	14.6	14.9	10.4	16.7	13.9
Zr	147	137	143	154	147	130	153	149
Hf	4.4	4.1	3.8	4.5	4.0	3.8	4.2	4.3
Nb	10	10	7	9	8	9	10	9
Ta	0.72	0.67	0.64	0.59	0.59	0.59	0.73	0.65
Th	7.1	6.6	5.8	5.9	4.8	6.1	7.2	6.8
U	2.8	2.6	2.4	2.5	3.0	3.5	2.8	3.4
Nb/Ta	13.7	15.0	11.4	15.9	13.5	15.3	13.1	14.5

Zr/Hf	33.5	33.7	37.5	34.3	36.4	34.4	36.3	34.8
Th/U	2.6	2.6	2.4	2.4	1.6	1.8	2.6	2.0
Nb/U	3.6	3.9	3.1	3.8	2.7	2.6	3.5	2.8
Sc	22	20	18	16	17	19	21	19
Co	16	19	20	13	5	15	10	3
Ni	59	62	75	57	55	86	49	19
Au (ppb)	4.0	3.8	0.4	0.3	3.1	3.7	6.5	1.2
Ir	<5	<5	<5	<5	<5	<5	<5	<5
Mo	<2	3.7	2.5	2.6	3.4	<2	4.9	7.0
Ge	1.1	0.9	1.4	1.2	1.2	1.3	1.4	1.1
Sn	1.3	1.2	<1	<1	<1	<1	1.1	1.1
Cu	152	53	67	59	45	58	35	121
Ag	4.0	3.8	0.4	0.3	3.1	3.7	6.5	1.2
Zn	149.0	157.3	135.8	156.8	77.7	185.0	115.6	68.0
Cd	0.9	1.3	<0.5	0.5	<0.5	0.5	<0.5	<0.5
Hg (ppb)	356	373	128	96	281	41	43	56
Pb	16	14	9	21	5	8	10	3
Ga	22	20	18	17	19	18	20	18
In	<0.1	<0.1	<0.1	<0.1	<0.1	<0.1	<0.1	<0.1
Tl	0.49	0.48	0.44	0.38	0.60	0.51	0.63	0.28
As	14.9	19.6	18.5	15.2	56.4	210.0	19.5	16.1
Sb	0.9	1.4	1.3	1.0	30.3	0.3	3.2	0.3
Bi	1.29	0.97	0.69	0.55	0.42	0.14	0.48	0.67
Se	0.71	0.88	0.90	0.66	0.59	0.64	0.41	0.95
Te	<0.1	<0.1	<0.1	<0.1	<0.1	0.1	<0.1	0.1
V	165.4	152.4	159.8	125.1	142.0	142.3	182.0	136.8
Cr	109.3	96.3	110.5	81.3	94.4	92.4	106.2	81.6
W	1.1	1.0	0.8	0.9	2.8	1.0	1.1	0.7
Br	<0.5	<0.5	<0.5	<0.5	<0.5	<0.5	<0.5	<0.5

---

---

nd, not determined

Table 5. U-Th-Pb, Sm-Nd and Rb-Sr isotope data for feldspars and whole rocks (wr) of the Kodiak batholith and igneous rocks flanking the batholith, Kodiak Island

Sample	Rock Type	$^{206}\text{Pb}/^{204}\text{Pb}$	$^{207}\text{Pb}/^{204}\text{Pb}$	$^{208}\text{Pb}/^{204}\text{Pb}$	Th	U	Pb	$^{238}\text{U}/^{204}\text{Pb}$	Sm	Nd	$^{143}\text{Nd}/^{144}\text{Nd}$	$^{147}\text{Sm}/^{144}\text{Nd}$	$\epsilon_{\text{Nd}}$	$T_{\text{DM}}$	Rb	Sr	$^{87}\text{Sr}$
					ppm	ppm	ppm	$\mu^1$	ppm	ppm	measured <sup>2</sup>		(59 Ma)	(Ga)	ppm	ppm	mea:
<b>Southern Zone</b>																	
RA02AK22	Granodiorite	18.924	15.580	38.520	4.98	2.26	16.98	9.97	4.46	19.77	$0.512538 \pm 7$	0.1364	-1.4	1.01	71.4	196.4	0.706
RA02AK19	Tonalite	18.911	15.576	38.504	7.26	2.30	16.08	9.48	4.38	20.89	$0.512576 \pm 7$	0.1268	-0.6	0.84	74.5	199.4	0.706
RA02AK21	Tonalite	18.929	15.604	38.618	6.67	3.02	18.00	9.60	4.87	21.15	$0.512546 \pm 5$	0.1393	-1.3	1.03	92.8	180.3	0.706
RA02AK20	Granodiorite	nd	nd	nd	4.17	2.43	16.90	nd	3.97	15.63	$0.512721 \pm 6$	0.1537	2.0	0.84	74.8	220.5	1
RA02AK17A	Granodiorite	18.928	15.584	38.350	7.41	2.28	16.89	9.51	4.46	20.27	$0.512556 \pm 9$	0.1331	-1.1	0.94	89.5	158.9	1
RA02AK17B	Granodiorite	18.925	15.599	38.575	7.41	2.28	16.89	9.58	4.46	20.27	nd	nd	nd	nd	89.5	158.9	1
RA02AK18	Granodiorite	18.929	15.608	38.534	6.12	2.53	16.05	9.61	4.06	18.26	$0.512595 \pm 3$	0.1345	-0.3	0.88	75.2	191.9	0.706
<b>Central Zone</b>																	
RA02AK28	Tonalite	18.933	15.591	38.568	9.59	2.74	11.35	9.54	5.47	28.36	$0.512730 \pm 6$	0.1164	2.4	0.52	80.1	191.2	0.706
01PH121A	Tonalite	18.960	15.575	38.547	5.25	1.89	24.72	9.47	4.40	20.49	$0.512467 \pm 9$	0.1300	-2.8	1.06	72.0	213.3	0.706
01PH116A, wr	Tonalite	18.898	15.564	38.524	2.79	1.34	24.02	9.44	3.04	13.32	$0.512728 \pm 5$	0.1381	2.2	0.66	41.3	249.1	0.705
RA02AK30	Tonalite	18.946	15.618	38.660	3.65	2.23	15.05	9.65	3.61	15.19	$0.512855 \pm 5$	0.1437	4.7	0.45	70.1	239.0	0.705
RA02AK10	Tonalite	18.903	15.590	38.537	3.51	2.06	13.34	9.54	4.23	18.28	$0.512546 \pm 3$	0.1399	-1.3	1.04	61.9	241.5	0.704
RA02AK12	Tonalite	18.918	15.590	38.522	4.91	1.81	23.01	9.54	3.47	15.93	$0.512556 \pm 6$	0.1317	-1.1	0.92	61.7	258.7	0.706
RA02AK26	Granodiorite	18.918	15.600	38.583	6.44	2.79	14.57	9.58	4.56	20.89	$0.512340 \pm 4$	0.1321	-0.3	0.85	88.8	198.8	0.706
RA02AK25	Tonalite	18.919	15.564	38.444	6.49	2.07	15.03	9.43	4.55	21.07	$0.512542 \pm 3$	0.1306	-1.3	0.93	80.4	216.7	0.706
RA02AK39A	Tonalite	18.936	15.600	38.577	4.93	2.12	25.04	9.58	4.24	19.70	$0.512565 \pm 7$	0.1302	-0.9	0.89	79.0	193.8	0.705
RA02AK39B	Tonalite	18.920	15.573	38.507	4.93	2.12	25.00	9.47	4.24	19.70	$0.512505 \pm 3$	0.1302	-2.0	1.00	79.0	193.8	1
RA02AK24	Tonalite	18.943	15.589	38.517	6.03	2.14	18.42	9.53	4.28	19.85	$0.512626 \pm 4$	0.1305	0.3	0.78	80.4	197.7	0.706
<b>Northern Zone</b>																	
RA02AK36	Granodiorite	18.884	15.587	38.497	5.18	1.66	24.71	9.53	3.77	17.64	$0.512650 \pm 6$	0.1293	0.8	0.73	79.9	191.2	0.704
01KD56A	Granodiorite	18.899	15.603	38.580	4.60	2.05	35.77	9.60	3.64	17.20	$0.512649 \pm 4$	0.1410	-1.8	1.11	56.4	242.8	1
01KD60B	Granodiorite	18.872	15.563	38.449	4.52	1.37	39.77	9.44	3.54	16.72	$0.512446 \pm 4$	0.1277	-3.7	1.07	71.6	187.5	0.705
RA02AK40	Tonalite	18.874	15.567	38.514	4.81	1.19	9.01	9.45	3.33	16.15	$0.512589 \pm 7$	0.1247	-0.4	0.80	76.5	251.9	0.705
RA02AK16	Granodiorite	18.893	15.579	38.508	6.46	1.62	24.00	9.50	4.04	17.32	$0.512521 \pm 4$	0.1410	-1.8	1.11	84.5	159.7	0.706
<b>Northern Satellite Group</b>																	
RA02AK31	Granodiorite	18.850	15.611	38.609	4.97	3.11	18.51	9.71	3.69	16.43	$0.512617 \pm 7$	0.1358	0.0	0.86	91.1	163.9	0.705
01KD70C	Leucogranite	18.918	15.595	38.556	1.23	3.26	72.09	9.56	1.25	4.53	nd	nd	nd	nd	124.8	33.9	1
<b>Western Satellite Group</b>																	
RA02AK15	Granodiorite	18.887	15.576	38.497	5.49	1.48	27.13	9.49	3.40	15.37	$0.512632 \pm 4$	0.1337	0.4	0.80	59.9	204.8	0.705
<b>Eastern Satellite Group<sup>3</sup></b>																	
01PH107B	Leucogranite	18.935	15.567	38.554	2.25	2.19	17.50	9.44	0.86	4.68	$0.512933 \pm 5$	0.1117	6.4	0.20	107.7	88.8	0.706
01KD72B	Granodiorite	18.926	15.587	38.543	8.59	4.08	18.37	9.53	6.41	29.07	$0.512550 \pm 6$	0.1334	-1.2	0.95	86.2	194.5	0.706
01KD74B	Granodiorite	18.948	15.577	38.610	9.20	2.21	23.50	9.48	7.28	33.97	$0.512535 \pm 7$	0.1297	-1.5	0.94	78.8	179.1	0.707
01KD75D	Diorite	18.969	15.578	38.514	2.20	1.07	4.99	9.48	1.44	5.02	$0.512511 \pm 8$	0.1738	-2.3	2.12	30.7	158.9	0.703
01KD141A	Tonalite	18.836	15.577	38.414	5.78	2.49	21.71	9.50	5.11	21.07	nd	nd	nd	nd	76.0	235.7	0.704
<b>Eastern Satellite Group<sup>4</sup></b>																	
01PH104B, wr	Gabbro	18.854	15.558	38.478	0.33	0.15	5.01	9.42	3.29	9.82	$0.512499 \pm 6$	0.2028	-2.7	nd	34.0	275.9	0.705
01KD137A, wr	Basalt	19.054	15.543	38.322	0.28	0.25	4.97	9.33	3.65	10.80	$0.512852 \pm 4$	0.2042	4.2	nd	3.2	461.0	0.705

nd, not determined

<sup>1</sup> $\mu$  calculated using Stacey and Kramers (1974)<sup>2</sup>Analytical errors on  $^{143}\text{Nd}/^{144}\text{Nd}$ ,  $^{87}\text{Sr}/^{86}\text{Sr}$  measurements represent ( $2\sigma$ ).<sup>3</sup>Inner: trenchward belt of rocks adjacent to batholith; intruded the Kodiak Formation and the Ghost Rocks Formation<sup>4</sup>Outer: trenchward belt of rocks; intruded the Ghost Rocks Formation

Table 6. U-Th-Pb, Sm-Nd and Rb-Sr whole-rock isotope data for the Kodiak Formation and Ghost Rocks Formation, Kodiak Island

Sample	$^{206}\text{Pb}/^{204}\text{Pb}$	$^{207}\text{Pb}/^{204}\text{Pb}$	$^{208}\text{Pb}/^{204}\text{Pb}$	Th ppm	U ppm	Pb ppm	$^{238}\text{U}/^{204}\text{Pb}$ $\mu^1$	Sm ppm	Nd ppm	$^{143}\text{Nd}/^{144}\text{Nd}$ measured <sup>2</sup>	$^{147}\text{Sm}/^{144}\text{Nd}$	$\epsilon_{\text{Nd}}$ (59 Ma)	$T_{\text{DM}}$ (Ga)	Rb ppm	Sr ppm	$^{87}\text{Sr}/^{86}\text{Sr}$ measured <sup>2</sup>
<b>Ghost Rocks Formation</b>																
RA02AK01	19.166	15.640	38.814	7.09	2.75	16.04	9.71	4.625	20.921	$0.512549 \pm 2$	0.1337	-1.22	0.96	91.33	132.80	$0.708219 \pm 2$
RA02AK02	19.029	15.588	38.636	6.64	2.58	13.73	9.52	4.402	19.999	$0.512490 \pm 5$	0.1331	-2.37	1.06	86.57	120.89	$0.708496 \pm 7$
<b>Kodiak Formation</b>																
RA02AK03	19.057	15.607	38.581	5.77	2.39	8.99	9.59	5.052	24.279	$0.512432 \pm 5$	0.1258	-3.45	1.07	68.75	182.89	$0.707029 \pm 8$
RA02AK04	18.981	15.567	38.484	5.90	2.51	21.07	9.44	4.039	18.359	$0.512533 \pm 6$	0.1331	-1.53	0.98	72.62	237.35	$0.706438 \pm 7$
RA02AK34	19.048	15.579	38.552	4.80	2.98	4.78	9.48	4.742	20.872	$0.512383 \pm 4$	0.1373	-4.49	1.33	169.88	100.86	$0.709573 \pm 4$
RA02AK43	18.978	15.580	38.561	6.14	3.45	8.08	9.49	4.163	18.439	$0.512409 \pm 4$	0.1365	-3.98	1.27	99.99	274.84	$0.707693 \pm 5$
RA02AK11	19.051	15.629	38.725	7.16	2.75	10.15	9.68	4.809	21.785	$0.512269 \pm 3$	0.1335	-6.68	1.49	97.60	128.95	$0.708908 \pm 6$
RA02AK13 (inclusion)	18.983	15.583	38.556	6.75	3.40	3.05	9.50	4.834	22.571	$0.512580 \pm 6$	0.1295	-0.57	0.86	46.29	275.89	$0.705843 \pm 4$

<sup>1</sup> $\mu$  calculated using Stacey and Kramers (1974)<sup>2</sup>Analytical errors on  $^{143}\text{Nd}/^{144}\text{Nd}$ ,  $^{87}\text{Sr}/^{86}\text{Sr}$  measurements represent (2  $\sigma$ ).